1-1-2015

Emulsion Stabilization with Janus Particles

Fuquan Tu
University of Pennsylvania, tufq06@gmail.com

Emulsion Stabilization with Janus Particles

Abstract
Emulsions are dispersions of droplets of one fluid within a second, immiscible fluid and have a wide range of applications from foodstuffs to pharmaceuticals to personal care products and agrochemicals. Emulsions are intrinsically unstable because of large interfacial area associated with the system. To obtain stable emulsions, the interfaces between immiscible fluids must be stabilized by emulsifying agents such as surfactants and colloidal particles. Surfactants refer to surface-active agents which prefer to segregate to interfaces between two immiscible fluids. Their surface activity originates from their amphiphilic structure. Colloidal particles can stabilize emulsions due to their tendency to attach strongly to the interface. It has been demonstrated that particles with amphiphilic structure (also known as Janus particles) can be synthesized. An important potential application of Janus particles comes from the fact that they could make unique solid surfactants, however, several questions needs to be answered: (1) It has been recognized for more than 100 years that surfactant molecules and homogeneous particles can attach to interfaces and stabilize emulsions. How would Janus particles be different from and, more importantly, advantageous over molecular surfactants and homogeneous particles in emulsion stabilization? (2) How does the structure or geometry of Janus particles influence their properties as solid surfactants? To answer these questions, thermodynamics of emulsion stabilization using amphiphilic Janus particles is investigated showing that they can indeed generate thermodynamically stable emulsion whereas emulsions stabilized by surfactant molecules and homogeneous particles are only kinetically stable. In addition, a new synthesis method is developed enabling the bulk synthesis of highly uniform pH-responsive Janus particles that are able to completely reverse their surfactant properties in response to changes in the solution pH. These Janus particles can stabilize different types of simple emulsions (oil-in-water and water-in-oil) at different pH and, more importantly, induce phase inversion of emulsions in response to changes in solution pH. Furthermore, one-step formation of stable multiple emulsions is demonstrated using these amphiphilic Janus. Multiple emulsions stabilized by these stimuli-responsive Janus particles can be induced to release the encapsulant by simply increasing the pH of the continuous phase. In conclusion, Janus particles represent promising systems as solid surfactants for making stable and smart emulsions.

Degree Type
Dissertation

Degree Name
Doctor of Philosophy (PhD)

Graduate Group
Chemical and Biomolecular Engineering

First Advisor
Daeyeon Lee

Keywords
amphiphilic, emulsion, Janus particle, stimuli-responsive

EMULSION STABILIZATION WITH JANUS PARTICLES

Fuquan Tu

A DISSERTATION

in

Chemical and Biomolecular Engineering

Presented to the Faculties of the University of Pennsylvania

in

Partial Fulfillment of the Requirements for the

Degree of Doctor of Philosophy

2015

Supervisor of Dissertation

_____

Daeyeon Lee, Associate Professor, Chemical and Biomolecular Engineering

Graduate Group Chairperson

_____

Raymond J. Gorte, Professor, Chemical and Biomolecular Engineering

Dissertation Committee

Russell J. Composto, Professor, Materials Science and Engineering

Daniel A. Hammer, Professor, Chemical and Biomolecular Engineering

Kathleen J. Stebe, Professor, Chemical and Biomolecular Engineering

EMULSION STABILIZATION WITH JANUS PARTICLES

To my family

Acknowledgements

Without the support of numerous individuals, the completion of this thesis would not have been possible and I am grateful for all of their support. First of all, I would like to thank my advisor Professor Daeyeon Lee for his guidance over the past four to five years. He introduced me to the world of colloids and interfacial science and also helped me develop my critic thinking and experimental skills, which are needed to be a qualified researcher. He is supportive, patient and always there to help when I experience difficulties in my research. His dedication and enthusiasm to science inspires me and keeps me motivated for the next big challenge.

I also would like to thank my thesis committee members Professor Composto, Professor Hammer, and Professor Stebe. It was very generous for Professor Burdick and Professor Kagan to let me use their equipment to conduct my research and I really appreciate Dr. Christopher Highley, Ryan Wade and Eric Wong's guidance in properly operating the equipment.

I feel really lucky to have met all the students and post-docs in the Lee group: Myung Han Lee, Bum Jun Park, Iris Yi, Kwadwo Tetty, Lei Zhang, Sang-Wook Lee, Zaki Estephan, Weifeng Wang, Seonju Yeo, Yun-Ru Huang, Elio Angilè, Teresa Brugarolas, Seongchul Park, Dongkyu Roh, Likai Hou, Weiyang Lim, Wei-Han Cheng, Jyo Lyn Hor,

Gang Duan, Sarah Hann, Ankit Kumar, Jacob Prosser, Tae Soup Shim, Martin Hasse and Rohini Gupta. It has been a wonderful experience and I really appreciate their kindness.

I am truly grateful for several people's help and time during my most difficult time of my thesis research. Dr. Kisun Yoon, Dr. Mark Panczyk and Professor Jin Woong Kim have offered me a lot of suggestions for my particle synthesis, and their help on the successful development of my own technique cannot be underestimated.

I would also like to thank my SEAS friends including Richard Tourdot, Amit Shavit, Cory Silva, Yifan Wang, Zhihao Jiang, Jiechang Hou and Huikuan Chao. We have had a lot of memorable times during the past few years.

Finally, I want to thank my parents for their patience and for supporting and encouraging me to pursue my dreams without reservation. I also would like to thank my sister. She always treats me as a role model, and this motivates me to become a self-disciplined, hard-working, and caring brother. I also want to thank Ms. Mei Wang for her support, help, and trust in both my personal life and career.

Without funding from PENN MRSEC though the National Science Foundation, the NSF CAREER Award, Biomolecular Materials programs at the DOE, the American Chemical Society Petroleum Research Fund, and Xerox, my research would not have been possible.

ABSTRACT

EMULSION STABILIZATION WITH JANUS PARTICLES

Fuquan Tu

Daeyeon Lee

Emulsions are dispersions of droplets of one fluid within a second, immiscible fluid and have a wide range of applications from foodstuffs to pharmaceuticals to personal care products and agrochemicals. Emulsions are intrinsically unstable because of large interfacial area associated with the system. To obtain stable emulsions, the interfaces between immiscible fluids must be stabilized by emulsifying agents such as surfactants and colloidal particles. Surfactants refer to surface-active agents which prefer to segregate to interfaces between two immiscible fluids. Their surface activity originates from their amphiphilic structure. Colloidal particles can stabilize emulsions due to their tendency to attach strongly to the interface. It has been demonstrated that particles with amphiphilic structure (also known as Janus particles) can be synthesized. An important potential application of Janus particles comes from the fact that they could make unique solid surfactants, however, several questions needs to be answered: (1) It has been recognized for more than 100 years that surfactant molecules and homogeneous particles can attach to interfaces and stabilize emulsions. How would Janus particles be different from and, more importantly, advantageous over molecular surfactants and homogeneous

particles in emulsion stabilization? (2) How does the structure or geometry of Janus particles influence their properties as solid surfactants? To answer these questions, thermodynamics of emulsion stabilization using amphiphilic Janus particles is investigated showing that they can indeed generate thermodynamically stable emulsion whereas emulsions stabilized by surfactant molecules and homogeneous particles are only kinetically stable. In addition, a new synthesis method is developed enabling the bulk synthesis of highly uniform pH-responsive Janus particles that are able to completely reverse their surfactant properties in response to changes in the solution pH. These Janus particles can stabilize different types of simple emulsions (oil-in-water and water-in-oil) at different pH and, more importantly, induce phase inversion of emulsions in response to changes in solution pH. Furthermore, one-step formation of stable multiple emulsions is demonstrated using these amphiphilic Janus. Multiple emulsions stabilized by these stimuli-responsive Janus particles can be induced to release the encapsulant by simply increasing the pH of the continuous phase. In conclusion, Janus particles represent promising systems as solid surfactants for making stable and smart emulsions.

Table of Contents

List of Tables

List of Figures

Chapter 1. Introduction

1.1 Backgroud

1.1.1 Emulsion

An emulsion is a stable dispersion of droplets of fluid within a second, immiscible fluid. Emulsions are widely encountered in a huge variety of industries, *e.g.* agrochemical, food, pharmaceutical, cosmetics, paint, printing and petroleum.[1,2] Emulsions are classified into three categories based upon the size of the dispersed droplets: (1) *macroemulsion*, opaque emulsions with particles >400 nm (0.4 μm), easily visible under a microscope; (2) *microemulsions*, transparent dispersions with droplets <100 nm (0.1 μm) in size; and (3) *nanoemulsions* (*miniemulsions*), a type that is blue-white, with particle sizes between those of the first two types (100-400 nm [0.1-0.4 μm]). *Multiple emulsions*[3], in which the dispersed droplets are themselves emulsions, have also been subject of considerable investigation.[4]

Macroemulsions are the most well-known emulsions of the three types[4], which is the only consideration in this thesis ("emulsion" will be used instead of "macroemulsion" later in this thesis for simplicity). There are two types of simple emulsions based on the nature of the dispersed phase: oil-in-water (O/W) and water-in-oil (W/O). In the case of O/W type, oil phase is the dispersed phase while water phase is the continuous phase. Emulsions are obtained by shearing two immiscible fluids, leading to the fragmentation of one phase

into the other, in the presence of a third component called the *emulsifying agent*, which can be either surface-active agents such as surfactant molecules and polymer surfactants or finely divided solids, *e.g.* homogeneous colloidal particles. The function of emulsifying agents is to stabilize emulsion for a sufficient time by adsorption or attachment to the fluid-fluid interfaces.

1.1.1.1 Surfactant

Surfactants are surface-active agents and include small surfactant molecules, *e.g.* sodium dodecyl sulfate (SDS) as well as polymeric surfactants such as polyvinyl alcohol (PVA). Their surface activity comes from the fact that they possess both hydrophilic and lipophilic properties, leading to the preferential adsorption to interfaces between two immiscible fluids. The surface activity of surfactants and their ability to stabilize emulsions strongly depend on their molecular structure and the degree of hydrophilicity/lipophilicity as often represented by hydrophile-lipophile balance (HLB) number.[5] For example, surfactants with HLB number >10 usually stabilize O/W emulsions while those with HLB number <10 stabilize W/O emulsions.

Emulsions stabilized by surfactants, in general, are thermodynamically unstable. The thermodynamics of emulsion stabilization can be considered by calculating the free energy change during emulsion formation which consists of an interfacial free energy term (ΔG_I) and a configuration entropy term ($-T\Delta S_{config}$).[6]

$$\Delta G_{em} = \Delta G_I - T\Delta S_{config} \quad (1\text{-}1)$$

The interfacial free energy term is equal to the increase in contact area between the oil and aqueous phases (ΔA) multiplied by the interfacial tension (γ) at the oil-water interface:

$$\Delta G_I = \gamma \Delta A \quad (1\text{-}2)$$

In most cases, especially macroemulsions considered here, $\gamma\Delta A >> -T\Delta S_{config}$, which means that ΔG_{em} is positive – that is, the formation of emulsions is nonspontaneous and the system is thermodynamically unstable.[2] Surfactants at fluid-fluid interfaces performs two functions: (1) it reduces the interfacial tension between the two fluids and consequently the thermodynamic instability of the system resulting from the increase in the interfacial area between the two phases. (2) It decreases the rate of coalescence of the dispersed droplets by forming mechanical, steric, and/or electrical barriers around them.[4] That is, emulsions are kinetically stabilized by surfactants.

1.1.1.2 Homogenous Particle

It has been known for more than 100 years that homogeneous particles even without amphiphilicity can stabilize emulsions. Ramsden was the first to report emulsion droplets stabilized by particles in 1903.[7] Interestingly, particle-stabilized emulsions are named after Pickering as "Pickering emulsion" for his first systematic study on particle-stabilized emulsions.[8]

Homogeneous particles with moderate wettability can strongly attach to fluid-fluid interfaces. Consider a spherical particle of radius r as shown in Figure 1.1 which is initially in one phase and is subsequently adsorbed to the fluid interface. The adsorption of the particle at the interface results in a reduction in the area of the fluid interface whose magnitude depends on the wettability of the particles characterized by three-phase contact angle θ (measured through the aqueous phase). The energy of attachment of a particle to a fluid–fluid interface is related not only to the contact angle but also to the tension of the interface γ. Assuming the particle is small enough (typically less than a few microns in diameter) so that the effect of gravity is negligible, the energy G_{de} required to remove the particle from the interface is given by

$$G_{de} = \pi r^2 \gamma \left(1 \pm \cos\theta\right)^2 \quad (1\text{-}3)$$

in which the sign inside the bracket is negative for removal into the aqueous phase, and positive for removal into the air or oil phase.[9] For a particle with neutral wetting (θ=90°) with a radius of r=10 nm and the interfacial tension of γ=0.036 Nm^{-1}, the detachment energy is 2750 kT which is orders of magnitude higher than thermal fluctuation (~kT) meaning that the adsorption of a particle to fluid interface is essentially irreversible.[10] This effectively irreversible adsorption leads to extreme stability for certain emulsions and is in contrast to the behavior of surfactant molecules which are usually in rapid dynamic equilibrium between the oil–water interface and the bulk phases.[10] However,

when the wettability of particles is too hydrophilic ($0° \leq \theta \leq 20°$) or too hydrophobic ($160° \leq \theta \leq 180°$), the detachment energy (G_{de}) falls rapidly to less than 10 kT.

The wettability of the particles not only affects the detachment energy but also determines the type of emulsion they can stabilize. The work of Finkle *et al.*[11] first recognized the relationship between the type of particles and emulsion type (o/w or w/o). They stated that in an emulsion containing solid particles, one of the liquids would probably wet the solid more than the other liquid, with the more poorly wetting liquid becoming the dispersed phase. That is, particles with contact angle $\theta < 90°$ stabilize O/W emulsion while those with $\theta > 90°$ stabilize W/O emulsion. These ideas are strongly supported by many following studies.[10,12,13]

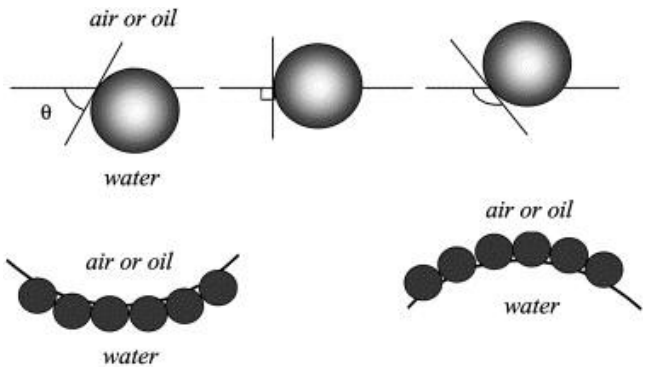

Figure 1.1 (upper) Position of a small spherical particle at a planar oil–water interface for a contact angle (measured through the aqueous phase) less than 90 ° (left), equal to 90 ° (centre) and greater than 90 ° (right). (lower) Corresponding probable positioning of particles at a curved interface. For θ<90°, solid-stabilised o/w emulsions may form (left). For θ>90°, solid-stabilised w/o emulsions may form (right). Figure reproduced from reference 10.

The significant difference in adsorption/desorption dynamics of homogeneous particles, however, does not alter the similar thermodynamic nature of Pickering emulsions from emulsion stabilized by surfactants. The free energy change for Pickering emulsions stabilized by homogeneous particles are given by

$$\Delta_{em}G = n_d \Delta_d G = n_d \left\{ A_{ow}\gamma_{ow} + n_p (\Delta_a G - T\Delta_a S) \right\} \quad (1\text{-}4)$$

where n_d and n_p are respectively the number of drops in the emulsion and the number of particles adsorbed onto a drop; the free energy of forming a particle-coated drop is denoted $\Delta_d G$. In equation (1-4), A_{ow} represents the surface area of a bare, notionally swollen drop (interfacial tension γ_{ow}) but with no particles adsorbed. $\Delta_a G$ is the free energy of adsorption of a particle to the drop surface excluding the entropy change, $\Delta_a S$, due to de-mixing of particles from the phase in which they are initially dispersed. The entropy of dispersion of the droplets in the continuous phase, which in the current context is very small, is ignored.[14] With moderate wettability, particles at droplet interfaces can act as effective steric barriers due to strong attachment giving Pickering emulsion superior stability over emulsions stabilized by surfactants.[1] However, it is generally believed that, like emulsion stabilized by surfactants, Pickering emulsions are nevertheless thermodynamically unstable.[10,15]

1.1.2 Janus Particle

In 1991, in his Nobel lecture, Pierre-Gilles de Gennes introduced the concept of "Janus particles" first made by C. Casagrande et al.[16] These are particles with opposite polarities on the two hemispheres.[17] Janus particles, according to de Gennes, resemble surfactant molecules in their amphiphilicity but should exhibit a unique property that is not observed in molecular amphiphiles when they assemble at an fluid-fluid interface. While a film of surfactant molecules at the interface would be dense, a film of Janus particles with interstices would form a "breathable skin" at the interface, through which exchange of chemicals can occur between the two phases.

In 1990s, not much was done on Janus particle research other than a limited number of publications in this area due to difficulty in the synthesis of Janus particles.[18] During the past 15 years, however, various synthesis methods are developed and motivations from a wide array of potential applications have emerged.[19] Janus particles exhibit unique assembly behaviors that are not observed in homogeneous particles and inspired new areas of potential applications due to improved performance over homogenous particles in a large variety of fields such as targeted drug delivery, biomedicine, electronics and sensors, optics, super-hydrophobic texitles, and many others.

One of the most promising applications of Janus particles is their use as solid surfactants for the stabilization of multiphasic mixtures such as emulsions. What's most exciting is that de Gennes' vision of a breathable skin made of a Janus particle monolayer at a fluid–fluid interface to allow for chemical exchange between the two fluid phases has recently

been realized in a study by Faria and co-workers.[20] Using Janus particles as solid surfactants, they are able to selectively catalyze reactions in both phases.

Research focusing on the application of Janus particles as solid surfactants has shown that these particles are able to stabilize emulsions and maintain their stability for an extended period of time, more effectively than homogeneous particles. For example, it was shown that Janus particles have significantly higher interfacial activity than their homogeneous counterparts, and thus, can effectively lower the interfacial tension between oil and water, as shown in Figure 1.2.[21] Janus particles synthesized by partial surface hydrophobization of hydrophilic silica particles are shown to effectively stabilized oil in water emulsions. In addition, O/W emulsions stabilized with Janus particles show superior long-term stability compared to those stabilized with homogeneous silica particles, as shown in Figure 1.3.[22]

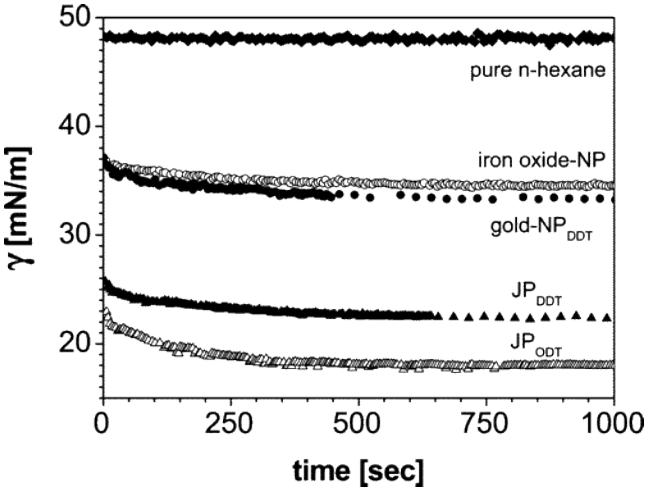

Figure 1.2 Comparisons between homogeneous iron-oxide nanoparticles and 1-dodecanethiol (DDT) modified Janus nanoparticles in decreasing the interfacial tension at a water–n-hexane interface. Reprinted with permission from reference 21.

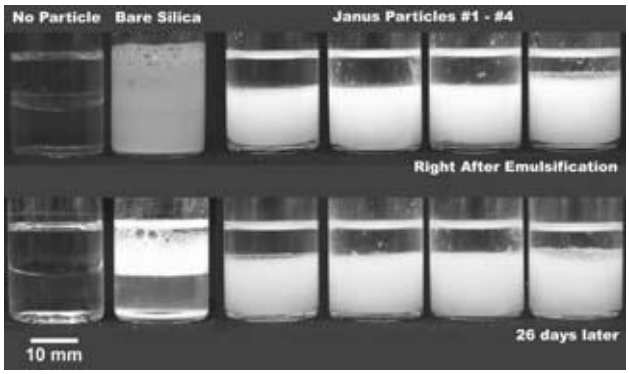

Figure 1.3 Comparison between emulsion stabilization (left) without particles, (second column) with unmodified silica particles, and (third to last columns) with Janus particles. Images were taken immediately after and 26 days after emulsification. Reprinted with permission from reference 22.

Non-spherical Janus particles also have been explored as emulsifiers. Janus dumbbells (or dimers) made of two partially fused spheres of opposing wettability (Figure 1.4) have been shown to exhibit considerable "surfactancy".[23] These particles are synthesized by

inducing phase separation between two incompatible polymers or polymer network via the seeded emulsion polymerization technique.[24] It was proposed that the shape (*i.e.*, the ratio of the size of the two spheres) could play an important role in determining the surface activity of these Janus dumbbells. These particles have the tendency to cover the interface with closely packed arrangements. Another remarkable observation was the stabilization of emulsion droplets that are non-spherical, as shown in Figure 1.4, which was hypothesized to occur due to jamming of dumbbells at the interface in time scales smaller than the relaxation time of the droplets. In another study, amphiphilic Janus nanosheets were explored for emulsion stabilization.[25] These plate-like Janus particles were found to be effective in decreasing the surface tension, demonstrated by a decrease in the size of emulsion droplets formed using these particles as emulsifiers. When used in emulsion polymerization, increasing the concentration of these amphiphilic nanosheets led to a decrease in the size of the synthesized polystyrene particles.

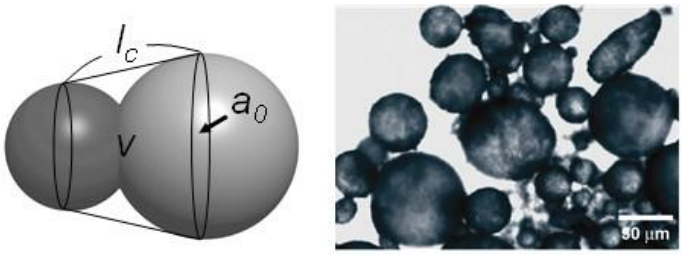

Figure 1.4 (Left) Schematic illustration of a Janus dumbbell with a parameter used to define the packing parameter ($P_{packing}=v/a_o l_c$) of a dumbbell; (right) non-spherical emulsion droplets formed by using amphiphilic dumbbells as colloid surfactants. Reprinted with permission from reference 23.

Used as solid surfactants, Janus particles have also facilitated the formation of new materials. It was demonstrated that Janus particles could compatibilize polymer blends much more effectively than block and graft copolymers, which, currently, are the state-of-the-art compatibilizers.[26,27] The effectiveness of Janus particles as polymer compatibilizers was attributed to their tendency to readily adsorb to polymer–polymer interfaces and to remain at the interfaces without micellization, even under high temperature and high shear conditions. Another study showed that when Janus particles were used as emulsifiers in mini-emulsion polymerization, no additives were required, unlike in Pickering emulsion polymerization using homogeneous particles.[28] Also, the size of the particles produced with Janus particles was shown to be very well controlled and monodisperse. The reason for such excellent performance of Janus particles as a stabilizer in emulsion polymerization was attributed to their strong tendency to adsorb to the oil–water interfaces.

In addition to these advances in experiments, a simulation study using dissipative particle dynamics was used to study the mechanism of coalescence between two emulsion droplets stabilized with Janus particles.[29] The nanoparticle surface coverage, their surface activity and the stability of the film forming between two coalescing droplets were found to be extremely critical in determining the stability of emulsions. At a comparable coverage, Janus nanoparticle-covered emulsions showed superior emulsion stability over those stabilized with homogeneous nanoparticles because of the high surface activity of Janus particles.

The main reason that Janus particles are able to stabilize emulsions more effectively than homogenous particles can be explained by their strong attachment to fluid interfaces. Due to the amphiphilicity of Janus particles, the desorption energy of a Janus particle from a fluid interface can be as large as three times that of a homogeneous particle.[30] Further extending this work, it was theoretically shown that spherical Janus particles can lead to the formation of thermodynamically stable Pickering emulsions.[14] In contrast, Pickering emulsions stabilized with homogeneous particles generally are only kinetically stable. The large attachment energy of Janus particles to fluid interfaces is able to overcome the energy penalty that is associated with creating a bare oil–water surface area during emulsion formation.

1.2 Motivations and Objectives

1.2.1 Motivations

Recent studies have shown that Janus particles have much higher adsorption energy and interfacial activity than their homogeneous counterparts. These studies inspire both theoretical and experimental investigation for a comprehensive understanding of the behaviors of Janus particles at fluid interfaces and their uses as solid surfactants for emulsion stabilization.

Although spherical Janus particles represent good model systems, good control over the geometry of Janus particles (e.g. position of Janus boundary) proves to be difficult. In

addition, the techniques to make them in a large quantity are still lacking. Pickering emulsion-templated method developed by Liang *et al.* improves the yields of spherical Janus particles by some extent.[31] This method, however, only offers limited tunability of the Janus boundary which separates the hydrophilic and hydrophobic portions.[32] This will greatly limit the application of Janus particles, especially when using them as solid surfactants for emulsion stabilization where large area of interface is presented thus requiring large amount of Janus particles. In contrast, non-spherical Janus particles, especially, dumbbell Janus particles can be easily synthesized in bulk using seeded emulsion polymerization. This method also allows good tunability on both the geometry and wettability of Janus particles. Therefore, theoretical work on using these non-spherical Janus particles as solid surfactant is imperative.

Furthermore, there has been a great interest in stimuli-responsive surfactants which allows the generation of smart emulsions. Studies on stimuli-responsive polymer surfactants have shown that the configuration or amphiphilicity of these polymer surfactants can be tuned by external stimuli allowing either destabilization or phase inversion to occur. These interesting behaviors of stimuli-responsive polymer surfactants inspires us to design synthesis scheme for making stimuli-responsive Janus particles which will allow us to explore the relationship between the geometry of Janus particles and their behaviors as solid surfactants.

1.2.2 Objectives

The main objective of this thesis is to explore answers both theoretically and experimentally to the following questions:

(1) Are Janus particles "better" solid surfactants than homogeneous particles?

(2) How can stimuli-responsive Janus particles be synthesized in large volume?

(3) How does the geometry of Janus particles influence their behavior as solid surfactants?

1.3 Thesis Outline

Chapter 2 answers the question whether Janus particles are better solid surfactant than homogeneous particles by considering the thermodynamics of emulsion stabilized by Janus dumbbells particles. It will be shown that, different from homogeneous particle-stabilized Pickering emulsion which are only kinetically stable, the use of Janus dumbbells as emulsion stabilizers leads to the formation of thermodynamically stable emulsions. Several other aspects are investigated including preferred droplet size and effect of particle geometry on the droplet size.

Chapter 3 presents a novel synthesis scheme for making uniform, amphiphilic and pH-responsive Janus particle in a large quantity. This synthesis method is based on seeded

emulsion polymerization and makes use of both polymer physics and chemistry. The tunability of this synthesis is studied. In addition, these Janus particles are used as solid surfactants to stabilize emulsion to investigate their ability to manipulate the properties of emulsions such as emulsion types and interactions in response to external stimuli, which reveals the relationship between the geometry of Janus particles and their behavior as solid surfactants.

Chapter 4 presents a systematically studies of emulsion stabilized by Janus particles synthesized in *Chapter 3* as a function of two parameters: pH and emulsion composition. An interesting finding is the formation of stable multiple emulsions stabilized by these Janus particles. Their triggered release by the change of solution pH again reveals the relationship between the geometry of Janus particles and their property as solid surfactant.

Chapter 5 shows a synthesis scheme for making Janus particles with pure compartments and geometrically anisotropic particles by a modifying the synthesis method introduced in *Chapter 3*. In the new synthesis scheme, the effect of surfactants, monomer and cross-linker is investigated to optimize the final particles.

The dissertation concludes with *Chapter 6*, which gives a brief summary on emulsion stabilization with amphiphilic Janus particles and recommendations for future studies.

Chapter 2. Thermodynamically Stable Emulsions Using Janus Dumbbells as Colloid Surfactants

2.1 Introduction

Emulsions are mixtures of two immiscible fluids that have a wide range of applications from foodstuffs to pharmaceuticals to personal care products and enhanced oil recovery.[1,33] One important property that is critical in the application of emulsions is their stability (e.g., shelf life of emulsion-based products). In general, emulsions stabilized with molecular surfactants tend to undergo destabilization via coalescence and Ostwald ripening.[10]

Pickering emulsions, which are emulsions stabilized using colloidal particles, have shown to possess superior stability compared to surfactant-stabilized emulsions.[8] This extended stability has been attributed to the fact that the desorption energy of a particle with a moderate contact angle from a liquid/liquid interface is typically several orders of magnitude greater than the thermal energy, k_BT. Therefore the adsorption of a particle to a liquid/liquid interface is essentially irreversible.[9] Although emulsions stabilized by homogeneous particles generally have better stability compared to those stabilized with surfactants, they are nevertheless only kinetically stable because the free energy of emulsion formation is positive.[34] The positive free energy of emulsion formation

indicates that Pickering emulsions could eventually undergo destabilization, like traditional emulsions stabilized by surfactants.[22,35,36]

A new class of colloidal particles with amphiphilic properties, also known as Janus particles[17], have shown great promise in the stabilization of emulsions. Janus particles with both hydrophilic and hydrophobic surfaces have shown to be more surface active than homogeneous particles.[21] In particular, theoretical work has shown that the adsorption energy of a Janus sphere to a fluid-fluid interface can be three times as high as that of the maximum adsorption energy of its homogeneous counterpart.[30] Furthermore, emulsions stabilized by Janus particles are reported to be more stable than those stabilized by homogeneous particles, and therefore they are advantageous in applications such as emulsion polymerization and emulsion-based microreactors for biofuel conversion.[20,22,25,28,37] Motivated by these results and other earlier work,[34,38] it was recently demonstrated theoretically that spherical Janus particles can give thermodynamically stable Pickering emulsions.[14]

To date, numerous methods for synthesizing spherical Janus particles have been reported[19,22,39-41]; however, these methods have some limitations. Methods based on the selective deposition of a material on a two-dimensional array of spherical particles on a planar substrate[16,42-44] or those based on microfluidic and electrospinning techniques[45-49] generate particles with high uniformity. However, these methods cannot be reliably used to generate Janus particles in a large quantity. In contrast, methods based on particle clusters[50] or Pickering emulsions[31,51-53] can generate Janus particles in larger quantities;

however, the uniformity of these particles based on these methods is not very high. We believe that these disadvantages significantly limit the application of spherical Janus particles in emulsion stabilization, which inherently presents a large surface area thus requires a large number of particles.

One recent development offers promise in generating Janus particles with high uniformity in a large quantity.[23] The synthesis of dumbbell particles (a.k.a., dimers, snowman particles and dicolloids) using seeded-emulsion polymerization is a well-developed technique both theoretically and experimentally.[54-56] Seeded-emulsion polymerization is ideal in two aspects. First, this method is a truly bulk synthesis technique, which allows large-scale generation of particles (e.g., > grams) and has a high probability of being adapted by industry for a large scale synthesis of Janus particles. Furthermore, it is possible to independently modify the two lobes of dumbbells[57] to impart and, more importantly, tune the amphiphilicity of these particles. Therefore, it is critical to investigate whether Janus dumbbells would function as effective colloid surfactants, and, more specifically, to study the thermodynamic stability of Janus dumbbell-stabilized emulsions and the effect of various particle parameters on the emulsification.

In this chapter, we calculate the free energy of the formation of emulsions stabilized with amphiphilic Janus dumbbells. Our numerical calculations clearly show that thermodynamically stable emulsions can be formed using Janus dumbbells as colloid surfactants. We show that under a given condition, there is an energy minimum that

predicts a preferred area for the oil-water interface that can be achieved when Janus dumbbells are used as emulsion stabilizers; this interfacial area can be used to predict a non-dimensionalized average droplet radius of the emulsion. We also present the effect of dumbbell geometry and emulsion composition on the average droplet size. We believe our work provides guidelines for synthesizing and utilizing Janus dumbbells as colloid surfactants in the stabilization of emulsions for a variety of applications.

2.2 Method

2.2.1 Geometry of Janus dumbbells

The geometry of Janus dumbbells studied in this work is shown in Figure 2.1 (a). A dumbbell particle consists of two partially fused spheres (also called lobes). R_A and R_P are the radii of hydrophobic and hydrophilic lobes, respectively. Symmetric Janus dumbbells have equal radii (R_A=R_P). The centers of these two lobes are separated by a distance d. The aspect ratio of a Janus dumbbell is defined as AR_d=(R_P+R_A+d)/(R_P+R_A). φ_P and φ_A are the angles which define the area of hydrophilic and hydrophobic lobes, respectively, which can be calculated with known R_A, R_P and AR_d. The volume of a single Janus dumbbell is

$$V_d = \frac{\pi R_P^3}{3}\left(2-3\cos\varphi_P+\left(\cos\varphi_P\right)^3\right)+\frac{\pi R_A^3}{3}\left(2-3\cos\varphi_A+\left(\cos\varphi_A\right)^3\right). \quad (2\text{-}1)$$

When the Janus dumbbells are symmetric, *i.e.*, $\cos\varphi_P=\cos\varphi_A=1-AR_d$, we have

$$V_d=\frac{2\pi R_A^3}{3}\left(3\left(AR_d\right)^2-\left(AR_d\right)^3\right). \quad (2\text{-}2)$$

The wettability of the two lobes of a Janus dumbbell is defined by three-phase contact angles through the water phase (inset in Figure 2.1 (a)). We consider the "supplementary wetting condition"; that is, the three phase contact angles of the hydrophilic and hydrophobic lobes are described by $\theta_P=90^\circ-\beta$ and $\theta_A=90^\circ+\beta$. A larger value of β, thus, represents a bigger difference in the wettability of the two lobes and a greater degree of amphiphilicity in the Janus dumbbells.

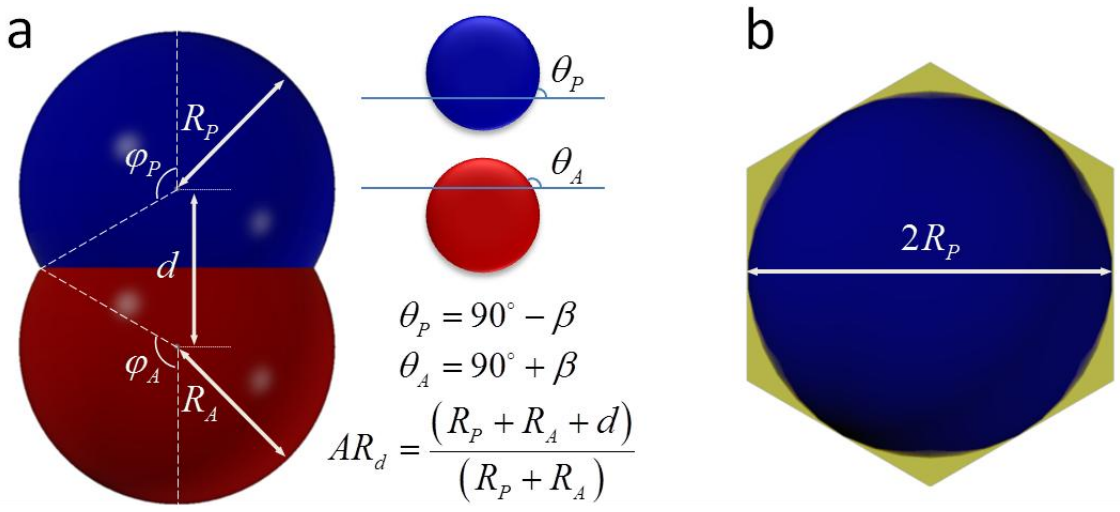

Figure 2.1 (a) Geometry and amphiphilicity of a Janus dumbbell. The blue and red colours represent hydrophilic and hydrophobic surfaces, respectively. (b) Top view of a symmetric Janus dumbbell attached to a hexagonal fluid-fluid interface, which circumscribes a lobe of the dumbbell.

2.2.2 Free energy of emulsion formation

The free energy of Pickering emulsion formation is the sum of free energy of droplet formation:

$$\Delta_{em}G = \sum_i \Delta_d G_i \qquad (2\text{-}3)$$

where i stands for the i^{th} droplet and $\Delta_d G_i$ stands for the free energy for creating the i^{th} droplet. The free energy of droplet formation is

$$\Delta_d G = A_{ow}\gamma_{ow} + n_p\left(\Delta_a G + U_{ele} + U_{vdw} + U_{hyd}\right) \qquad (2\text{-}4)$$

Where n_p is the number of dumbbells attached onto the surface of a single droplet; A_{ow} represents the surface area of a bare, notionally swollen droplet but with no dumbbells attached. γ_{ow} is the interfacial tension. $\Delta_a G$ is the free energy of adsorption of a dumbbell particle to the droplet surface excluding particle interactions. U_{ele}, U_{vdw} and U_{hyd} are energy contribution from electrostatic, van der Waals and hydration forces of attaching a single dumbbell particle to the formation of Janus dumbbell-covered emulsions, respectively. Janus dumbbell-covered emulsions are modeled by first creating notionally swollen droplets, and subsequently adsorbing Janus dumbbells to the droplet surfaces, which reduces the free energy of the system.[14,34]

When particles are adsorbed onto the interface of an emulsion droplet, particles will displace a small portion of the oil phase which leads to the swelling of the droplet as shown in Figure 2.2. A droplet with radius of R_0 becomes R after the adsorption of Janus dumbbells. A notionally swollen droplet can be regarded as a droplet with a cavity as shown in Figure 2.2 (c) such that the droplet has a radius of R but still maintains a volume of oil phase that is equal to the droplet shown in Figure 2.2 (a) and (b). This approach simplifies the calculation of free energy of droplet formation $\Delta_d G = A_{ow}\gamma_{ow} + n_p \Delta_a G$ where $A_{ow} = 4\pi R^2$ because we do not have to consider the adsorption of individual Janus dumbbells one at a time; instead, we can consider the attachment of n_p Janus dumbbells at a time for the calculation of $\Delta_d G$. The extra interface created by the cavity will eventually disappear when particles are adsorbed to the interface therefore there is no need to consider the free energy for creating this interface in the free energy of droplet formation.

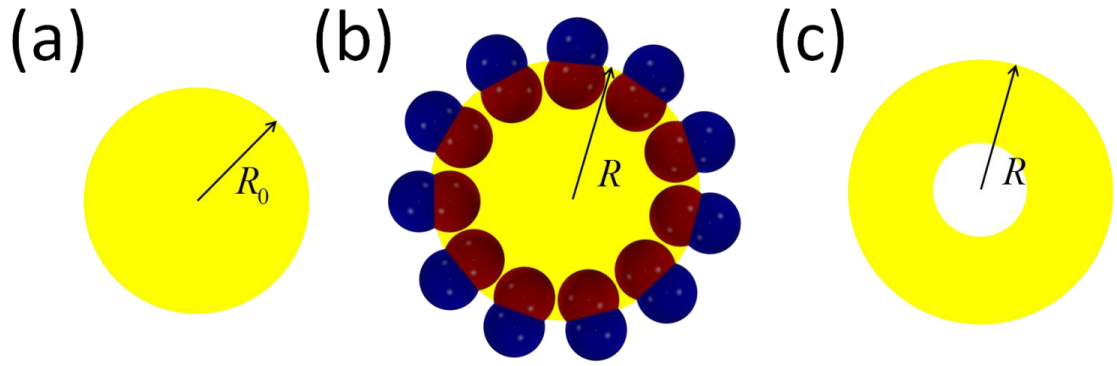

Figure 2.2 (a) A bare oil droplet with a radius of R_0. (b) The droplet in (a) covered with close-packed Janus dumbbells with a slightly larger radius R. (c) Notionally swollen droplet that has a radius of R but has the same volume of oil phase as that in (a) and (b).

To proceed with the calculation, we apply the following conditions:

1. R_A=100 nm, whereas R_P can be larger than 100 nm.

2. The hydrophilic and hydrophobic lobes satisfy the so-called supplementary wetting condition which indicates that the sum of the two contact angles (θ_P and θ_A) is 180°.

3. Amphiphilic dumbbells form a close-packed layer on the droplet interface.[23]

4. Amphiphilic dumbbells are initially dispersed in the aqueous phase.

5. The emulsion consists of oil-in-water droplets with a total volume of 1 m^3 (V_w+V_o=1 m^3).

6. The oil-water interfacial tension (γ_{ow}) is 50 mN/m, similar to *n*-decane/water interfacial tension.[58]

Here we only consider amphiphilic dumbbells with the upright configuration at the oil-water interface.[59,60] In the upright configuration, the long axis of a Janus dumbbell lies perpendicular to the oil-water interface, and the wettability separation line (Janus boundary) lies at the fluid interface. This condition imposes certain constraints on the geometry and wettability (*i.e.*, amphiphilicity β) of amphiphilic dumbbells which we will discuss later. We consider both monodisperse and polydisperse emulsions. We also assume that the Janus boundary does not cause undulation in the fluid interface, thus does not induce lateral capillary attractions between Janus dumbbells.[61-65]

2.3 Results and Discussion

2.3.1 Free energy of emulsion formation

We first consider the situation, in which the radius of droplets is much larger than the size of the amphiphilic dumbbells, *i.e.*, $R \geq 50R_A$ and the dumbbells are symmetric. Under this condition, particles can be assumed to form hexagonally close-packed structure on the droplet surface[14] because of the large radius of curvature of the droplet.[66] Thus the surface area of each droplet can be divided into n_p hexagonal elements. We modify Equation (2-4) so that

$$\frac{\Delta_d G}{n_p} = \frac{A_{ow}}{n_p}\gamma_{ow} + \Delta_a G + U_{ele} + U_{vdw} + U_{hyd} \quad (2\text{-}5)$$

where $A_{ow}/n_p \approx A_{hex}$ and A_{hex} is the area of the hexagonal element as shown in Figure 2.1 (b). The free energy of emulsion formation, therefore, will be negative (*i.e.*, thermodynamically stable emulsion) if the free energy of creating this element is negative. The free energy for creating the hexagonal element can be expressed as

$$\Delta_{hex}^{IN} G = \Delta_{hex} G + U_{ele} + U_{vdw} + U_{hyd} \quad (2\text{-}6)$$

where $\Delta_{hex}^{IN} G = \Delta_d G / n_p$ and $\Delta_{hex} G = A_{hex}\gamma_{ow} + \Delta_a G$. $\Delta_{hex} G$ consists of two parts: creating a hexagonal interface and the adsorption of a Janus dumbbell to this interface. The free energy change due to the adsorption of one Janus dumbbell to the interface from the bulk phase ($\Delta_a G$) is the energy difference between a particle at the interface and a particle in the bulk phase[59] (aqueous phase in this context) and can be expressed as

$$\Delta_a G = \pi R_A^2 \gamma_{ow} \left[A R_d^2 - 2 A R_d \left(1 + \sin\beta\right) \right] + \frac{\gamma_{ow}}{R} V_d \quad (2\text{-}7)$$

for symmetric Janus dumbbells. The last term on the right hand side of Equation (2-7) is due to the pressure difference between inside and outside of the droplet, which becomes negligible when the droplet size is large compared to the particle size.[67] The contribution of particle-particle interactions such as electrostatic repulsion, van der Waals interaction and hydration force to the free energy of emulsion formation will be shown to be negligible.

We compare the magnitudes of potential energies associated with electrostatic interactions, van der Waals interactions and hydration interactions to the free energy of creating a hexagonal element illustrated in Figure 2.1 (b). We incorporate the three interactions mentioned above using the following approach.[14]

The free energy for creating a hexagonal element while considering particle-particle interactions can be expressed as $\Delta_{hex}^{IN}G = \Delta_{hex}G + U_{ele} + U_{vdw} + U_{hyd}$ as described in the main context. Notice that $U_{ele} = 3\Phi_{sph\text{-}sph}$, $U_{vdw} = 3V_{vdw}$ and $U_{hyd} = 3V_{hyd}$ where $\Phi_{sph\text{-}sph}$, V_{vdw} and V_{hyd} are pair potentials for electrostatic, van der Waals and hydration interactions, respectively. The factor 3 comes in because every dumbbell has six nearest neighbours. The free energy for creating the hexagon shown in Figure 2.1 (b) excluding particle-particle interactions is $\Delta_{hex}G = -3.5 \times 10^5\ k_BT$.

2.3.1.1 Electric double layer repulsion

There could be electrostatic double layer repulsion between the two hydrophilic lobes. This can be approximated with the potential energy of electrostatic repulsion between two equal-sized spheres. The formula is $\Phi_{sph\text{-}sph} = (64\pi a n_\infty k_B T \rho^2/\kappa^2)\exp(-\kappa S_0)$ following the Derjaguin approximation, where κ^{-1} is the Debye length and $\kappa^2 = 2z^2e^2n_\infty/\varepsilon\varepsilon_0 k_B T$. $\rho = \tanh(ze\Psi_\delta/4k_BT)$ and Ψ_δ is Stern potential. a is the radius of the sphere. n_∞ is the number density of ions in the bulk solution. S_0 is the shortest distance between these two

spheres. z is the number of charge.[68] For $|z\Psi_\delta|\geq 100$ mV (highly charged), z=1 and S_0=0, $\Phi_{sph\text{-}sph}/k_BT$=1122 with ε_{water}=80 and T=293 K. Each hexagonal element will be connected with six other hexagonal elements thus one dumbbell will have six nearest neighbors. Therefore, if electrostatic interaction is included, every hexagonal element created will result in another $3\Phi_{sph\text{-}sph}$ energy penalty. We see that $3\Phi_{sph\text{-}sph}$=3366 k_BT is much less than 1% of $\Delta_{hex}G$.

The calculation above most likely overestimates the electrostatic repulsion. First, stern potential larger than 100 mV is not very common. Usually, a smaller potential is expected. For example, Levine *et al*. estimated the double layer interaction between silica particles of 0.286 μm in radius that are close to each other using the surface potential of 25 mV and 50 mV. The estimated values of $\Phi_{sph\text{-}sph}$ for these particles were 65.5 k_BT and 300 k_BT, respectively.[69] Moreover, in the case of dumbbells, the polar lobes are not completely spherical, thus the electrostatic potential is expected to be smaller than the spherical case.

To consider the electrostatic interaction beyond the nearest neighbours, we need to consider the Debye length κ^{-1} which can be calculated using $\kappa^2 = 2z^2e^2N_{AV}C_\infty/\varepsilon\varepsilon_0k_BT$ where N_{AV} is the Avogadro's number and C_∞ is the concentration of ions in bulk solution. Assuming $C_\infty=10^{-4}$ M, Debye length in this case is $\kappa^{-1}\approx 30$ nm, which is much smaller than the radius of dumbbell lobes (R_A=100 nm). Therefore, electrostatic double layer interactions beyond the nearest neighbors can be ignored.

2.3.1.2 Van der Waals interaction

Following the idea of Levine et al.[70], the potential energy due to Van der Waals interaction can be approximated by the sum of two terms: attractive interactions between two spherical particles in the aqueous phase and oil phases, respectively. Thus the pair potential for van der Waals interaction is $V_{vdw}=-(A_{pwp}a/12S_0+A_{pdp}a/12S_0)$ where A_{pwp} is the Hamaker constant for two polystyrene surfaces in water, and A_{pdp} is the Hamaker constant for two polystyrene surfaces in decane. S_0 is the nearest separation between two surfaces. We estimate A_{pdp} using $A_{pdp}=[A_d^{1/2}-A_p^{1/2}]^2$ (where $A_d=3.97\times10^{-20}$ J (decane) and and $A_p=6.5\times10^{-20}$ J.[5]). The two Hamaker constants are found to be $A_{pwp}=1.4\times10^{-20}$ J and $A_{pdp}=0.31\times10^{-20}$ J. If we use $S_0=0.1$ nm, $3V_{vdw}=-352\ k_BT$ which is negligible compared to $\Delta_{hex}G=-3.5\times10^5\ k_BT$.

2.3.1.3 Hydration force

When two hydrophilic surfaces are very close to each other (distance in a few nm range), there will be a strong repulsive hydration force that decays exponentially.[71] The hydration potential energy is expressed as $V_{hyd}=\pi rP_o\lambda^2\exp(-D/\lambda)$ where λ is a decay length, P_o is the hydration force constant and D is the closest separation of particle surfaces. Using

λ=0.6 nm and P_o=3×10^6 Nm^{-2},[72] which are reasonable estimates for particles with β=40 °, $3V_{hyd}$=251 k_BT (D=0 and r=100 nm) which is negligible compared to $\Delta_{hex}G$=-3.5×10^5 k_BT.

Therefore, $\Delta_{hex}^{IN}G \approx \Delta_{hex}G$ which simplifies the calculation of Equation (2-4) such that

$$\Delta_d G = A_{ow}\gamma_{ow} + n_p \Delta_a G \qquad (2\text{-}8)$$

We can further normalize $\Delta_{hex}G$ by the area of the hexagon as

$$\Delta_{hex}G / A_{hex} = \gamma_{ow}\left\{1 + \frac{\pi}{2\sqrt{3}}\left[AR_d^2 - 2AR_d\left(1+\sin\beta\right)\right]\right\} \qquad (2\text{-}9)$$

to obtain the free energy of creating a unit area of the hexagonal element.

This calculation demonstrates that Janus dumbbells can lead to the formation of thermodynamically stable emulsions. Figure 2.3 shows the free energy as a function of the aspect ratio and the amphiphilicity of Janus dumbbells. The free energy of emulsion formation is indeed negative and become more negative as the amphiphilicity increases. More interestingly, the free energy also decreases as the aspect ratio increases despite the fact that the displaced area at the oil-water interface by a dumbbell decreases as the aspect ratio is increased (*i.e.*, the cross-section area of the neck of a dumbbell decreases). This trend can be explained by the fact that for Janus dumbbells in the upright configuration, their tendency for preferential wetting (*i.e.*, aqueous phase wets the hydrophilic lobes and oil phase wets the hydrophobic lobes) outweighs their tendency to maximize the displaced interface at the oil-water interface.[59] Although our calculations

are performed for oil-in-water emulsions, the same conclusions can be drawn for water-in-oil emulsions. We also believe that these particles can form thermodynamically stable foams if Janus dumbbells with proper geometry and surface wettability are used.

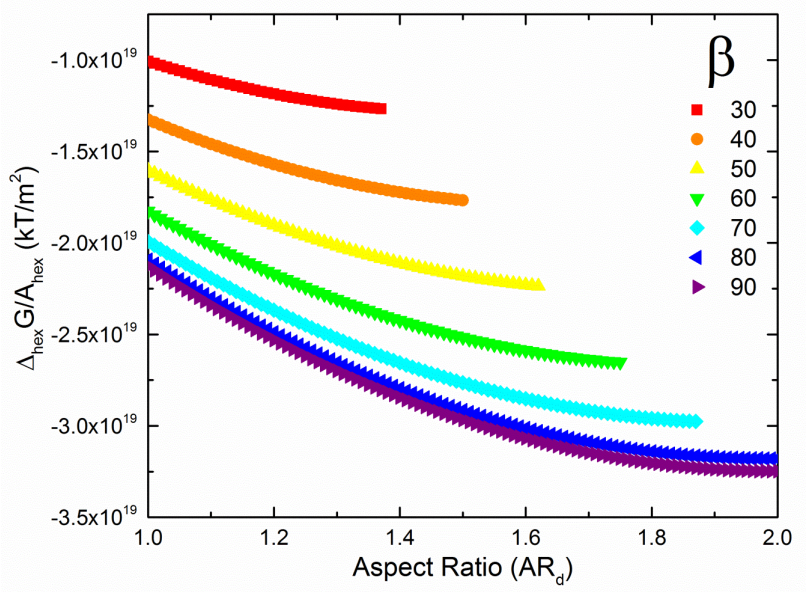

Figure 2.3 Free energy of creating a unit area of a hexagonal element in Figure 2.1 (b) with a symmetric dumbbell as a function of the aspect ratio and amphiphilicity of Janus dumbbells.

To demonstrate the thermodynamic stability of Janus dumbbell-stabilized emulsions in a more direct fashion, we calculate the free energy of emulsion formation for a specific system that has the equal volumes (0.5 m^3) of the aqueous and the oil phases. We consider an emulsion that consists of monodisperse oil droplets whose radii are 10 μm when no dumbbell is adsorbed at droplet surface[73] and adjust the number of Janus dumbbells available in the system to ensure that the droplet interface is fully covered.

Because the emulsion consists of monodisperse droplets, Equation (2-3) becomes

$$\Delta_{em}G = n_d\Delta_d G = n_d\left(A_{ow}\gamma_{ow} + n_p\Delta_a G\right) \quad (2\text{-}10)$$

where n_d is the total number of droplets in the emulsion. As shown in Figure 2.4, the free energy of emulsion formation in most part of the plot is negative, indicating that these emulsions are thermodynamically stable. The free energy of emulsion formation becomes more negative as the aspect ratio and the degree of amphiphilicity increase. The free energy is positive only when the degree of the amphiphilicity of dumbbells is very small ($\beta \leq 2°$). Notice that Janus dumbbells with AR_d=1 and β=0 correspond to homogeneous spherical particles with a three-phase contact angle of 90°. Free energy data is omitted for Janus dumbbells that do not have the upright configuration.[59]

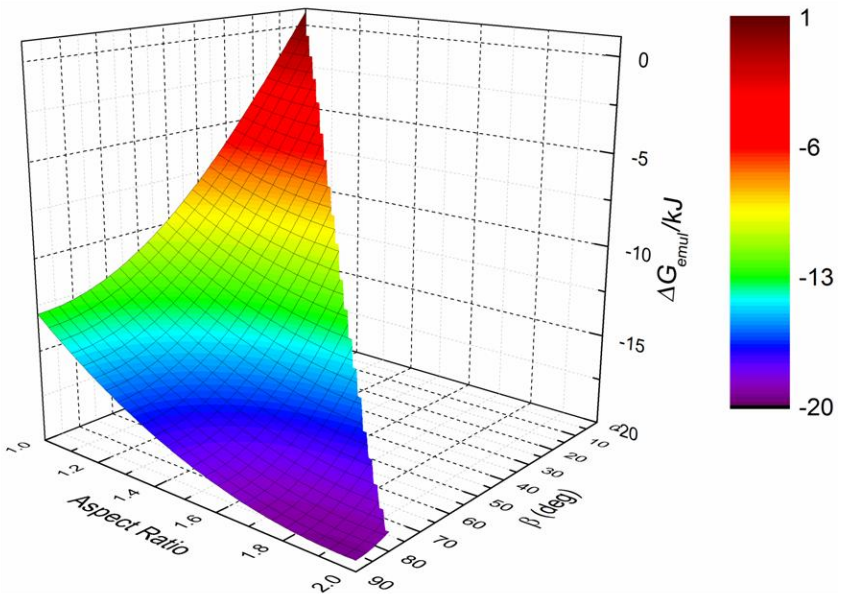

Figure 2.4 Free energy of emulsion formation as a function of the amphiphilicity and the aspect ratio of Janus dumbbells. The emulsions modeled in this calculation consist of oil droplets of a radius of 10 μm and have a 0.5 m^3 aqueous phase and a 0.5 m^3 oil phase.

2.3.2 Preferred area of interface

To test whether an emulsion system prefers a particular droplet size under a given condition, we calculate the free energy of emulsion formation using Equation (2-10) as a function of droplet radius provided that we have a sufficient supply of dumbbells in the system (*i.e.*, the system has enough particles to cover the surface of emulsion droplets with a close-packed layer). Thermodynamic equilibrium would be reached if a global minimum in the free energy of emulsion formation as a function of droplet radius is observed. To test this idea, we assume a particular condition; the emulsion consists of a

0.2 m^3 oil phase and a 0.8 m^3 aqueous phase with monodisperse droplets, and Janus dumbbells in the system are symmetric and have an aspect ratio of 1.5. In addition, the dumbbells are assumed to have the highest degree of amphiphilicity, *i.e.*, β=90 º, which ensures that the Janus dumbbells maintain their upright configuration even if the radius of droplet becomes comparable to that of the dumbbell.[59] Theoretical work has shown that Janus boundary detaches from the oil-water interface when the droplet radius becomes comparable to the size of a Janus particle.[67] If the Janus boundary detaches from the oil-water interface, such a Janus dumbbell can adopt a tilted configuration, complicating the determination of the free energy of emulsion formation. For $R<50R_A$, the assumption of hexagonal close-packing is no longer a valid approximation; thus, densest packings of Janus dumbbells with icosahedral symmetry are used.[74]

As shown in Figure 2.5, the free energy of emulsion formation keeps decreasing until the droplet radius is around 400 nm, at which point the free energy reaches a minimum. The existence of a free energy minimum can be explained by considering the following equation:

$$\Delta_{em}G = n_d n_p \left(\frac{A_{ow}}{n_p} \gamma_{ow} + \Delta_a G \right). \quad (2\text{-}11)$$

As can be seen in Equation (2-11), the total number of Janus dumbbells ($n_d n_p$) needed to cover the droplet surface increases as the droplet radius decreases. However, as droplet radius decreases, the fraction of displaced surface area at the interface of droplets by

Janus dumbbells decreases as a result of deviation from hexagonal close-packing, which makes $((A_{ow}/n_p)\gamma_{ow}+\Delta_a G)$ less negative. Therefore, the total free energy eventually increases as the droplet radius decreases beyond a critical value (the equilibrium radius). This result indicates that, theoretically, there exists a thermodynamic equilibrium droplet radius for this particular condition; however, the volume fraction of dumbbells required to cover the entire oil-water interface for this equilibrium radius is around 60 vol%, which is challenging and impractical to achieve experimentally. If the volume fraction of oil phase becomes too large, then it may not be possible to reach the equilibrium diameter because of the lack of particles in the aqueous phase (*e.g.*, an emulsion of 35 vol% oil phase requires > 100 vol% particle in the aqueous phase to completely cover the emulsion surface). As long as enough Janus dumbbells can be suspended in the water phase to completely cover the emulsion droplet surface, the size of the equilibrium droplet, thus the number of particles on the droplet surface, remains constant; that is, $\Delta_d G/v_{drop}$ (where v_{drop} = volume of a droplet) is minimum at $R = R_{eq}$ regardless of emulsion composition.

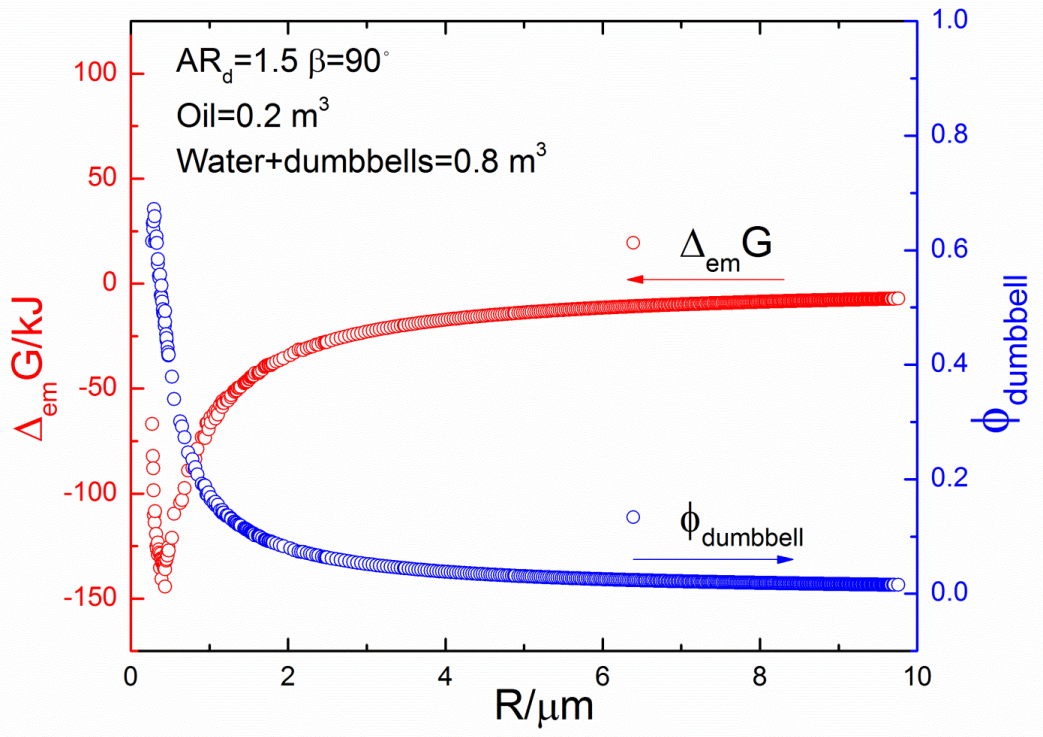

Figure 2.5 Free energy of emulsion formation (red) and the corresponding volume fraction of dumbbells in the aqueous phase needed to form a close-packed layer on the droplet surface (blue) as a function of droplet radius. The Janus dumbbells have an aspect ratio of 1.5 with a high amphiphilicity of β=90°. The emulsion consists of a mixture of a 0.2 m^3 oil phase and a 0.8 m^3 aqueous phase.

To consider more typical emulsification processes, we fix the volume fraction of dumbbells to be 2 vol% of the aqueous phase. In this calculation, Janus dumbbells have an aspect ratio of 1.5 and β=40°, and emulsions are generated from a mixture of 0.2 m^3 oil and 0.8 m^3 aqueous phases with monodisperse droplets. It can be inferred from Figure 2.5 that the volume fraction of dumbbells needed to form close-packed layer at the droplet interface increases as the droplet radius decreases. Thus, for a constant volume fraction of dumbbells in a constant volume of water, the range of droplet radius within which dumbbells can form a close-packed monolayer has a lower limit. When the amount

of dumbbells is enough to form a close-packed monolayer on the surface of emulsion droplets, the free energy of emulsion formation continues to decrease with the droplet radius because the adsorption of every Janus dumbbell increases the number of hexagons (shown in Figure 2.1 b) on the droplet surface. The addition of each hexagon to the droplet surface reduces the free energy of the system until all of the Janus dumbbells are consumed to cover droplet surface as shown by the blue circles in Figure 2.6. Once there are no more Janus dumbbells available in the aqueous phase, a further decrease in the droplet radius leads to an increase in the free energy (red squares in Figure 2.6). The increase in the free energy is due to non-close packing of Janus dumbbells on the interface, thus the exposure of bare oil-water interface. In other words, with a limited number of Janus dumbbells, there is a total oil-water interfacial area (S_{pf}) for a specific system that results in the lowest energy state, which can be achieved when all of the available Janus dumbbells attach to the droplet as a close-packed monolayer to minimize the free energy of the system. We note that emulsions with non-close packed dumbbell monolayer are nevertheless thermodynamically stable as long as the number of interface-adsorbed dumbbells is high enough to over-compensate the energy of bare oil-water interface formation. Based on Figure 2.6, the droplet radius with minimum free energy is large enough to apply the hexagonal close packing approximation ($R \geq 50R_A$). The total oil-water interfacial energy that results in the lowest energy state thus can be approximated with the number of Janus dumbbells in the system such that

$$S_{pf} = \left(\frac{V_w \phi_{ds}}{V_d} \right) A_{hex} \quad (2\text{-}12)$$

where ϕ_{ds} is the volume fraction of dumbbells in the aqueous phase. The term in the brackets in Equation (2-12) is essentially the number of Janus dumbbells in the system. Although the conclusion of total interfacial area that results in the lowest energy state is obtained under the assumption of a monodisperse emulsion, it also extends to polydisperse emulsions because the total number of Janus dumbbells remains constant.

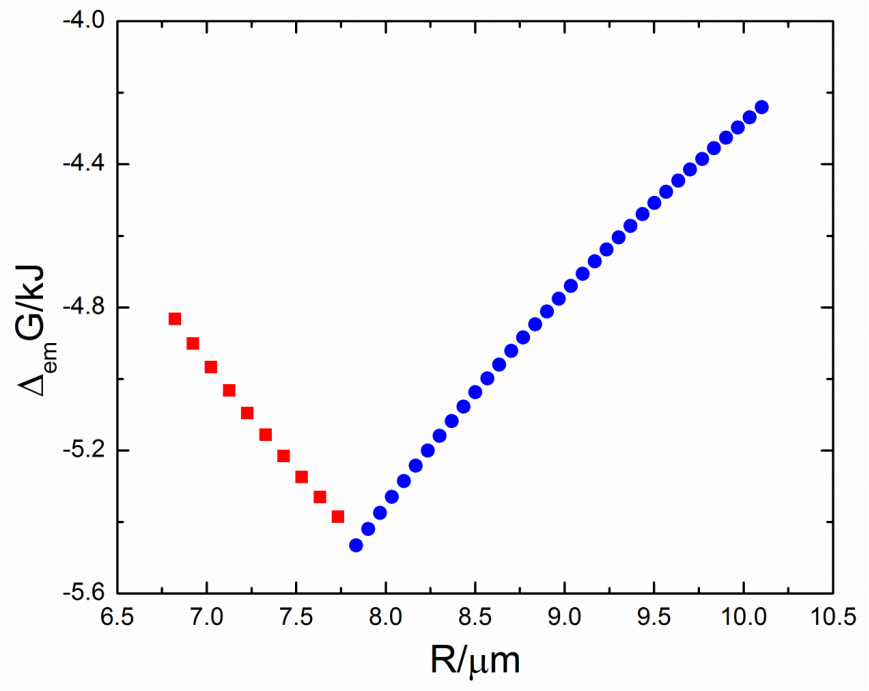

Figure 2.6 Free energy of emulsion formation as a function of droplet radius. Close packed and non-close packed states are represented by blue circles and red squares, respectively. The volume fraction of dumbbell is fixed at 2 vol%. Janus dumbbells have an aspect ratio of 1.5 and β=40 º. The emulsion consists of a 0.2 m^3 oil phase and a 0.8 m^3 aqueous phase.

The existence of preferred total interfacial area is reminiscent of an often-observed phenomenon called "limited coalescence" in Pickering emulsions. In limited coalescence, if the total amount of particles in an emulsion is initially insufficient to fully cover the oil-water interfaces, the emulsion droplets coalesce such that the total interfacial area between oil and water is progressively reduced until the particle layer at interface is dense enough to prevent further coalescence.[75] One major difference, of course, is that Janus dumbbells generate thermodynamically stable emulsions, whereas Pickering emulsions stabilized with homogeneous particles lead to kinetically stable emulsions.

2.3.3 Surface weighted average droplet radius for polydisperse emulsion

Emulsions generated using various bulk emulsification methods are polydisperse. Numerous studies have shown that the size distribution of many emulsions, especially Pickering emulsions, formed via conventional processes follow log-normal distribution.[75-78] Thus we assume that Pickering emulsions generated with Janus dumbbells obey log-normal distribution such that the distribution of the surface area density of droplets $S(R)$ has the following relation with the droplet radius R

$$S(R) = \frac{1}{\sigma\sqrt{2\pi}R} e^{-(\ln R - M)^2/2\sigma^2} \quad (2\text{-}13),$$

where M and σ are the mean and standard deviation of the variable's natural logarithm. R ranges from zero to infinity and, $S(R)dR$ represents the fraction of interface taken by

droplets with radius between R and $R+dR$. Using this distribution, we can convert S_{pf} into a more practical quantity: surface weighted average droplet radius $\overline{R}_{surf}$, which is also known as the Sauter mean radius $\overline{R}_{32}$ [79]. The average droplet radius $\overline{R}_{surf}$ is the first moment of $S(R)$, therefore

$$\overline{R}_{surf} = \int_0^\infty S(R) R dR = e^{M+\sigma^2/2} \quad \text{(2-14)}.$$

To calculate $\overline{R}_{surf}$, we set up an equation with volume balance of oil phase as

$$\int_0^\infty \frac{S_{pf} S(R) R dR}{3} - \frac{V_w \phi_{ds}}{2} = V_o \quad \text{(2-15)}.$$

The first term on the left hand side of Equation (2-15) is the total volume of droplets which consists of both oil and Janus dumbbells because every Janus dumbbell has one of its two lobes submerged in the droplets. The second term represents half of the total volume of dumbbells. By combining Equation (2-14) and (2-15), we obtain

$$e^{M+\sigma^2/2} = \frac{3}{S_{pf}} \left(V_o + \frac{V_w \phi_{ds}}{2} \right) \quad \text{(2-16)}.$$

Thus, the average radius of a polydisperse emulsion can be expressed as

$$\overline{R}_{surf} = \frac{3V_d}{V_w \phi_{ds} A_{hex}} \left(V_o + \frac{V_w \phi_{ds}}{2} \right) \quad \text{(2-17)}.$$

For symmetric Janus dumbbells, with Equation (2-2) and $A_{hex} = 2\sqrt{3}R_A^2$ we can non-

dimensionalize Equation (2-17) as

$$\mathbb{R}=\frac{\overline{R}_{surf}}{R_A}=\frac{\pi}{\sqrt{3}}\left(3\left(AR_d\right)^2-\left(AR_d\right)^3\right)\left(\frac{V_o}{V_w}\frac{1}{\phi_{ds}}+\frac{1}{2}\right) \quad (2\text{-}18).$$

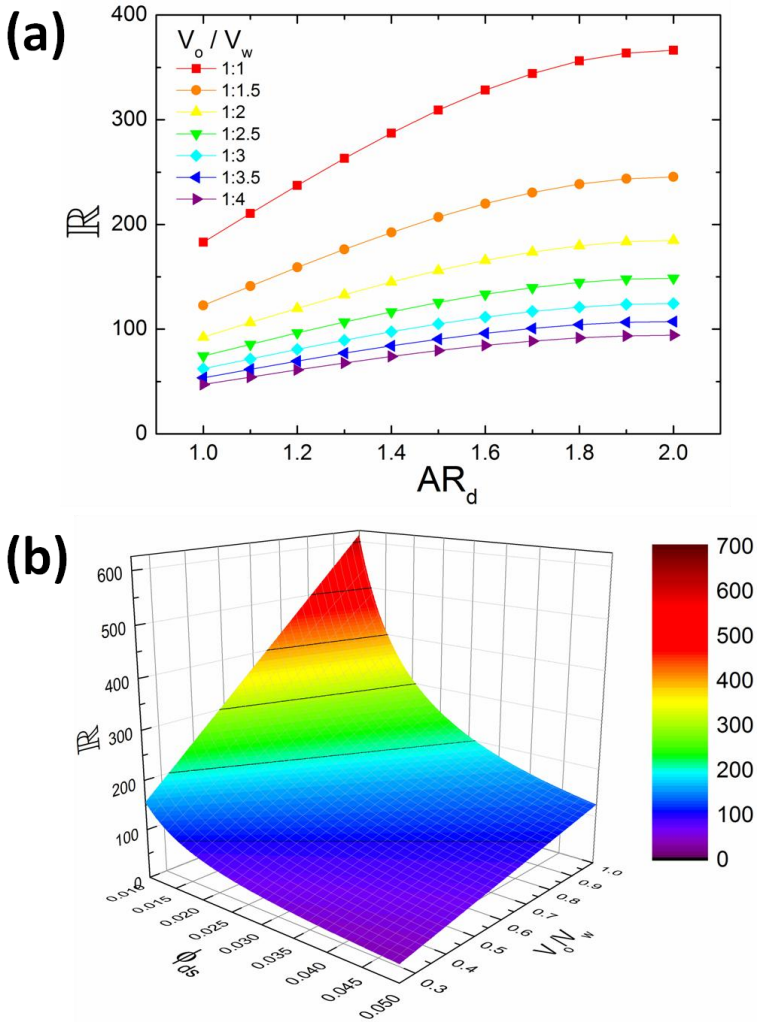

Figure 2.7 (a) Non-dimensionalized average droplet radius as a function of the dumbbell aspect ratio and volume ratio between oil and aqueous phases. The volume fraction of Janus dumbbell is 2 vol% of the aqueous phase. (b) Non-dimensionalized average droplet radius as a function of the volume fraction of Janus dumbbells and volume ratio between oil and aqueous phases. The Janus dumbbells have an aspect ratio of 1.5.

Using the approach described above, we determine the non-dimensionalized average droplet radius $\mathbb{R}$ based on the properties of Janus dumbbells and the composition of the fluids. Figure 2.7 (a) shows $\mathbb{R}$ as a function of the aspect ratio of Janus dumbbells (AR_d) as well as the volume ratio between the oil and aqueous phases (V_o/V_w). First, we notice that, for a fixed aspect ratio, the droplet radius increases with the volume ratio between oil and aqueous phases. This trend is because larger oil droplets have smaller specific surface area thus need fewer particles to form close-packed monolayer per unit volume of oil phase compared with smaller droplets. For a given volume ratio, the droplet radius also increases with the aspect ratio of Janus dumbbells. This increase is due to an increase in the volume of a single dumbbell with aspect ratio and in turn a decrease in the number of Janus dumbbells in the system.

In Pickering emulsification, two parameters that are readily tuned to change the emulsion properties are the volume fraction of the particles and the volume ratio between the oil and aqueous phases. To test how these two parameters change the droplet size, we determine $\mathbb{R}$ as a function of the volume fraction of Janus dumbbells (ϕ_{ds}) and the volume ratio between oil and aqueous phases (V_o/V_w) when the aspect ratio is fixed at 1.5. As shown in Figure 2.7 (b), $\mathbb{R}$ increases with the volume ratio between oil and aqueous phases because of the smaller specific surface area associated with larger droplets as discussed above. $\mathbb{R}$ also increases as the volume fraction of Janus dumbbells decreases because, for a fixed volume ratio, the number of dumbbells in the aqueous phase decreases with decreasing volume fraction of Janus dumbbells. Notice that in these more

practical cases, the non-dimensionalized average droplet radius $\mathbb{R}$ satisfies $\overline{R}_{surf} > 50R_A$, *i.e.*, $\mathbb{R} > 50$, indicating both hexagonal close-packing and Equation (2-12) are reasonable approximations.

2.3.4 Effect of asymmetry

The unique feature of Janus dumbbells is that the geometry, in addition to chemistry, of the particles can be precisely controlled.[23,55,56] In fact, the control of the geometry is expected to provide a unique means to change the packing of particles at the oil-water interface, affecting the emulsification process. We, therefore, investigate how the asymmetry of Janus dumbbells would affect the average droplet radius. The asymmetry is define as $\alpha = R_P/R_A$. We change the ratio of the hydrophilic to hydrophobic lobe radii while keeping the volume fraction of particles, the neck size of dumbbells and the volume ratio between oil and aqueous phases constant. The neck area of dumbbells is kept the same as that of symmetric dumbbells with an aspect ratio of 1.5 (*i.e.*, $3\pi R_A^2/4$). We use this condition because by fixing the neck area, we can exclusively examine the effect of asymmetry on the average droplet radius. We note that highly asymmetric Janus dumbbells are not considered here because those particles have been shown to adopt tilted orientations at equilibrium.[60]

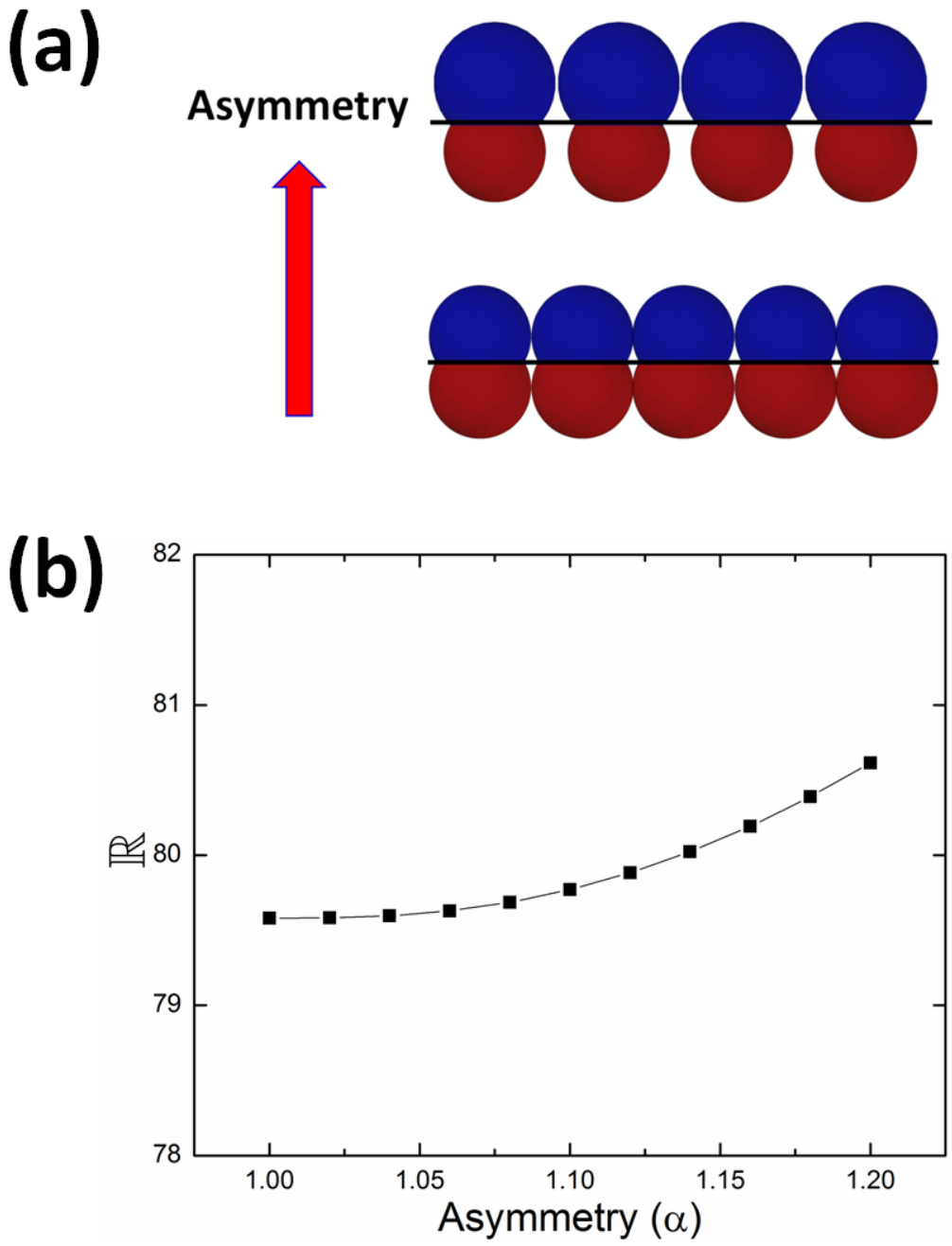

Figure 2.8 (a) Schematic illustration of the effect of increasing asymmetry of Janus dumbbells on their packing at the oil-water interface and (b) non-dimensionalized average droplet radius as a function of the ratio between radii of hydrophilic and hydrophobic lobes. Parameters used for this calculation are V_o/V_w=1/4 and ϕ_{ds}=2%.

As the particle asymmetry increases, hydrophilic lobes instead of hydrophobic lobes come in contact with each other as shown in Figure 2.8 (a) thus the preferred area of interface is determined as

$$S_{pf} = \left(\frac{V_w \phi_{ds}}{V_d} \right) \left(2\sqrt{3} R_P^2 \right) \quad \text{(2-19)}.$$

Following the same argument for symmetric Janus dumbbells, we obtain non-dimensionalized average droplet radius as

$$\mathbb{R} = \frac{\overline{R}_{surf}}{R_A} = \frac{\pi}{2\sqrt{3}\alpha^2} \left[\alpha^3 \left(2 - 3\cos\varphi_P + \left(\cos\varphi_P \right)^3 \right) + \frac{27}{8} \right] \left(\frac{V_o}{V_w} \frac{1}{\phi_{ds}} + \frac{1}{2} \right) \quad \text{(2-20)}$$

where $\cos\varphi_P = -(1 - 3/4\alpha^2)^{1/2}$. We use ϕ_{ds}=2% and V_o/V_w=1/4 for calculations.[80] The non-dimensionalized average droplet radius increases slightly with the asymmetry of Janus dumbbells, as shown in Figure 2.8 (b), which may seem unexpected because we expect fewer particles would be required to cover the same interfacial area when the asymmetry of dumbbells is increased. Fewer particles on the surface of each droplet would be expected to, in turn, result in a smaller average droplet radius. This somewhat counterintuitive increase in the average droplet size, however, is due to the reduction in the number of Janus dumbbells. It turns out that increasing hydrophilic lobes also increases the volume of each Janus dumbbell, which in turn decreases the number of Janus dumbbells in the system for a given particle volume fraction (ϕ_{ds}).

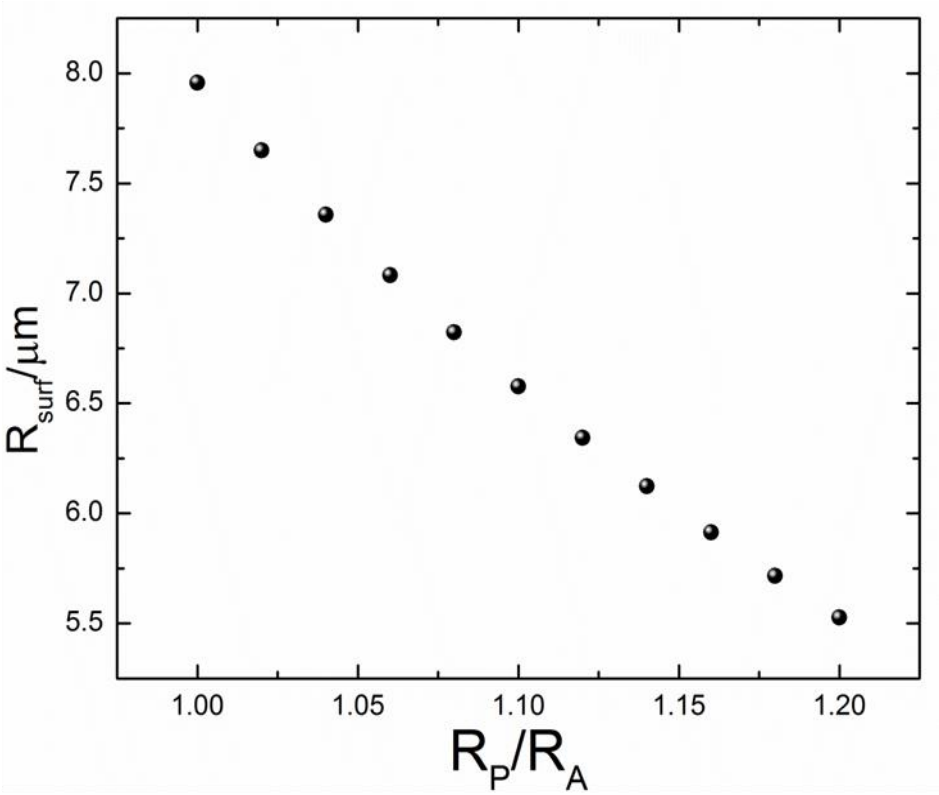

Figure 2.9 Effect of asymmetry of Janus dumbbells on the average droplet radius when the number of Janus dumbbells in the system (N_d) remains constant. The value of N_d is the same as the total number of symmetric Janus dumbbells with the aspect ratio of 1.5 in a system consisting of a 0.8 m^3 aqueous phase, 2 vol% of which is Janus dumbbells.

We perform a thought experiment in which we keep the number of Janus dumbbells in the system constant while changing the asymmetry of the dumbbell. The preferred area of interface in this case is

$$S_{pf} = N_d \left(2\sqrt{3}R_P^2\right) \quad (2\text{-}21)$$

where N_d is the total number of Janus dumbbells in the system. Here the value of N_d is the same as the total number of symmetric Janus dumbbells with the aspect ratio of 1.5 in a

system consisting of a 0.8 m^3 aqueous phase, 2 vol% of which is Janus dumbbells. The geometry of Janus dumbbells has a significant influence on the average droplet radius as shown in Figure 2.9.[81] In contrast to Figure 2.8 (b), the radius of droplets decreases as the asymmetry increases. Remarkably, even a small asymmetry in the shape of dumbbells ($R_P/R_A \geq 1.02$) leads to an appreciable decrease in the size of emulsion droplets. These results clearly illustrate that it is critical to carefully consider the concentration of particles as well as the geometry of Janus dumbbells in predicting the average droplet size of the resulting Picking emulsions.

2.4 Conclusions

We show that the use of Janus dumbbells as emulsion stabilizers leads to the formation of thermodynamically stable emulsions. For a given volume fraction of Janus dumbbells in the mixture system of a given composition, there exists thermodynamically preferred interfacial area, which can be achieved when all of the Janus dumbbells in the system are adsorbed to the droplet interface and form close-packed monolayers. Based on this result, the non-dimensionalized average droplet radius as a function of the geometry and the volume fraction of dumbbells and the emulsion compositions are predicted. Furthermore, we examine the effect of asymmetry of dumbbells and show that increasing the asymmetry of dumbbells increase the average droplet radius when the volume fraction of Janus dumbbells is fixed, whereas the average droplet radius decreases when the number

of Janus dumbbells is kept constant. We believe that our theoretical results will provide critical insights into the design and application of Janus dumbbells as colloid surfactants to generate thermodynamically stable Pickering emulsion.

Chapter 3. Shape-Changing and Amphiphilicity-Reversing Janus Particles with pH-Responsive Surfactant Properties

3.1 Introduction

Janus particles are biphasic colloids that have two sides with contrasting properties.[17,19,41,82] One of the most promising and practical applications of these Janus particles is in the stabilization of multiphasic mixtures such as emulsions.[23,25,26,37,50,83-85] Theoretical and experimental studies have shown that Janus particles offer advantages over their homogeneous counterparts as solid surfactants. The adsorption energy of a spherical Janus particle to an oil-water interface, for example, can be as large as three times that of its homogenous counterpart.[30] Such a result indicates that Janus particles have a very strong tendency to segregate to and remain at fluid interfaces. More recently, theoretical studies based on free energy calculations have shown that thermodynamically stable emulsions can be generated using Janus particles as solid surfactants.[14,86] In contrast, most Pickering emulsions generated with homogenous particles, except a few notable exceptions[87], are only kinetically stable. The thermodynamic stability of particle-stabilized emulsions can be understood by determining the free energy change during emulsification. While the free energy change is positive for emulsions stabilized with

homogenous particles[88], it can become negative for emulsions stabilized with Janus particles due to their large detachment energy from fluid interface.[14,86] Experimentally, it has been reported that a Janus particle-laden interface has a significantly smaller interfacial tension than a liquid-liquid interface with homogeneous particles, which indicates that Janus particles have much higher surface activity.[89-92] In addition, some emulsions that cannot be easily stabilized by homogenous particles exhibit excellent stability when Janus particles are used as emulsifiers.[22] Taking advantage of such excellent surfactant properties of Janus particles, recent studies have shown that Janus particle-stabilized emulsions can be used as microreactors for biofuel upgrade reactions and the subsequent separation of the reaction products.[93,94]

An emerging idea in this area is that the shape of Janus particles, in addition to their amphiphilicity, has a significant influence on their behavior and functionality as surface active agents.[63] Such a concept is inspired by the fundamental parameters that govern the behavior and properties of molecular amphiphiles: shape, characterized by the so-called packing parameter, and amphiphilicity, quantified in terms of hydrophile-lipophile balance (HLB).[5] The type of emulsions that can be stabilized by a particular molecular amphiphile, for example, can be accurately predicted by analyzing its packing parameter and HLB number.[5] Recent reports provide ample evidence that the behavior and properties of Janus particles as solid surfactants indeed depend on the shape as well as the chemistry of Janus particles. Both theoretical and experimental studies, for example, have shown that shape anisotropy is a critical factor that determines the configuration of Janus

particles as well as interparticle interactions at fluid interfaces.[59,60,95,96] The adsorption kinetics and packing behavior of non-spherical Janus particles also have been found to depend strongly on the particle shape.[97]

One intriguing class of molecular surfactants that exhibit behaviors that have both fundamental and practical significance is stimuli-responsive amphiphiles. These molecules change their shape and amphiphilicity in response to external stimuli such as temperature, pH and light, which in turn change their properties and functionality as surfactants.[98,99] A diblock copolymer composed of a hydrophobic block and a pH-sensitive hydrophilic block, for example, assembles into a variety of different aggregate structures depending on the pH of the solution.[100-102] Another study has shown that the type of emulsions (*i.e.*, oil-in-water vs. water-in-oil) generated with a hydrophobically modified pH-sensitive polymer as the stabilizer depends on the pH of the aqueous phase.[103] A recent study has even shown that the generation and phase inversion of multiple emulsions is possible using single pH-sensitive amphiphilic copolymer surfactant.[104] The changes in the shape and HLB of these amphiphilic molecules in response to changes in the solution pH are responsible for these observed phenomena. Despite many interesting and important examples of stimuli-responsive molecular surfactants, only a few examples have been reported on the application of stimuli-responsive Janus particles as solid surfactants. Janus particles described in these previous studies[105-107] have somewhat limited ranges of amphiphilicity- and shape-tunability and thus cannot be used for inducing phase inversion of emulsions or for stabilizing different

types of emulsions as have been demonstrated by stimuli-responsive molecular surfactants.

In this chapter, we present the synthesis of pH-responsive Janus particles that can completely switch their amphiphilicity due to drastic changes in their shape and chemistry. The surfactant properties of these Janus particles can be drastically altered to enable stabilization of different types of emulsions and induce phase inversion of emulsions. Our synthesis method utilizes seeded emulsion polymerization, thus enables the generation of a large amount of highly uniform particles.[24,39,40,55,108-112] The pH-responsiveness of these Janus particles can be tailored by changing the composition of the particles generated via the seeded emulsion polymerization. We demonstrate the type of emulsions that are stabilized by these amphiphilicity-reversing and shape-changing Janus particles depends on the solution pH and that these emulsions undergo phase inversion in response to changes in the pH of the aqueous phase. We also demonstrate that the interaction between emulsion droplets stabilized by these particles can be controlled by changing the pH of the continuous phase. Our results present a new class of colloidal materials that will further widen the functionality and properties of Janus particles as dynamically tunable solid surfactants.

3.2 Experimental Section

3.2.1 Synthesis of amphiphilic Janus particles

Amphiphilic Janus particles are synthesized by seeded emulsion polymerization followed by acid hydrolysis. The monodisperse seed particles composed of linear polystyrene (LPS) are synthesized by dispersion polymerization. First, 0.03 gram polyvinylpyrrolidone (PVP, Mw ~ 55,000) is dissolved in 75 ml isopropyl alcohol (IPA, 99.9%) in a 100 ml flask. Then 9 ml deionized (DI) water containing 0.02 gram ammonium persulfate (APS, 98%) as initiator is added to the flask followed by adding 6.6 ml styrene (≥99%). After the flask is sealed with a rubber stopper and Teflon® tape, the mixture is well mixed by shaking the flask for 60 seconds. Subsequently the mixture is purged with nitrogen for 5 minutes. The flask is mounted onto a tumbler (IKA® RW16 basic) and immersed in oil bath at 70 °C. The flask is tumbled at 100 revolutions per minute (rpm) for 24 hours for polymerization. After polymerization, the particles are washed four times with DI water using centrifugation. 20 wt% LPS dispersion is prepared by dispersing LPS particles in 1 wt% poly vinyl alcohol (PVA, Mw 13,000-23,000, 87-89% hydrolyzed) aqueous solution. A 20 wt% monomer emulsion is prepared by vortexing a mixture consisting of styrene, *tert*-butyl acrylate (*t*BA, 98%), 1 vol% divinylbenzene (DVB, 55%) and 0.5 wt% initiator 2,2'-Azobis(2.4-dimethyl valeronitrile) (V-65B) (Wako) with 1 wt% PVA aqueous solution. LPS particles are swollen with the monomer mixture by mixing the LPS dispersion and the monomer emulsion. The volume ratio of the LPS and the monomer mixture is 20:80. The particle-monomer mixture is mounted on a rotator (Glas-Col®) and rotated for 8 hours at 60 rpm. Seeded emulsion polymerization is performed by tumbling the particle-monomer mixture in an oil bath at 70 °C at 100 rpm for 10 hours. After seed

emulsion polymerization, the particles are washed with DI water for least 6 times by centrifugation to remove PVA and unreacted monomer. The particles from seeded emulsion polymerization are then stirred in an acid mixture consisting of 80 vol% trifluoroacetic acid (TFA, 99%) and 20 vol% formic acid (FA, ≥95%) at 1200 rpm for 24 hours for hydrolysis of *t*BA. The volume ratio of particles and acid mixture is 1:40. The hydrolyzed particles are washed with DI water for 10 times by centrifugation.

3.2.2 Emulsification, phase inversion and emulsion characterization

3 ml toluene (99.8%) containing 0.01 wt% Nile Red (technical grade) and 3 ml of an aqueous suspension containing 0.5 wt% (Sty50/AA50) Janus particles are added in a glass vial and homogenized at 9500 rpm for 60 seconds using a homogenizer (Ultra-Turrax® T25 basic). The pH of the aqueous phases is adjusted using 1.0 M NaOH or 1.0 N HCl solutions. For phase inversion, 20 μL of 1.0 N HCl and 1.0 M NaOH are added in oil-in-water (O/W) emulsion (6.0 mL) generated with (Sty50/AA50) Janus particles in pH 11.0 and water-in-oil (W/O) emulsion (6.0 mL) generated with (Sty50/AA50) Janus particles in DI water, respectively. The emulsions are thoroughly mixed using a vortex mixer for 30 seconds and subsequently homogenized at 9500 rpm for 60 seconds. To image emulsion droplets using fluorescence microscopy, a drop of emulsions is placed in between two glass slides. To image (W/O) emulsions, glass slides are silanized using 1 vol% octadecyltrichlorosilane (OTS, ≥90%) in toluene for 30 seconds followed by heat

treatment on a hot plate at 150 °C for 30 minutes. To image (Sty50/AA50) Janus particles on emulsion surfaces, we replace toluene with styrene and add 1 wt% V-65B to enable polymerization of the oil phase. Polymerized emulsion samples are washed thoroughly with DI water before imaging.

To characterize the interactions between emulsion droplets, toluene-in-water emulsions are prepared by first homogenizing a mixture of 1 ml toluene and 4 ml 0.5 wt% (Sty50/AA50) Janus particles dispersed in aqueous solution of either pH 2.2 or pH 11.0 at 9500 rpm for 60 seconds followed by vortexing for 30 seconds. The emulsions are transferred into a glass syringe and injected into a glass microchannel with a 1×1 mm^2 square cross-section. The flow pattern of the toluene-in-water emulsions is recorded by a fast camera (Phantom v7.1).

3.3 Results and Discussions

3.3.1 Synthesis of amphiphilic Janus particles

The generation of amphiphilic Janus particles is inspired by the synthesis of pH-responsive amphiphilic diblock copolymer, poly(styrene-b-acrylic acid) (PS-b-PAA). PS-b-PAA diblock copolymers are typically synthesized by sequentially polymerizing styrene and tertiary butyl acrylate (*t*BA) to make poly(styrene-b-*t*BA) and then subsequently hydrolyzing the *t*BA repeating units to form the acrylic acid block.[113-116]

We use an analogous method to synthesize amphiphilic Janus particles using seeded emulsion polymerization as schematically illustrated in Figure 3.1 (a).

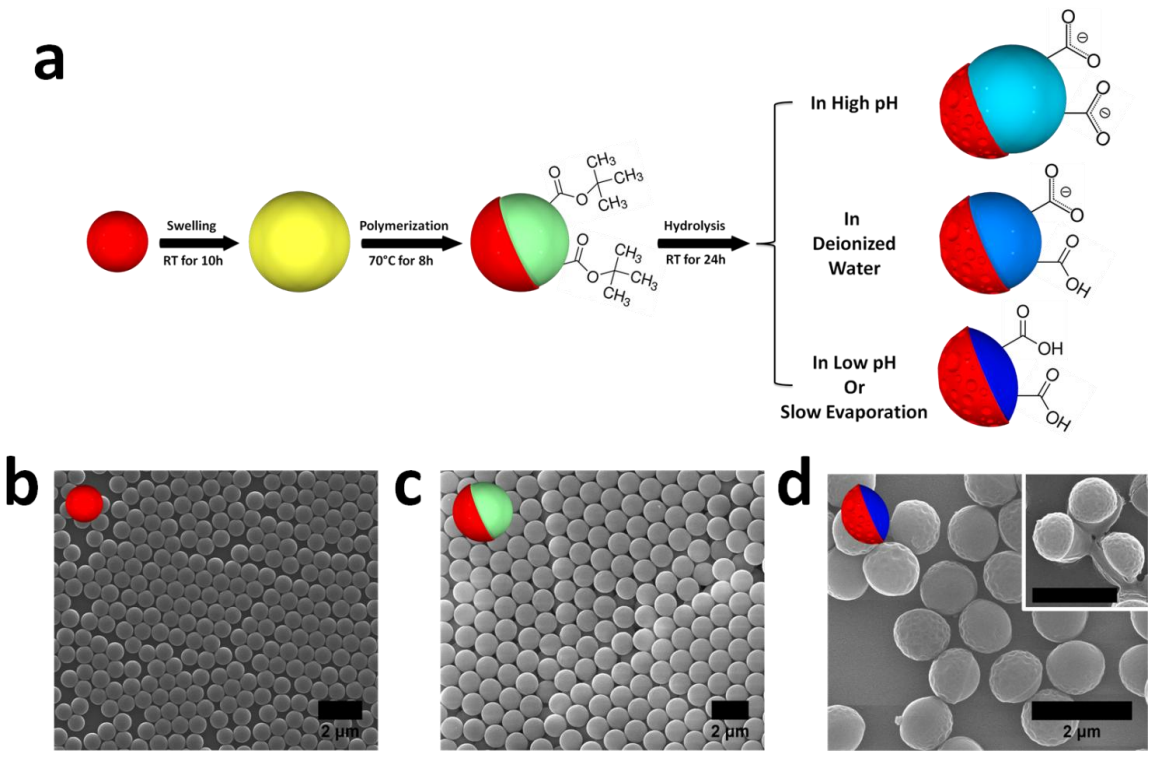

Figure 3.1 (a) Schematic illustration for the synthesis of amphiphilic Janus particles by seeded emulsion polymerization followed by acid hydrolysis. Scanning electron microscope (SEM) images of (b) linear polystyrene (LPS) seed particles, (c) P(S-co-*t*BA)/LPS composite particles and (d) (Sty/AA) Janus particles after hydrolysis. The inset of the image in (d) shows hydrolyzed composite particles prepared by fast evaporation with AA-rich side collapsed (scale bar = 2 μm).

Monodisperse particles (~ 0.75 μm in diameter) composed of linear polystyrene (LPS) are synthesized by dispersion polymerization (Figure 3.1 (b)).[117] These LPS seed particles are swollen with a monomer emulsion composed of styrene, *t*BA, divinylbenzene (DVB) (1 vol%), 2,2'-azobis(2.4-dimethyl valeronitrile) (0.5 wt%;

initiator) and 1 wt% poly vinyl alcohol (PVA) aqueous solution for 10 hours. The volume ratio of LPS particles and the monomer mixture is 20:80, while the ratio of styrene and *t*BA in the monomer mixture is 50:50. These swollen LPS particles are kept at 70 ℃ for 8 hours for polymerization, which produces ~ 1.1 μm-composite particles consisting of LPS and a network of copolymer styrene and *t*BA, as shown in Figure 3.1 (c). *t*BA repeating units in the copolymer network are subsequently hydrolyzed using a 80:20 mixture of trifluoroacetic acid (TFA) and formic acid (FA) to form acrylic acid (AA). The hydrolysis of the composite particles is confirmed with Fourier transform infrared spectroscopy (FTIR). The disappearance of peaks associated with *t*BA at 1368 cm^{-1}, 1392 cm^{-1}, 1255 cm^{-1} and 1148 cm^{-1} peaks and a broadening and shift in the peak associated with carbonyl (-C=O) from 1725 cm^{-1} to 1705 cm^{-1} before and after hydrolysis are both indications of successful conversion of *t*BA to acrylic acid as shown in Figure 3.2. The presence of 1452 cm^{-1} and 1491 cm^{-1} peaks is attributed to the aromatic rings in polystyrene.[118,119]

The hydrolysis of the composite particles leads to a drastic change in the morphology of the particles as seen in Figure 3.1 (d). The hydrolyzed particles become acorn shapes with one smooth side and one rough side. This highly asymmetric shape strongly suggests that some type of phase separation occurred within each composite particle during seeded emulsion polymerization. In fact, a very careful examination of the composite particles before hydrolysis shows evidence of phase. Although morphological changes before hydrolysis induced by phase separation is not as prominent as that after hydrolysis, phase

separation nevertheless can be observed by careful examination of the surface of P(S-co-*t*BA)/LPS composite particles. We place a dashed line outlining the boundary between the two phases of each particle to distinguish the two sides (Figure 3.3).

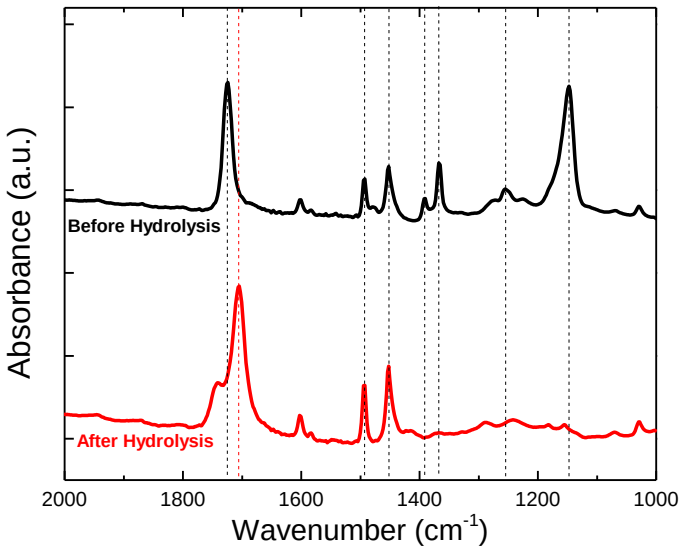

Figure 3.2 Fourier transform infrared spectroscopy (FTIR) of P(S-co-*t*BA)/LPS composite particles before (black) and after (red) hydrolysis.

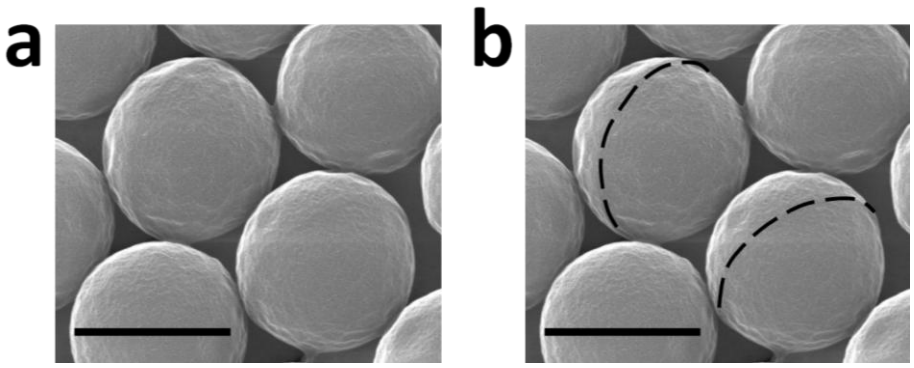

Figure 3.3 Scanning electron microscope images of P(S-co-*t*BA)/LPS composite particles show the boundary of smooth surface and slightly rougher surface ((b) marked by black dashed line) (scale bar = 1μm).

We believe the copolymerization of the two monomers in the presence of LPS induces phase separation in the composite particles. Instantaneous copolymer composition as a function of monomer conversion is calculated using formula as shown in Equation (2-1).[120]

$$1-\frac{M}{M_0}=1-\left[\frac{f_S}{(f_S)_0}\right]^{\alpha}\left[\frac{f_{tBA}}{(f_{tBA})_0}\right]^{\beta}\left[\frac{(f_S)_0-\delta}{f_S-\delta}\right]^{\gamma} \qquad (2\text{-}1)$$

M/M_0 stands for the remaining mole fraction of two monomers in the reaction medium, thus 1- M/M_0 represents the mole fraction of two monomers that have been reacted or converted. f_S and f_{tBA} represent the mole fraction of styrene and *t*BA in the reaction medium, respectively, while $(f_S)_0$ and $(f_{tBA})_0$ represent the initial mole fraction of styrene and *t*BA in the reaction medium. Other parameters are listed as in Equation (2-2), (2-3), (2-4), (2-5), (2-6) and (2-7).

$$\alpha=\frac{r_{tBA}}{(1-r_{tBA})} \qquad (2\text{-}2)$$

$$\beta=\frac{r_S}{(1-r_S)} \qquad (2\text{-}3)$$

$$\gamma=\frac{(1-r_S r_{tBA})}{(1-r_S)(1-r_{tBA})} \qquad (2\text{-}4)$$

$$\delta=\frac{(1-r_{tBA})}{(2-r_S-r_{tBA})} \qquad (2\text{-}5)$$

$$F_S = \frac{r_S f_S^2 + f_S f_{tBA}}{r_S f_S^2 + 2 f_S f_{tBA} + r_{tBA} f_{tBA}^2} \quad (2\text{-}6)$$

$$F_S = 1 - F_{tBA} \quad (2\text{-}7)$$

r_S = 0.89 and r_{tBA} = 0.29 are the reactivity ratio for styrene and *t*BA, respectively. F_S and F_{tBA} are the mole fraction of styrene and *t*BA in the instantaneous copolymer chains, which are solved numerically for different degrees of conversion. As seen in Figure 3.4, the network strands generated in the early stage of copolymerization is rich in styrene. The mole fraction of styrene gradually decreases as degree of conversion increases. When the degree of conversion is around 80%, mole fraction of *t*BA in the network strands starts to dominate over styrene and eventually increase to 100%.

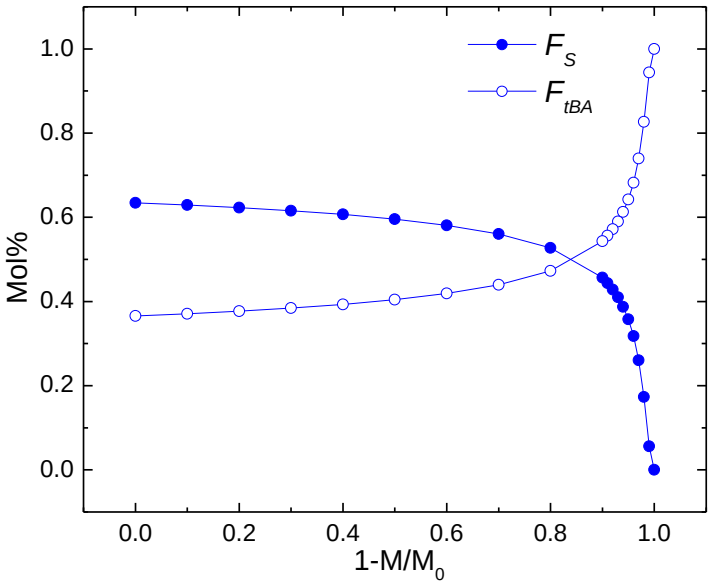

Figure 3.4 Instantaneous copolymer composition as a function of degree of monomer conversion calculated for copolymerization of styrene and *t*BA from Equation (2-1).

The reactivity ratios, which characterize the selectivity of an end group of a polymerizing chain to react with either monomer during copolymerization, of styrene and *t*BA are 0.89 and 0.29, respectively, in toluene medium.[121] Because of the reactivity ratios of the two monomers are quite different, composition of the polymer network formed with these two monomers is expected to shift as the polymerization of monomers proceeds; that is, the network strands generated in the early stage of polymerization is rich in styrene. These strands likely have an appreciable miscibility with LPS of the seed particles. However, as the conversion approaches completion, the network strands synthesized in the late stage become rich in *t*BA. These network strands likely has low miscibility with LPS and also with styrene-rich part of the network because of the high Flory-Huggins interaction parameter between styrene and *t*BA.[122] Thus, the composite particles undergo polymerization-induced phase separation resulting in the formation of styrene-rich and *t*BA-rich regions. Interestingly, no signs of phase separation are observed if particles composed of styrene and *t*BA are synthesized in the absence of LPS as shown in Figure 3.5, emphasizing the importance of LPS in inducing the phase separation.

Styrene-tBA composite particles are synthesized without LPS seed particles to reveal the necessity of LPS in inducing the phase separation we observe in the P(S-co-*t*BA)/LPS composite particles shown in Figure S2. A monomer mixture consisting of styrene, *tert*-butyl acrylate (*t*BA, 98%), 1 vol% divinylbenzene (DVB, 55%) and 0.5 wt% initiator 2,2'-Azobis(2.4-dimethyl valeronitrile) (V-65B) (Wako) are emulsified in 1 wt% poly vinyl alcohol (PVA) aqueous solution by vortexing. The volume ratio of styrene and *t*BA

is 50:50. The monomer emulsion is then tumbled in oil bath at 70 ℃ for 24 hours for polymerization. The particles are washed with deionized water for 6 times before acid hydrolysis by a mixture of 80 vol% trifluoroacetic acid and 20% formic acid for 24 hours. The volume of particles and acid mixture is 1:40. The hydrolyzed particles are washed with deionized water 10 times before imaging.

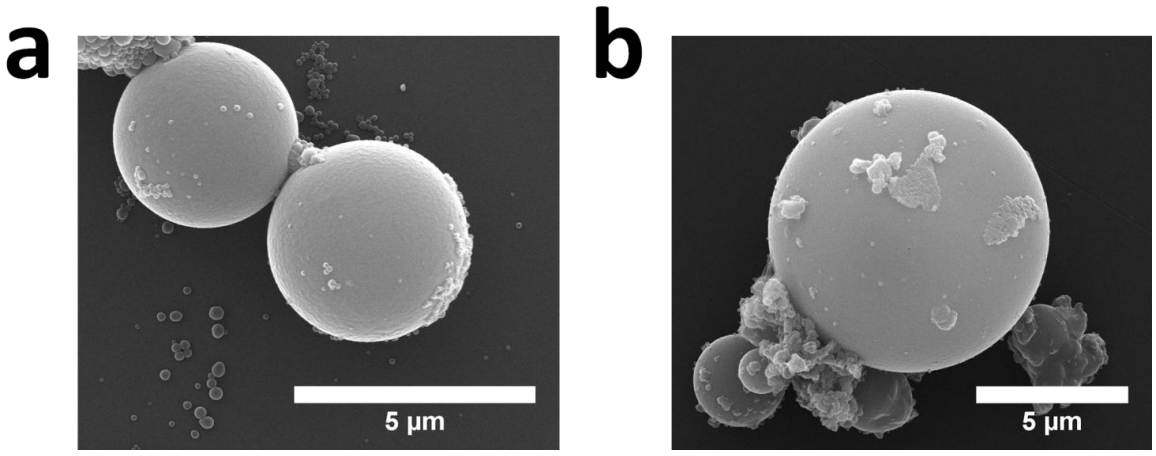

Figure 3.5 Styrene-*t*BA composite particles synthesized by emulsion polymerization without LPS seed particles (a) before and (b) after hydrolysis (scale bar = 5 μm).

As shown in Figure 3.5, there is no morphological change before and after hydrolysis as P(S-co-*t*BA)/LPS composite particles synthesized using seeded emulsion polymerization as shown in Figure 3.1. This result likely shows the importance and necessity of LPS seed particles for successful phase separation during polymerization. Phase separation in seeded emulsion polymerization has been observed in poly(methyl methacrylate)-seeded emulsion polymerization of styrene, in which different particle morphologies were found by changing polymerizing conditions.[123]

Although the evidence for phase separation is quite clear, it is not straightforward to distinguish which side of the hydrolyzed composite particles is rich in AA. To indentify the chemical natures of the two sides, we subject these particles to rapid drying from an aqueous suspension. Rapid dehydration under high vacuum does not allow the AA-rich side, which likely becomes swollen in water, to relax back to form a smooth hemisphere thus leading to disfigurement of the AA-rich side as shown in the inset of Figure 3.1 (d). Because of its hydrophobicity and the lack of swelling in water, the styrene-rich side is not expected to show any significant difference in the morphology even after rapid drying. These results strongly suggest that the rough side of the composite particles is the styrene-rich (Sty-rich) side. We believe the small dimples that are present on the surface of the Sty-rich side are small domains of acrylic acid. Despite the presence of these small domains of carboxylic acid groups, we expect Sty-rich domain to remain hydrophobic. Studies have shown that PS particles functionalized with surface carboxylic acid groups have relatively hydrophobic surfaces at the interface between oil and water (three phase contact angle > 130).[124] In the rest of this chapter, we refer to these hydrolyzed composite particles as (Sty/AA) Janus particles.

3.3.2 Shape-changing property of (Sty/AA) Janus particles

Polymer networks containing high mole fractions of acrylic acid units are known to have pH-responsiveness; that is, they swell and deswell in high and low pH conditions,

respectively. Such a stimuli-responsive property of AA-rich network makes our Janus particles change their shape and behavior quite drastically in response to changes in solution pH. As shown in Figure 3.6 (a), at pH = 2.2, (Sty50/AA50) Janus particles[125] remain oblate-like and form clusters in the suspension. The formation of these clusters indicates that these particles interact attractively, which is reminiscent of the aggregation of amphiphilic molecules in water (*e.g.*, micelle formation). The aggregation of the particles is likely due to the protonation of acrylic acid groups and the loss of surface charge, leading to the reduction of electrostatic repulsive interactions between particles.[51,126-129] When these (Sty50/AA50) Janus particles are dispersed in deionized water (pH = 5.5 - 6.0), however, these particles become individually dispersed and, at the same time, become more or less spherical in shape as shown in Figure 3.6 (b). Such a shape change likely stems from slight hydration of the AA-rich side and partial ionization of carboxylic acid groups, which keep the particles apart via electrostatic repulsion. When the basicity of the suspension is further increased to pH 11.0, these Janus particles transform their shape from spheres to dumbbells (also known as snowmen, dimers and dicolloids), as shown in Figure 3.6 (c). The AA-rich lobes of these Janus dumbbells become almost transparent due to significant swelling in the high pH environment.

The pH-sensitivity of these Janus particles can be tuned by controlling the composition of the monomer mixture that is used for seeded emulsion polymerization. To demonstrate such tunability, we synthesize two additional composite particles with the styrene:*t*BA ratios of 75:25 and 25:75. As shown in Figure 3.6, the pH-sensitivity of these two

amphiphilic Janus particles in different pH solutions are quite different. (Sty75/AA25) Janus particles (Figure 3.6 (d)) remain spherical at pH = 11.0 (Figure 3.6 (f)), whereas (Sty25/AA75) Janus particles (Figure 3.6 (e)) transform to dumbbell shapes in deionized water (pH = 5.5 - 6) (Figure 3.6 (g)). The changes in the responsiveness (*i.e.*, swellability) of the AA-rich sides likely stems from the changes in their composition. In short, our results demonstrate that the aggregation/dispersion behavior and shape of (Sty/AA) Janus particles are highly sensitive to the solution pH and that their pH sensitivity can be tailored by tuning the ratio of styrene and *t*BA used for the synthesis of these particles.

One way to characterize the shape changes that are observed in these particles as a function of the solution pH is to use the concept of packing parameter, which is typically used to characterize the shape of molecular surfactants and the size ratio of hydrophilic and hydrophobic segments within a molecular surfactant.[5] For example, while the (Sty50/AA50) Janus particles have a packing parameter that is larger than 1.0 in acidic solutions, the packing parameter of the same particle decreases below 1.0 in basic solutions.[5] Such a drastic shape change, we believe, leads to reversal in the amphiphilicity of these particles; that is, in the language of hydrophile-lypophile balance (HLB), (Sty/AA) Janus particles have lypophile-dominant property in acidic solutions, whereas they completely switch to become hydrophile-dominant solid amphiphile in basic solutions. The implications of such an amphiphilicity-reversing property of (Sty/AA) Janus particles are described below.

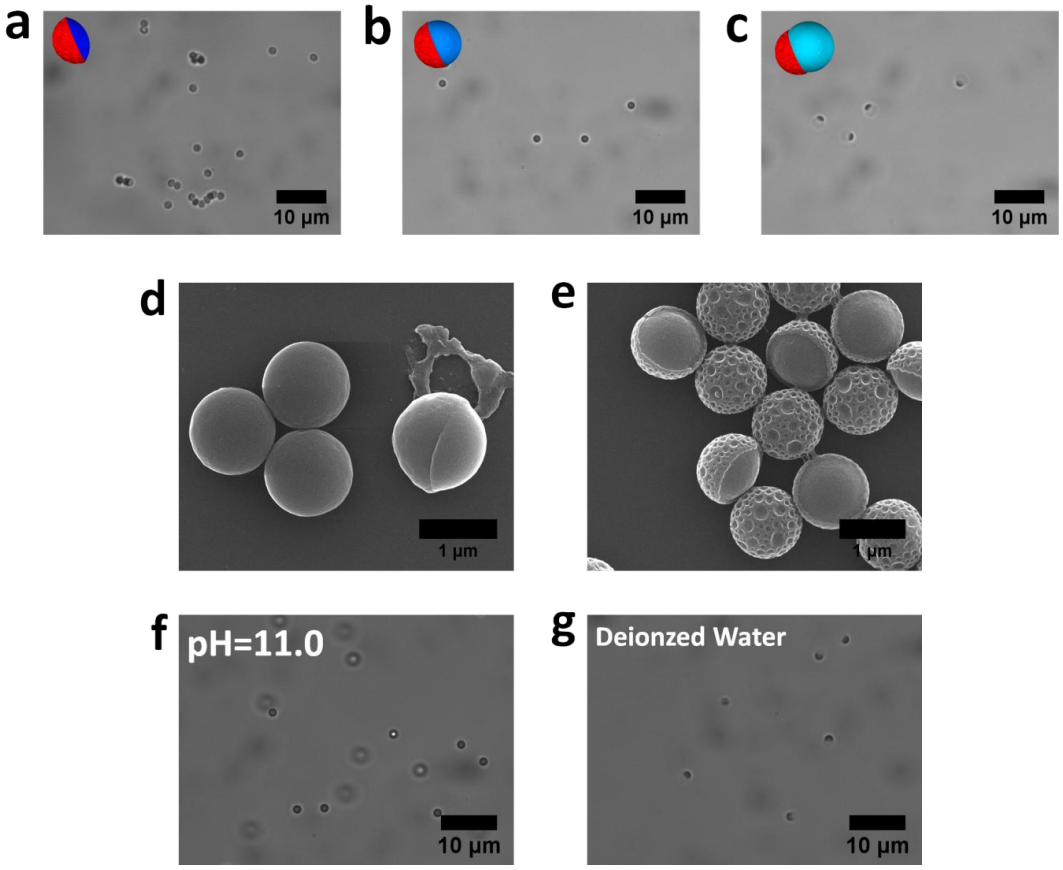

Figure 3.6 Microscope images of (Sty/AA) Janus particles made with 50 vol% of both styrene and *t*BA in the monomer mixture (Sty50/AA50) in (a) pH =2.2, (b) DI, and (c) pH=11.0 water. (Sty/AA) Janus particles swollen by monomer mixtures with styrene:*t*BA ratios of (d) 75:25 and (e) 25:75. Microscopy images of (f) (Sty75/AA25) Janus particles in pH=11.0 water and (g) (Sty25/AA75) Janus particles in DI water (pH=5.5 – 6) (scale bar = 10 μm in a, b, c, f and g; scale bar = 1 μm in d and e).

In addition to the tunability of pH responsiveness, the synthesis scheme developed here also allows us to tune the Janus boundary between styrene-rich side and acrylic acid-rich side. This can be done by increasing the volume ratio between monomer and polystyrene seeds (swelling ratio V_{mono}/V_{PS}) during the swelling step. As shown in Figure 3.7, with

increasing swelling ratio from 3:1 to 7:1, the Janus boundary continually moves towards rough styrene-rich side.

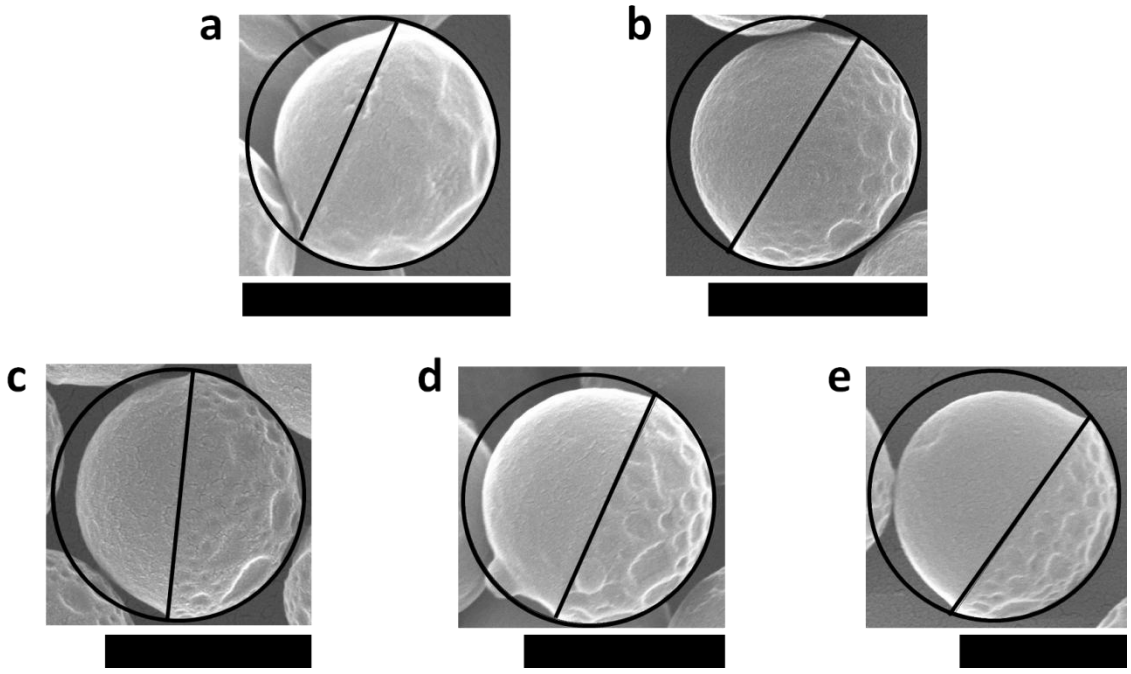

Figure 3.7 SEM images of (Sty50/AA50) Janus particles with increasing swelling ratio V_{mono}/V_{PS}: (a) 3:1, (b) 4:1, (c) 5:1, (d) 6:1 and (e) 7:1. The scale bar is 1 μm.

3.3.3 Controlling the type of Pickering emulsion stabilized by (Sty/AA) Janus particles

One of the most promising and practical applications of Janus particles is in the stabilization of multiphasic mixtures such as emulsions. As summarized in Introduction, recent studies have shown that thermodynamically stable emulsions can be generated using amphiphilic Janus particles.[14,86] Because our (Sty/AA) Janus particles comprise two

sides with significantly different preferences toward oil and water (*i.e.*, not just the wettability but also swellability in different media), we believe our particles would make excellent solid surfactants. Moreover, the shape-changing and thus amphiphilicity-reversing properties of these (Sty/AA) Janus particles could significantly change their surfactant properties; that is, analogous to how the shape of molecular surfactants determine the type of emulsions they can stabilize, the type of emulsions that can be stabilized by these solid amphiphiles may depend on the particle shape and amphiphilicity.

To test this idea, we generate emulsions while keeping the volume ratio of oil and aqueous phases constant at 50:50. By keeping the volumes of the two phases equal to each other, it allows the system to generate the type of emulsion that the Janus particles prefer and avoid the influences of dominant fluid phase in determining the final emulsion type.[130,131] An oil-soluble dye, Nile Red, is added to facilitate emulsion characterization, and Janus particles are dispersed in the aqueous phase. As shown in Figure 3.8, emulsions made with particles in pH 2.2 water and in deionized (DI) water sediment to the bottom of the vials with excess oil phase remaining on top of the settled emulsions. In contrast, the emulsion made at pH 11.0 creams with an aqueous phase forming at the bottom. Given that the density of toluene is smaller than that of water, these observations suggest that emulsions made with pH 2.2 and DI water are water-in-oil (W/O) emulsions, whereas the emulsion made at pH 11.0 is an oil-in-water (O/W) type. This prediction is further confirmed by the fluorescence microscopy images of the emulsions as shown in

Figure 3.8. The fluorescence microscopy images indicate that emulsion droplets made at pH 2.2 and DI water are composed of aqueous phase (dark dispersed phase), whereas those made at pH 11.0 are oil droplets (bright dispersed phase). The size of W/O emulsion droplets is significantly larger than that of O/W emulsions likely because of the high charge of (Sty50/AA50) Janus particles at pH 11.0, leading to strong repulsive interparticle interactions. An analogous trend has been observed in emulsions that were stabilized with silica and latex particles.[132]

To observe the aggregation structures as well as the orientations of (Sty50/AA50) Janus particles at the interface of emulsion droplets, we replace toluene with a polymerizable oil phase, styrene, which has similar property and chemical structure as toluene. The oil phase contains 3 ml styrene with 0.5 wt% 2,2'-Azobis(2.4-dimethyl valeronitrile) as initiator, whereas the aqueous phase contains 3 ml 0.5 wt% (Sty50/AA50) Janus particles under pH 2.2 or pH 11.0. Emulsions are made by homogenization at 9500 rpm for 60 seconds. The emulsions are subsequently placed in an oil bath at 70 ℃ for polymerization of styrene for 24 hours. Polymerized samples are washed with deionized water thoroughly before imaging.[10,40]

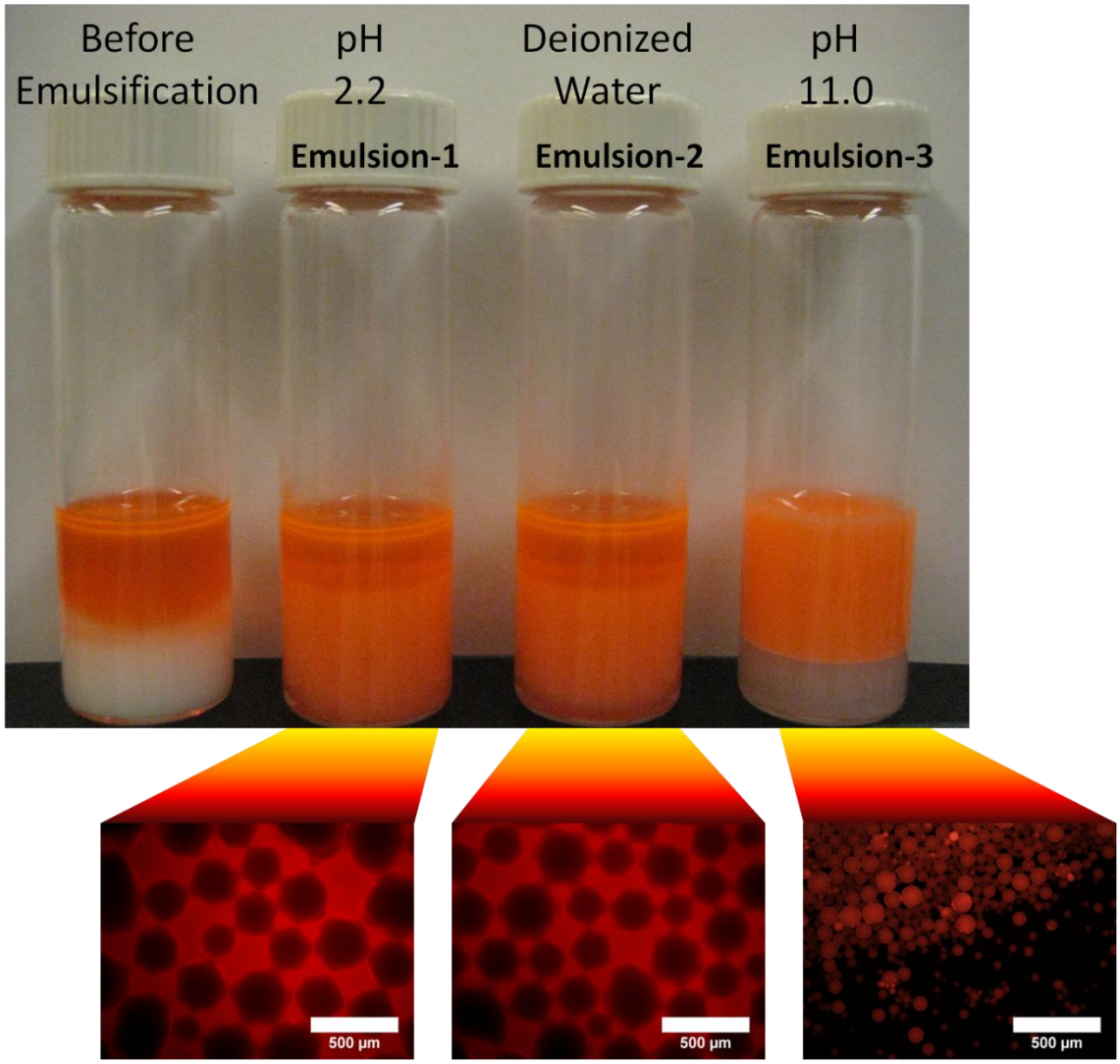

Figure 3.8 Macroscopic and fluorescence microscopy images of emulsions made with aqueous phases of pH 2.2, deionized water (water-in-oil emulsion) and aqueous phase of pH=11.0 (oil-in-water emulsion). The volume ratio of oil and water phases is kept 50:50 in all cases, and the oil phase contains 0.01 wt% Nile Red (scale bar = 500 µm).

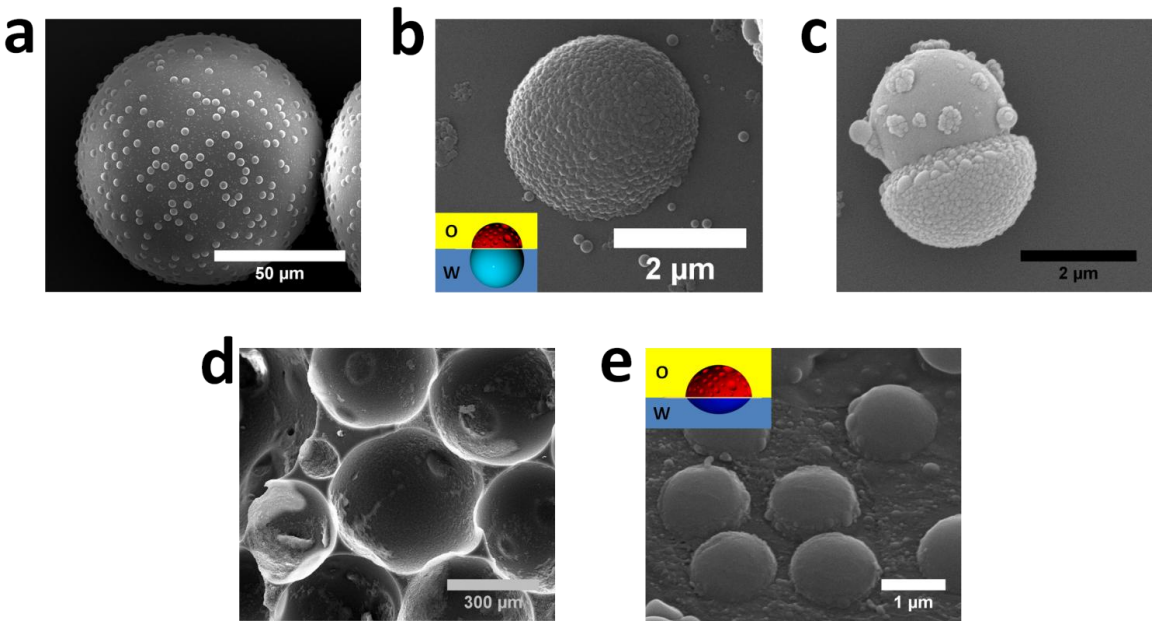

Figure 3.9 Scanning electron microscopy images of polymerized styrene-in-water emulsion (a,b and c) and water-in-styrene emulsion (d and e). (a) Image of a polymerized styrene emulsion droplet made at pH 11.0 with (Sty50/AA50) Janus particles on the surface (scale bar = 50 µm). (b) High magnification image of an embedded (Sty50/AA50) Janus particle on the surface (scale bar = 2 µm). (c) A free (Sty50/AA50) Janus particle on substrate (scale bar = 2 µm). (d) Image of polymerized water-in-styrene emulsions (scale bar = 300 µm). (e) (Sty50/AA50) Janus particles embedded in the surface of the polymerized styrene phase in (d) (scale bar = 1 µm).

In the case of styrene-in-water emulsion droplets stabilized with (Sty50/AA50) Janus particles at pH 11.0, we observe particles imbedded in the polymerized droplet as shown in Figure 3.9 (a). In addition, we also find some free particles that are not embedded in the polymerized droplets as seen in Figure 3.9 (c). The exposed dome of the imbedded particles as shown in Figure 3.9 (b) resembles one lobe of the free particles in both shape and size, which we believe to be the AA-rich lobe. This phenomenon also indicates that the other lobe of (Sty50/AA50) Janus particles is fully immersed in the styrene emulsion

before polymerization. The mushroom-shaped free particles are also a strong indication that our (Sty50/AA50) Janus particles are dumbbells at pH 11.0. We believe we are able to observe the dumbbell shape because styrene used as the dispersed oil phase also swells (Sty50/AA50) particles and undergoes polymerization, changing their shape and size from their original states.

In the case of water-in-styrene emulsion droplets stabilized with (Sty50/AA50) Janus particles at pH 2.2, the large concave surfaces that are observed in Figure 3.9 (d) represent the polymerized continuous phase. On the surface of the polymerized styrene phase, we find (Sty50/AA50) Janus particles embedded in the polymerized surface as shown in Figure 3.9 (e). Particles that are embedded in the surface have circular outline, indicating that (Sty50/AA50) Janus particles immerse styrene-rich side in oil phase while expose AA-rich side to the aqueous phase; that is, no particles are showing tilted orientations at the interface. These observations strongly indicate that (Sty50/AA50) Janus particles indeed take the upright orientation on emulsion surface due to their high amphiphilicity; that is, each side of these Janus particles fully resides in its preferred fluid phase, and the boundary between the two sides are pinned at the W/O or O/W interface.

Our results clearly demonstrate that (Sty/AA) Janus particles can change their preferred emulsion type in response to pH changes in the aqueous phase and stabilize different types of emulsion. The preferred emulsion type as a function of the solution pH can be attributed to the changes in the shape leading to the reversal of the amphiphilicity of (Sty/AA) Janus particles, which is analogous to the effect of the packing parameter and

the HLB of molecular surfactants, respectively, on the type of emulsions that they are able to stabilize. The upright orientation of these Janus particles at the water-oil interface likely plays an important role in maximizing the effect of particle shape change on the emulsion type that can be stabilized with these particles.[86]

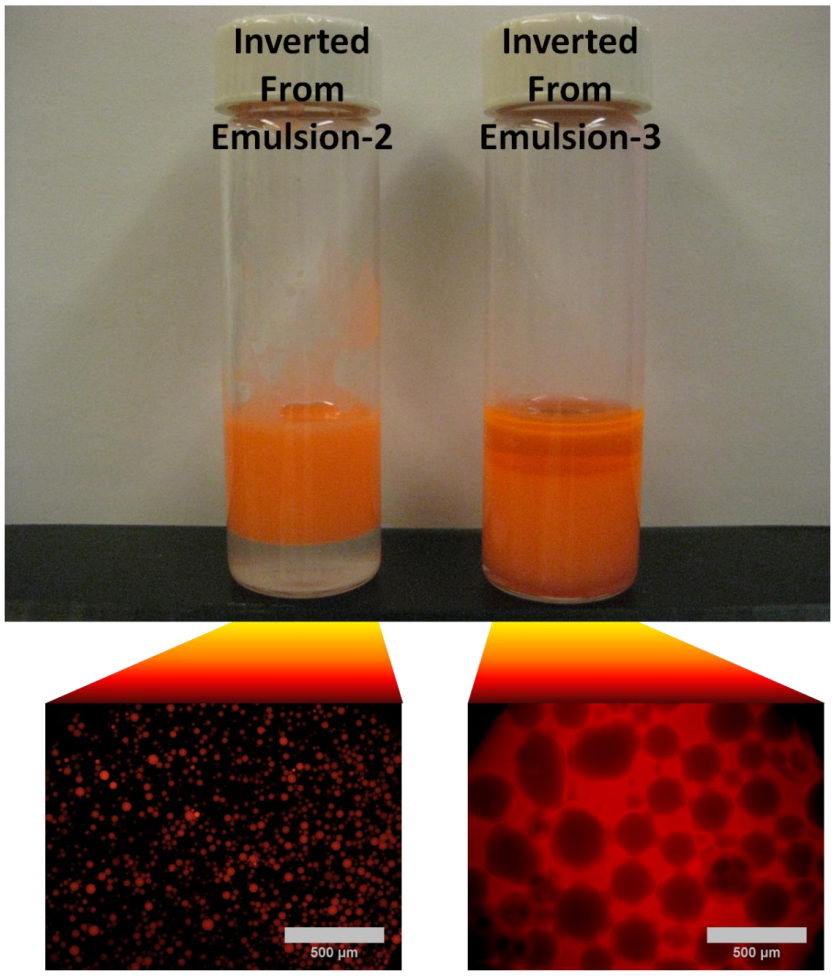

Figure 3.10 Images of emulsions inverted from Emulsion-2 and Emulsion-3 in Figure 3.7 by adding ~ 20 µL of 1 M NaOH and 1 N HCl, respectively. Fluorescence microscopy images of emulsions inverted from (b) Emulsion-2 and (c) Emulsion-3, respectively (scale bar = 500 µm).

The W/O emulsion made with (Sty/AA) Janus particles in deionized water presents another unique aspect because it does not conform to the so-called Bancroft or Finkle rules, which state that the continuous phase of an emulsion is the one in which the emulsifier is preferentially solubilized (Bancroft) or dispersed (Finkle).[11] Using the pH-responsiveness and amphiphilicity-reversing properties of the (Sty/AA) Janus particles, it is possible to generate emulsions that both follow (pH 11.0) and violate (deionized water) these empirical rules. Interestingly, such behaviors have also been observed in Pickering emulsions stabilized with homogenous particles with proper choice of aqueous and oil phases.[133,134]

The fact that the type of emulsions generated with (Sty/AA) Janus particles is controlled by the pH of the aqueous phase strongly suggests that one type of emulsion generated under one condition can be inverted into the other type simply by changing the solution pH. Phase inversion emulsification triggered by an external stimulus (also known as transitional phase inversion emulsification) is an important process by which emulsions with highly viscous dispersed phases can be generated and requires changes in the HLB as well as the shape of stimuli-responsive surfactants or the wettability of homogenous particles that stabilize the original emulsions.[104,135-138] We demonstrate the transitional phase inversion of emulsions stabilized with (Sty50/AA50) Janus particles by adding a small amount of highly concentrated basic and acid solution (~ 20 μL of 1.0 M NaOH and 1.0 N HCl, respectively) into 6 ml of W/O and O/W emulsions originally generated with DI water and pH 11.0 (Emulsion-2 and Emulsion-3 in Figure 3.8), respectively.

Upon vigorous mixing, the Emulsions-2 and -3 become O/W and W/O emulsions, respectively (Figure 3.10); that is, the types of final emulsions are inverted and opposite of the starting emulsions in both cases. By changing the shape of the AA-rich side and relative size of styrene- and AA-rich sides, the amphiphilicity of these particles reverses in response to changes in solution pH, which eventually leads to the phase inversion of the emulsions. We believe this is the first demonstration of transitional phase inversion of Pickering emulsions stabilized with Janus particles, which is facilitated by the dynamic tunability of the shape as well as the reversible amphiphilicity of the pH-responsive (Sty/AA) Janus particles.

3.3.4 Controlling the interactions between Pickering emulsion droplets

Interactions between emulsion droplets have an important effect on the rheological properties of emulsions[139,140], which in turn change the properties of emulsion-based products such as shelf stability and sensorial properties.[135] Thus, emulsifiers that enable the control over the interactions between emulsion droplets without causing destabilization are highly desirable. The pH-dependent aggregation/dispersion behavior of (Sty50/AA50) Janus particles in the bulk aqueous phase, as seen in Figure 3.6 (a), suggests that the interactions of Pickering droplets stabilized with these particles could also depend on the pH of the solution. To test this hypothesis, we generate oil-in-water (O/W) emulsions at pH 2.2 or pH 11.0 and study the interactions between Pickering

emulsion droplets. Unlike the above case when the oil:water ratio was kept 50:50, by decreasing the volume fraction of oil significantly (oil:water = 20:80), O/W emulsions can be generated regardless of the pH of the aqueous phase.

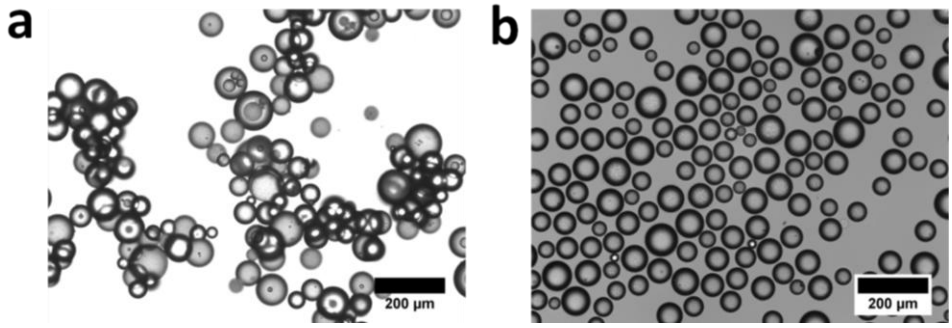

Figure 3.11 Microscope images of toluene-in-water emulsions made with (Sty50/AA50) Janus particles dispersed in (a) pH 2.2 and (b) pH 11.0 aqueous solutions. The volume ratio of oil to water is 20:80 (scale bar = 200 μm).

The difference in the interactions between emulsions under acidic and basic conditions can be indirectly observed by the morphology of emulsion droplets. O/W emulsion generated at pH 2.2 shows droplets that are aggregated to form clusters as shown in Figure 3.11 (a). In contrast, when the pH of the emulsion is switched to pH 11.0, the droplets become well-separated as shown in Figure 3.11 (b), indicating repulsive interactions.

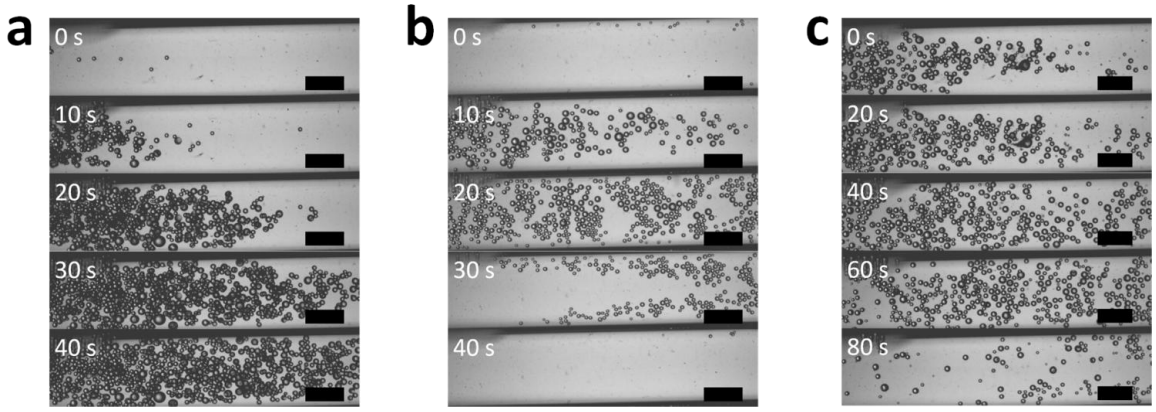

Figure 3.12 Microscope images of toluene-in-water emulsion stabilized by (Sty50/AA50) Janus particles made at (a) pH 2.2 and (b) pH 11.0 flowing inside a glass capillary microchannel. (c) Attractive toluene-in-water emulsion made at pH 2.2 that are stuck to the microchannel being washed away by a pH 11.0 aqueous solution. (scale bar = 500 μm).

The tunable interactions between Pickering emulsions stabilized with (Sty50/AA50) Janus particles can be more clearly demonstrated by observing the flow behavior of these emulsions under different pH conditions. When an emulsion prepared at pH 2.2 flow across a microchannel made of glass (1 × 1 mm^2 square cross-section), droplets stick to the glass surface and to each other as they flow in the channel as shown in Figure 3.12 (a). Droplets also move in clusters rather than as individual droplets, strongly indicating that these emulsion droplets interact attractively and are very adhesive. Emulsion droplets prepared at pH 11.0, however, do not stick to the channel wall and flow freely in the channel as single droplets as shown in Figure 3.12 (b), indicating that these emulsion droplets are repulsive. When an emulsion is introduced in the channel at pH 2.2 initially and then the pH of the continuous phase is changed to pH 11.0, the emulsion droplets that are originally stuck to the glass channel surface and to each other suddenly become

individually dispersed and flow freely down the channel as shown in Figure 3.12 (c). Again these results clearly demonstrate that the interactions between emulsion droplets can be readily tuned by changing the solution condition without destabilizing the emulsion.

3.4 Conclusions

In this chapter, we have presented a bulk synthesis scheme for generating highly uniform pH-responsive Janus particles. These Janus particles not only drastically change their shape but also completely reverse their amphiphilicity in response to changes in the solution pH. These pH-sensitive changes of shape are analogous to the changes that are observed in pH-responsive amphiphilic molecules; that is, the packing geometry and amphiphilicity of these Janus particles are dynamically tunable using solution pH as environmental stimuli. We demonstrate that the type of emulsions generated using these amphiphilicity-reversing and shape-tunable Janus particles depends strongly on the acidity/basicity of the aqueous phase and that emulsions can be inverted to the opposite types by either lowering or raising the pH of the aqueous phases. The pH-dependent aggregation/dispersion behavior of our Janus particles are utilized to generated both attractive and repulsive emulsions at low and high pH conditions, respectively. Furthermore, attractive and repulsive interactions between emulsion droplets can be controlled on demand by changing the pH of continuous phase. Our findings offer a new

class of dynamically tunable colloidal materials that would widen the functionality and applications of Janus particles as solid surfactants. In particular, the ability to enable phase inversion opens up new possibilities in generating emulsions and particles that are not readily obtainable using traditional emulsion formation processes.[141] Also dynamically tunable interactions between Janus particle-stabilized emulsions could lead to new applications in pH-responsive complex fluids that can drastically change their rheological properties.

Chapter 4. One-Step Encapsulation and Triggered Release Based on Janus Particle-Stabilized Multiple Emulsions

4.1 Introduction

Multiple emulsions are hierarchical multiphasic systems in which dispersed droplets of one liquid contain smaller droplets of another liquid.[142] The ability to carry cargos with drastically different polarities and the possibility to induce the triggered release of encapsulated actives make multiple emulsions extremely useful in various fields including pharmaceuticals[143], cosmetics[144], agricultural[145] and food industry.[146] However, the practical applications of multiple emulsions are impeded by the lack of simple methods to prepare multiple emulsions with high stability. In most cases, multiple emulsions are generated by two-step bulk emulsification using a combination of lipophilic and hydrophilic surfactants.[142,147] In addition to the complexity of implementing two-step emulsification, the possibilities of disrupting the primary W/O emulsion during the second emulsification step potentially pose a challenge in the encapsulation of active ingredients.[148] Depending on the combination of surfactants used to generate multiple emulsions, different mechanisms may induce their destabilization which in turn limits their practical applications.[142,149] Although the preparation of stable

multiple emulsions with good stability using one-step emulsification has been demonstrated[104,150-158], the combination of simple formulation, high stability and triggered release functionality has proven to be extremely challenging to achieve because high stability and triggered release are somewhat incompatible properties; that is, highly stable multiple emulsions would not easily undergo destabilization to release the encapsulated actives.

Amphiphilic Janus particles that have stimuli-responsive properties represent a promising surfactant system to overcome these limitations. It has been shown that not only highly stable emulsions can be generated with amphiphilic Janus particles, but also the destabilization of emulsions can be achieved by using stimuli-responsive Janus particles as emulsifiers.[105,106,159-161] More importantly, our recent work has shown that inversion of emulsion can also be achieved with stimuli-responsive Janus particles.[162] However, all of the studies that have shown emulsion stabilization using Janus particles have thus far resulted in the formation of simple emulsions.[105,106,159-161] The generation of Janus particle-stabilized multiple emulsions could be especially beneficial since such emulsions could be highly stable, providing a long term protection of the encapsulated species, and at the same time allowing for the release of encapsulants when an external stimulus is applied.

We are inspired by recent studies that have demonstrated the one-step generation of multiple emulsions via inversion mechanisms with diblock copolymer surfactants.[104,153,158] In this chapter, we demonstrate for the first time that highly stable

multiple emulsions can be generated in one-step by using stimuli-responsive amphiphilic Janus particles. We show that by changing the solution pH, we can induce the triggered release of encapsulated hydrophilic species from these multiple emulsions. We investigate the effect of various processing parameters on the formation of double emulsions and the triggered release from Janus particle-stabilized double emulsions.

4.2 Experimental Section

4.2.1 Particle Synthesis

(Sty50/AA50) Janus particles are synthesized by seeded emulsion polymerization followed by acid hydrolysis as reported previously.[162] Briefly, 20 wt% linear polystyrene (LPS) dispersion is prepared by dispersing LPS particles in 1 wt% poly vinyl alcohol (PVA, Mw 13,000-23,000, 87-89% hydrolyzed) aqueous solution. A 20 wt% monomer emulsion is prepared by vortexing a mixture consisting of styrene, *tert*-butyl acrylate (*t*BA, 98%), 1 vol% divinylbenzene (DVB, 55%) and 0.5 wt% initiator 2,2'-Azobis(2.4-dimethyl valeronitrile) (V-65B) (Wako) with 1 wt% PVA aqueous solution. LPS particles are swollen with the monomer mixture by mixing the LPS dispersion and the monomer emulsion. The volume ratio of the LPS and the monomer mixture is 20:80. The particle-monomer mixture is mounted on a rotator (Glas-Col®) and rotated for 8 hours at 60 rpm. Seeded emulsion polymerization is performed by tumbling the particle-monomer mixture in an oil bath at 70 ℃ at 100 rpm for 10 hours. After seed emulsion

polymerization, the particles are washed with DI water for least 6 times by centrifugation to remove PVA and unreacted monomer. The particles from seeded emulsion polymerization are then stirred in an acid mixture consisting of 80 vol% trifluoroacetic acid (TFA, 99%) and 20 vol% formic acid (FA, ≥95%) at 1200 rpm for 24 hours for hydrolysis of *t*BA. The volume ratio of particles and acid mixture is 1:40. The hydrolyzed particles are washed with DI water for 10 times by centrifugation.

4.2.2 Emulsion Stabilization and Triggered Release

The emulsions stabilized by Janus particles were prepared by homogenizing toluene and Janus particle dispersion in aqueous solution using a homogenizer (Ultra-Turrax T25 basic) at 9500 rpm for 60 seconds unless otherwise noted. The total emulsion volume was kept at 6 mL for all samples. The oil phase may contain 0.01 wt% nile red (technical grade) and the water phase may contain 1.5×10^{-4} wt% calcein (Sigma) to facilitate the characterization of emulsion. The agitation to multiple emulsion is done by tumbling the glass vial containing the multiple emulsion with a tumbler (IKA RW16 basic) at 120 rpm for 2 minutes. Triggered release is done by injecting 400 μL 1M NaOH solution into multiple emulsion followed by agitation. Evolution of multiple emulsions during increasing pH is done by injecting multiple emulsion into a petri dish (containing 9 mL deionized water) covered with a glass slide and 1 mL 1M NaOH to increase the pH. Snapshots are taken using an upright microscope (Zeiss).

4.3 Results and Discussions

4.3.1 Phase Diagram of (Sty50/AA50) Janus Particle-stabilized Emulsions

Emulsions we study in this work are stabilized with stimuli-responsive Janus particles that drastically switch their surfactant properties in response to changes in the solution pH as shown in Figure 4.1. Each Janus particle comprises rough apolar and smooth polar regions that are rich in styrene (Sty) and in acrylic acid (AA), respectively; we call this particle (Sty50/AA50) Janus.[162] We have shown that emulsions stabilized with these Janus particles undergo phase inversion from oil (toluene)-in-water to water-in-oil (toluene) emulsions (or vice versa) by simply changing the solution pH while keeping the volume fraction of the oil phase constant (ϕ_o = 0.5).[162]

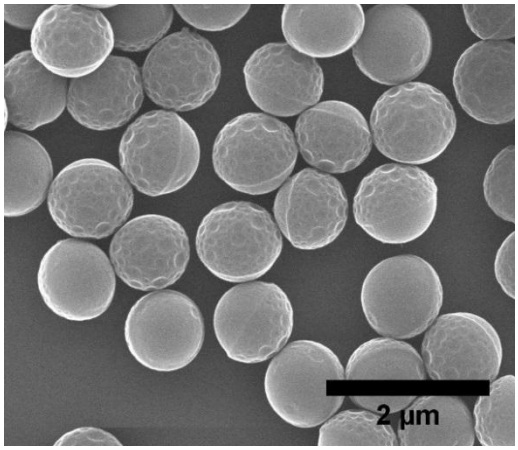

Figure 4.1 SEM image of (Sty50/AA50) Janus particles. The scale bar is 2 µm.

Interestingly, in our attempt to induce the so-called catastrophic phase inversion[163], in which the volume fraction of the oil (toluene) phase (ϕ_o) is decreased while keeping the solution condition (i.e., pH and ionic strength) constant, we observe that highly stable water-in-oil-in-water (W/O/W) multiple emulsions are generated in one emulsification step.

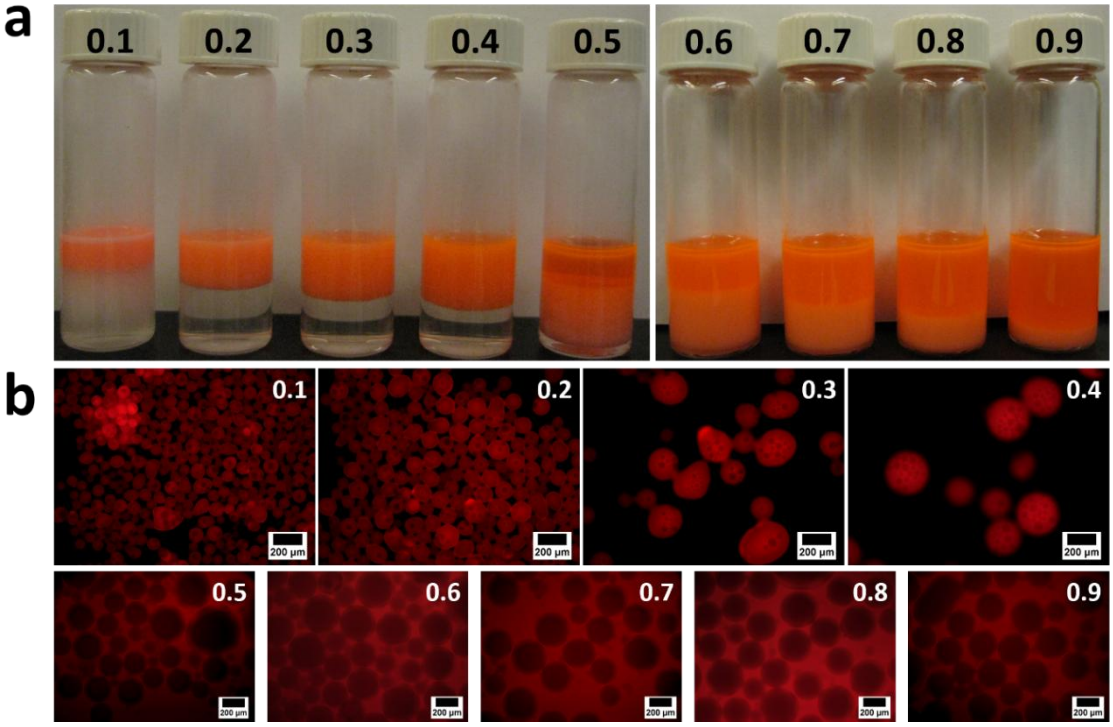

Figure 4.2 (a) Photo and (b) fluorescent microscopy images of emulsion stabilized by 0.5wt% (Sty50/AA50) Janus particles at pH5.0 with different volume fraction of oil phase (ϕ_o). The scale bar for fluorescent images is 200 μm.

Nine emulsions are generated with different volume fraction of oil phase (ϕ_o) as shown in Figure 4.2 (a). The water phase has a pH of 5.0 and contains 0.5% (Sty50/AA50) Janus

particles. The oil phase is toluene with 0.01wt% Nile Red. When $\phi_o \geq 0.5$, emulsion type is W/O emulsion as confirmed by fluorescent microscopy as shown in the second row of Figure 4.2 (b). The red fluorescence of these emulsions is coming from the continuous phase and dark droplets are observed indicating that these are W/O simple emulsions. When $\phi_o < 0.5$, W/O/W multiple emulsions are formed. As shown in the first row of Figure 4.2 (b), the continuous phase is dark indicating that water is continuous phase. Red fluorescence is coming from the emulsion droplets with black spots indicating the formation of W/O/W multiple emulsions. The stabilization of multiple emulsion is achieved by the adsorption of Janus particles to both outer and inner oil-water interfaces. Images of one multiple emulsion droplet taken at different focal planes are shown in Figure 4.3; Janus particles adsorbed at the two oil-water interfaces can be clearly observed. In the absence of Janus particles, no emulsions are stabilized.

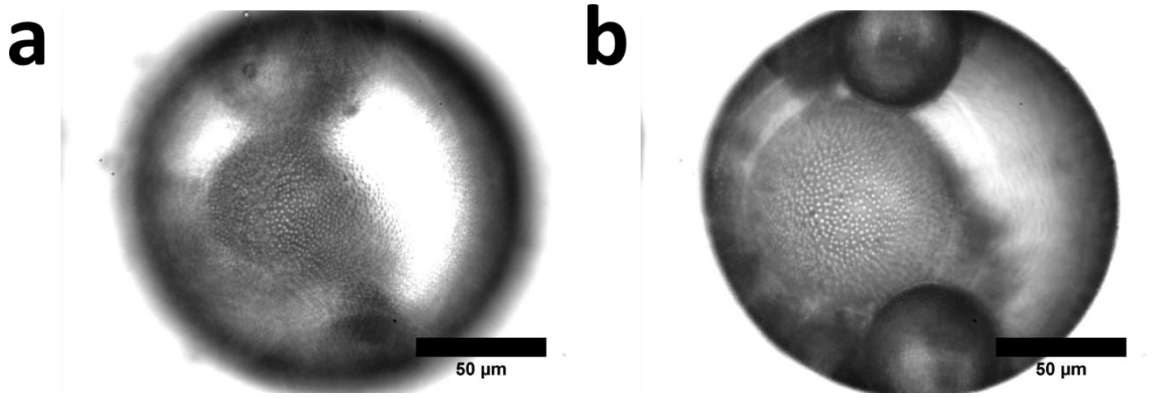

Figure 4.3 Microscopy images of a multiple emulsion droplet showing Janus particles adsorbed at both (a) outer and (b) inner oil-water interfaces.

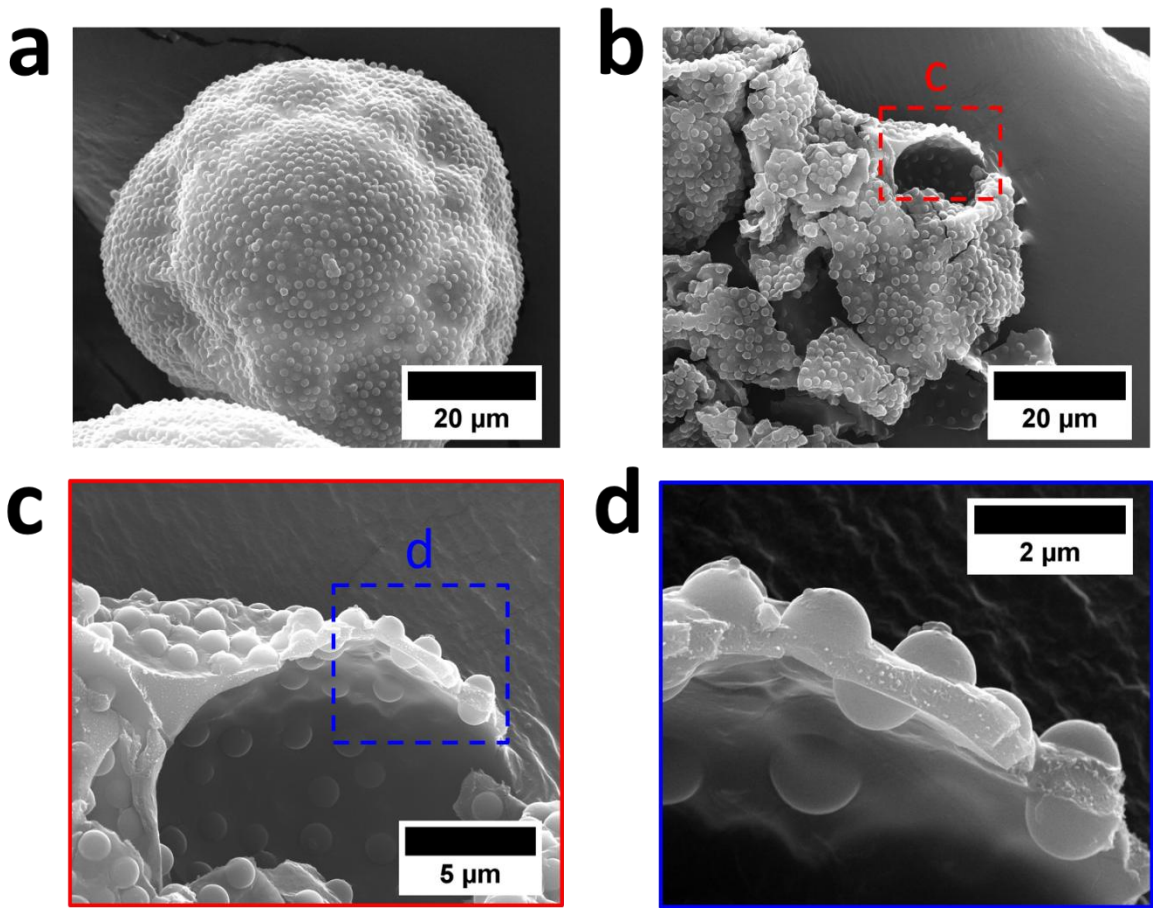

Figure 4.4 SEM images of (a) intact and (b-d) broken multiple emulsion stabilized by (Sty50/AA50) Janus particles. (c) and (d) are taken from the red and blue dashed areas in (b) and (c), respectively. The scale bars are 20 µm for (a) and (b), 5 µm for (c) and 2 µm for (d).

We modify a previously reported gel trapping method to directly visualize the orientation of Janus particles at the two oil-water interfaces of multiple emulsions. The SEM samples are prepared by emulsifying chloroform containing 5 wt% linear polystyrene (M_w=45k) together with deionied water containing 0.5wt% (Sty50/AA50) Janus particles. The volume fraction of oil phase is 0.2. The multiple emulsions solidified by evaporating

chloroform, which traps Janus particles at the oil-water interfaces. As shown in Figure 4.4 (a), the outer interface is densely covered with Janus particles. Samples in Figure 4.4 (b-d) are prepared by breaking the solidified multiple emulsions between two glass slides. As shown in Figure 4.4 (b-d), we can clearly see that Janus particles are adsorbed on both the inner and outer interfaces of the multiple emulsion. As shown in Figure 4.1, the smooth side of (Sty50/AA50) Janus particles is rich in acrylic acid and thus is hydrophilic.[1] The exposed sides of Janus particles adsorbed at the both inner and outer interfaces of multiple emulsion shown in Figure 4.4 (d) has very smooth surfaces, indicating that the exposed sides are rich in acrylic acid, which is the hydrophilic side of (Sty50/AA50) Janus particles. These results clearly demonstrate that the Janus particles adopt the so-called upright orientation (*i.e.*, each side is exposed to the preferred fluid phase) at the surface.

Although the generation of W/O/W multiple emulsions during catastrophic phase inversion have been well-documented[164], such W/O/W multiple emulsions are found to be transient or extremely unstable. In stark contrast, our W/O/W multiple emulsions stabilized by (Sty50/AA50) Janus particles are not temporary emulsions. To demonstrate the stability of multiple emulsions stabilized by (Sty50/AA50) Janus particles, we take photos and microscopy images of a multiple emulsion two hours and more than three months after preparation. Figure 4.5 (a), (b) and (c) are taken on June 10th 2014. Figure 4.5 (d), (e) and (f) are taken on September 27th 2014. Comparing Figure 4.5 (a) and (d), no macroscopic changes can be observed. Comparing Figure 4.5 (c) and (f), multiple

emulsion droplets contain large number of aqueous inner droplets that show green fluorescence (calcein) after 3 months of storage. These observations indicate that the multiple emulsions remain stable for at least three months.

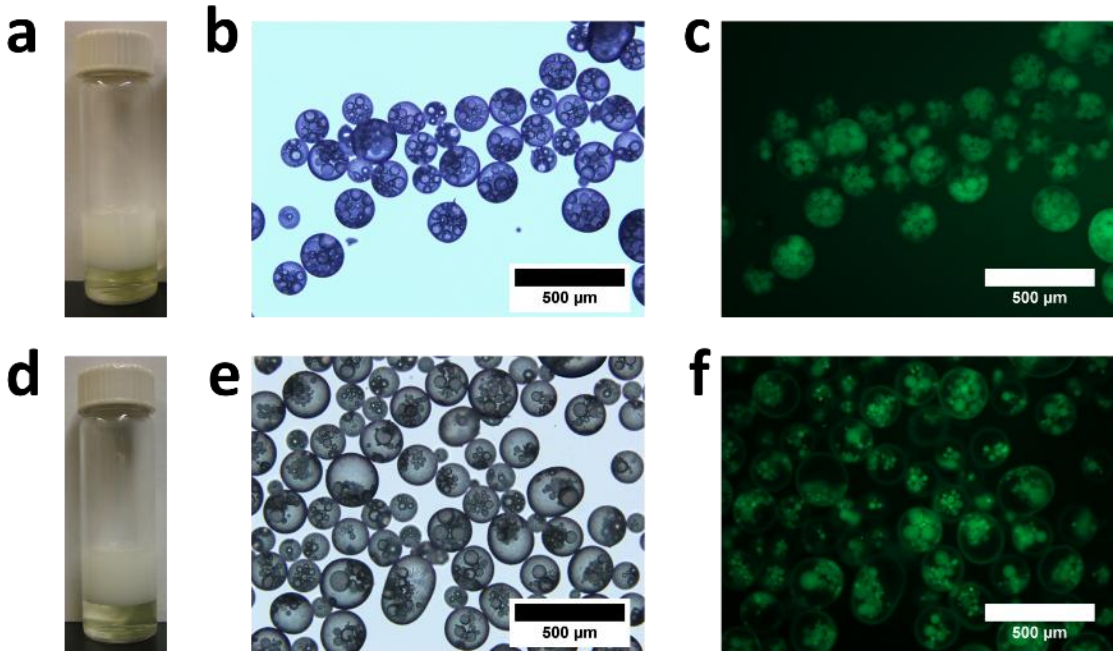

Figure 4.5 Photos and Microscopy images of multiple emulsion (a-c) two hours and (d-f) more than three months after emulsification. Multiple emulsions are made from 1 wt% (Sty50/AA50) Janus particle dispersed in deionized water and toluene with ϕ_o = 0.4. 1.5×10-4 wt% calcein added in the water phase. The scale bar is 500 µm.

To determine conditions that lead to the generation of such highly stable multiple W/O/W emulsions, we study the effect of the solution pH of the water phase and the volume fraction of oil phase (ϕ_o) on the type of emulsion generated using (Sty50/AA50) Janus particles. As shown in Figure 4.6 (c), the effects of these two parameters can be summarized as a phase diagram, which can be divided into four regions. When the pH of

the water phase is 11, the preferred emulsion type is O/W emulsion because the hydrophilic acrylic acid-rich (AA-rich) side is larger than the hydrophobic styrene-rich (Sty-rich) side, giving Janus particle more hydrophilic characteristics due to the ionization of the AA-rich side.[162] The upper left region where pH = 11 and $\phi_o \leq 0.5$ represents simple O/W emulsions. However, when $\phi_o > 0.5$, stable emulsions cannot be generated and these mixtures separate into two macroscopic oil and water phases in less than one minute after homogenization. When the pH of the water phase is lower than 11, the preferred emulsion type is W/O emulsion because (Sty50/AA50) Janus particle behaviours are dominated by their lipophilic characteristics due to the protonation of the AA-rich side.[162] At pH < 11, simple W/O emulsions are generated when $\phi_o \geq 0.5$. These simple W/O emulsions are transformed to W/O/W multiple emulsions by decreasing the oil fraction ϕ_o below 0.5. This one-step emulsification method is advantageous over traditional two-step emulsification method because it greatly simplifies the process for the preparation of multiple emulsions and prevents the possible loss of encapsulated species during the second emulsification process involved in the conventional two-step method.

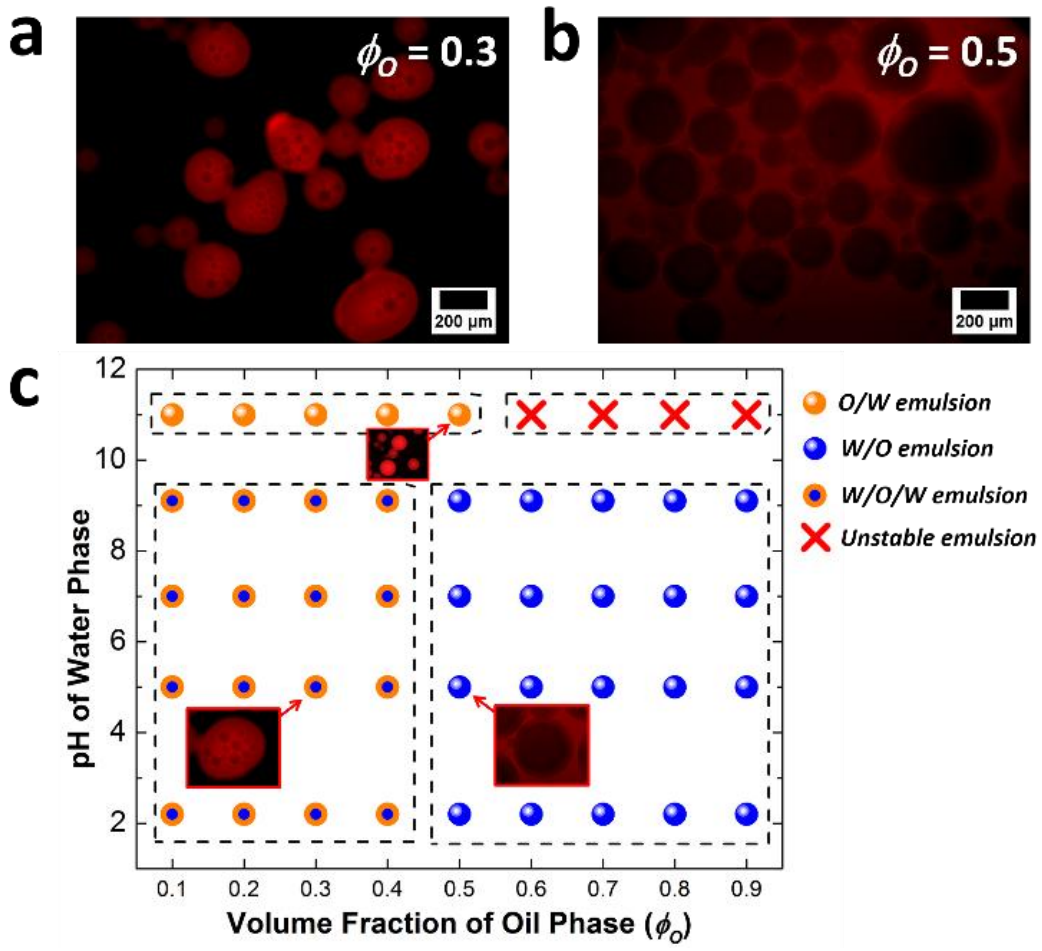

Figure 4.6 Fluorescent microscopy images of emulsion stabilized by 0.5wt% (Sty50/AA50) Janus particles at pH5.0 with volume fraction of oil phase (ϕ_o) equal to (a) 0.3 and (b) 0.5, respectively. The scale bar for fluorescent images is 200 μm. (c) Phase diagram of emulsion made with (Sty50/AA50) Janus particles as a function of both pH of water phase and volume fraction of oil phase (ϕ_o).

It has been proposed that catastrophic phase inversion is induced by increasing the effective volume fraction of the dispersed phase.[165] The effective volume fraction of the dispersed phase is increased by the inclusion of the continuous phase into the droplets of dispersed phase with prolonged emulsification; that is, the effective volume fraction of

the continuous phase decreases.[165] This idea indicates that the time of emulsification is important in achieving catastrophic phase inversion. To test this idea, we monitor the evolution of emulsions as a function of emulsification time. The volume fraction of oil phase ϕ_o is kept constant at 0.4. Based on the phase diagram in Figure 4.6, this composition should give a W/O/W multiple emulsion. When the time of emulsification is less than 20 seconds, however, W/O simple emulsions are observed as shown in Figure 4.7, which is evident from the sedimentation of the emulsion phase and the red fluorescence coming from the continuous phase. When the time of emulsification is increased above 25 seconds, W/O/W multiple emulsion are generated, which can be seen by the emulsion phase creaming to the top and the red fluorescence coming from the dispersed phase. These observations are in agreement with the phase diagram in Figure 4.6 (c). The observed phenomena indicate that at the very early stage of emulsification, the type of emulsion generated is dominated by the intrinsic properties of (Sty50/AA50) Janus particles - shape and amphiphilicity - rather than the composition of the two-phase mixture. As the time of emulsification increases, W/O emulsion suddenly inverts to W/O/W multiple emulsion which is consistent with the inclusion mechanism. Previous studies have observed similar phenomena that lead to the formation of W/O/W double emulsions.[13] The exact pathway by which W/O emulsions inverts into W/O/W emulsions, however, is not fully understood and warrants future investigation. We believe the reason W/O/W multiple emulsions generated with (Sty50/AA50) Janus particles are highly stable unlike those generated during phase inversion of common surfactant-stabilized

emulsions is due to their tendency to attach strongly and remain at the fluid interfaces, unlike molecular surfactants that easily desorb. In fact, studies have shown that the detachment energy of Janus particles from fluid-fluid interfaces is several orders of magnitude greater than thermal energy, k_BT.[59,63,86]

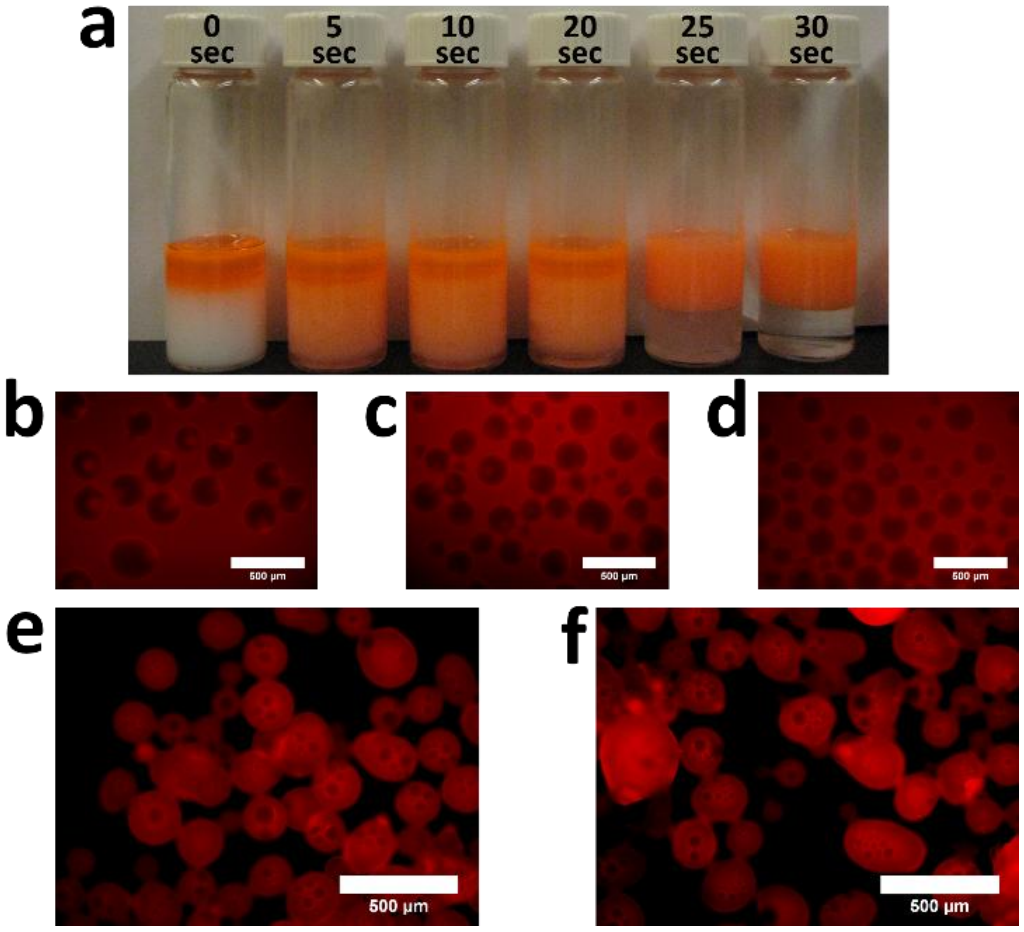

Figure 4.7 (a) Photo and (b-f) fluorescence microscopy images of emulsions made with different time of emulsification: (b) 5, (c) 10, (d) 20, (e) 25 and (f) 30 seconds, respectively. Each glass vial is labelled with time of emulsification. Emulsions are made with ϕ_o = 0.4. Water phase consists of deionized water and 0.5 wt% Janus particles. The scale bars for fluorescent images are 500 µm.

4.3.2 One-step Encapsulation by Janus Particle-stabilized Multiple Emulsion

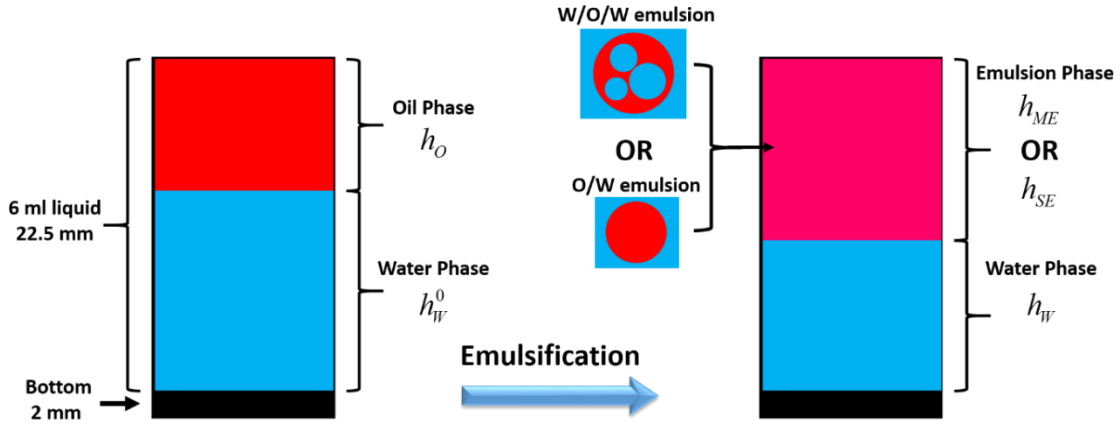

Figure 4.8 Schematic illustration of parameters for the calculation of packing fraction and encapsulation fraction.

The one-step generation of W/O/W multiple emulsions represents an excellent encapsulation technique because these emulsions can carry and protect hydrophilic species in the aqueous inner droplets, which is important in a number of applications. Although a few studies on preparation of multiple emulsions by one-step emulsification with only one emulsifier have been reported, little is known about how various parameters affect the encapsulation process. To determine how encapsulation is affected by the solution conditions, we carry out a systematic study on the effect of several important parameters on the encapsulation fraction of these Janus particle-stabilized multiple emulsion. The encapsulation fraction (ε) is defined as the volume ratio of encapsulated water phase and the original water phase before emulsification, thus should have a formula as shown in Equation (4-1)

$$\varepsilon = \frac{V_{encap}}{V_W^0} \quad (4\text{-}1)$$

where V_{encap} and V^0_W represent the volume of encapsulated water phase and original water phase, respectively. Because $V_{encap}=V_{ME}P-V_O$, therefore we rewrite Equation (4-1) as

$$\varepsilon = \frac{V_{ME}P - V_O}{V_W^0} \quad (4\text{-}2)$$

where V_{ME} and V_O denote for the volume of multiple emulsion phase and oil phase, respectively. P represents the packing fraction of emulsion droplets in emulsion phase. Because the height is directly proportional to the volume in a cylindrical glass vial, Equation (4-2) can also be written as

$$\varepsilon = \frac{h_{ME}P - h_O}{h_W^0} \quad (4\text{-}3)$$

where h_{ME}, h_O and h^0_W denote for the height of multiple emulsion phase, oil phase and original water phase in a vial, respectively, as shown in Figure 4.8. The height of different phases can be directly measured. The packing fraction of emulsion droplets needs to be determined with simple emulsions as shown in Figure 4.8. The packing fraction can be calculated as

$$P = \frac{h_O}{h_{SE}} \qquad (4\text{-}4)$$

where h_O and h_{SE} denote for the heights of oil phase and simple emulsion phase, respectively. The height of emulsion phase and that of water phase is related by

$h_{SE} = 22.5 - h_W$ (4-5) and

$h_{ME} = 22.5 - h_W$ (4-6)

Because the total volume of the liquid is fixed at 6 ml which corresponds to 22.5 mm in height in the glass vial as shown in Figure 4.8. As shown in Table 4.1, the average packing fraction *P* as determined using simple O/W emulsion at pH 11.0 is 0.67 which is consistent with the packing of polydisperse spheres and emulsions.[2]

Table 4.1 Parameters obtained from O/W emulsion in Figure 4.9 (a) and packing fraction calculated for each case.

V_O/V_W	10:90	20:80	30:70	40:60	50:50
h_O (mm)	2.25	4.5	6.75	9	11.25
h_W (mm)	19	16	12	9	6
h_{SE} (mm)	3.5	6.5	10.5	13.5	16.5
P	0.64	0.69	0.64	0.67	0.68

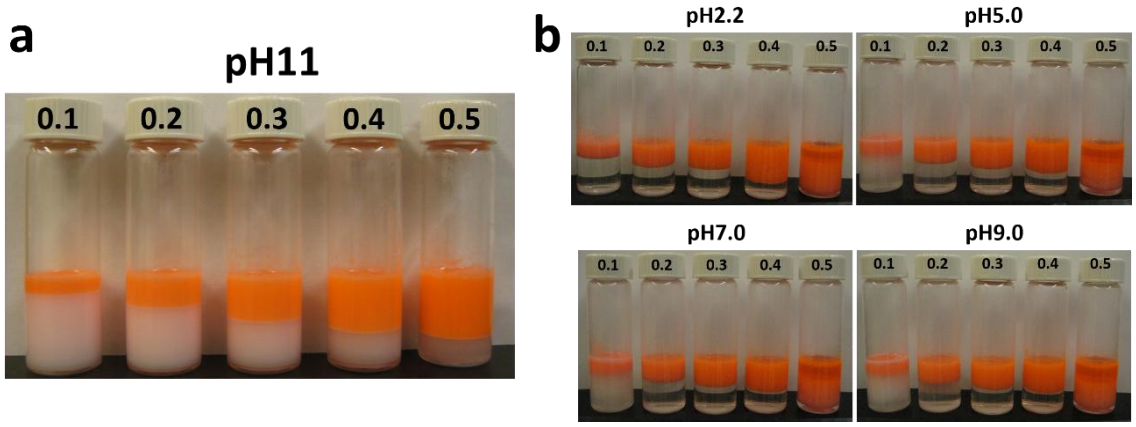

Figure 4.9 Emulsions made at (a) pH11.0 and (b) pH lower than 11.0 with different ϕ_o for calculating (a) packing parameter and (b) encapsulation fraction, respectively. In all cases, particle concentration is kept as 0.5 wt%.

The encapsulation fraction is first determined as a function of volume fraction of oil phase (ϕ_o) and pH of water phase as shown in Figure 4.10 (a). The concentration of (Sty50/AA50) Janus particles in water phase is kept constant at 0.5 wt%. For a given ϕ_o, the pH of water phase does not have a significant effect on the encapsulation fraction; however, the encapsulation fraction is apparently higher at pH 2.2 than higher pH. This apparent increase is probably because the packing fraction *P* is overestimated for emulsion droplets at pH 2.2 resulting in a higher encapsulation fraction. We have shown previously that emulsion droplets tend to aggregate and form clusters at pH 2.2 indicating emulsion droplets have strong attractions between each other.[162] Strong attractive emulsion droplets are known to form loosely packed flocculates in the emulsion phase.[146] For a given pH, the encapsulation fraction decreases with increasing ϕ_o. At pH 7.0, for example, the encapsulation fraction is increased by more than a factor of two by

decreasing the volume fraction of oil from 0.4 to 0.1. This enhancement is probably because the volume fraction of particles in the total mixture is decreasing with increasing ϕ_o. With a larger amount of particles, more water phase is expected to be encapsulated. To confirm this hypothesis, we study the effect of particle concentration on encapsulation fraction by keeping the particle concentration and pH solution at ϕ_o = 0.4 and pH 7.0, respectively. As shown in Figure 4.10 (b), the encapsulation fraction increases by more than 10 folds from 3% to 33% as particle concentration increases from 0.5% to 3%, which indicates that particle concentration is indeed a critical parameter affecting the encapsulation process.

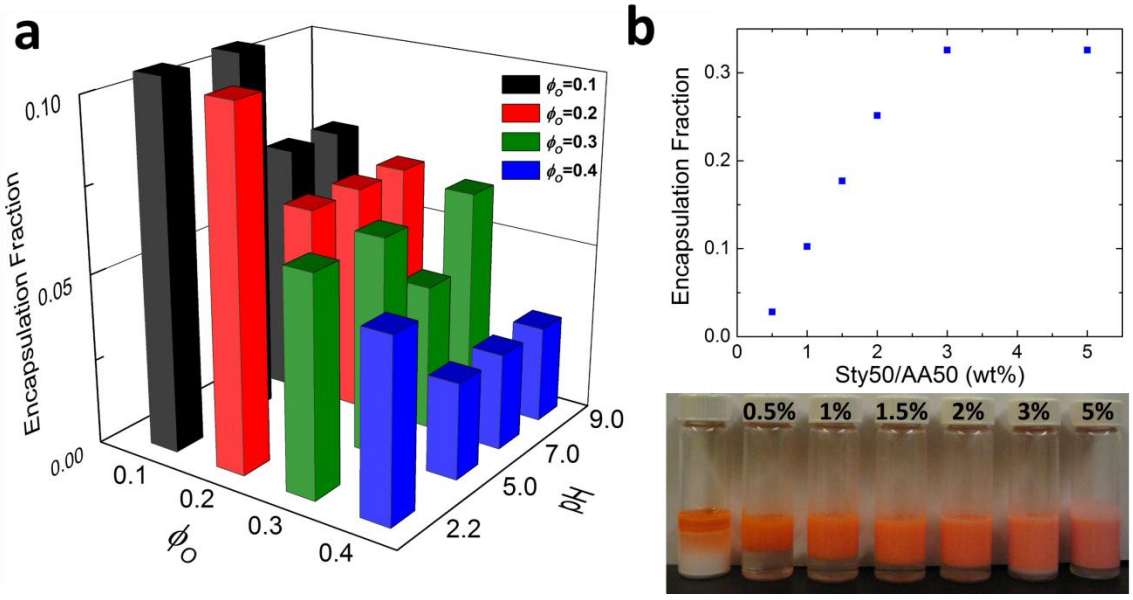

Figure 4.10 (a) Encapsulation fraction as a function of ϕ_o and pH of water phases. Particle concentration is kept at 0.5 wt%. (b) Encapsulation fraction as a function of particle concentration. ϕ_o and pH are kept 0.4 and 7.0, respectively.

4.3.3 Triggered Release

Triggered release from multiple emulsions is highly desirable for various applications that require the protection of active species under "normal" conditions and the release of the actives upon significant changes in the environment. As discussed above, one-step formation of stable multiple emulsions and the triggered release of encapsulants may seem incompatible and contradictory properties since triggered release requires the destabilization of multiple emulsions. The phase diagram in Figure 4.6 (c), however, provides us with a clear roadmap to overcome such a limitation. Triggered release from double emulsions should be possible by simply increasing the solution pH. We directly observe a triggered release process by monitoring the changes in the morphology of the same W/O/W multiple emulsion droplet upon pH increase and take images of it at different time.

Two significant changes are observed during the release of the inner water droplets as shown in Figure 4.11 (a). The number of inner droplets decreases significantly, indicating effective release of the inner droplets. The destabilization of inner water droplets is likely due to the swelling of the AA-rich side of (Sty50/AA50) Janus particles, which make them favor the interface of O/W emulsion rather than that of the inner W/O interface. Thus the inner droplets become unstable and undergo coalescence with each other and with the continuous phase. More interestingly, the outer O/W interface undergoes drastic changes in its appearance, and, at the end of these changes, a thick layer of particles covering the droplet surface is observed. Two factors are likely to be responsible for

these observed changes. The change in the shape of the Janus particle leads to an increased packing fraction of the particles and stronger lateral repulsion at the interface, which could push some particles out of the interface. In addition, as the inner aqueous droplets are expelled from the oil droplet, Janus particles that were covering the inner droplets accumulate at the outer O/W interface. Both of these factors lead to the formation of multilayers of Janus particles at the O/W interface. Results shown in Figure 4.11 (a) clearly suggest that when the pH of the continuous phase is raised, hydroxide ions (OH-) are able to transport through the oil phase of W/O/W multiple emulsions to induce the destabilization of the inner aqueous droplets. To facilitate and accelerate this transport process and thus the subsequent release of the inner drops, we apply a gentle agitation by tumbling the vial containing a W/O/W multiple emulsion (ϕ_o = 0.4 and 1 wt% (Sty50/AA50)) at 120 rpm for 2 min. We add a fluorescent dye, calcein, in the aqueous phase as a model encapsulant. As shown in Figure 4.11 (b), the boundary between emulsion phase and water phase is the same for multiple emulsions before and after agitation when no changes in the pH of the solution are induced. Fluorescent microscopy images of these two multiple emulsions also do not show significant difference as shown in Figure 4.11 (c) and (d). When the solution pH of the multiple emulsion is raised by adding a small volume (400 μL) of 1.0 M NaOH, we observe a drastic increase in the height of the water phase indicating release of aqueous inner droplets from the multiple emulsion (Figure 4.11 (b)). In addition, fluorescence microscopy images shown in Figure 4.11 (c) and (e) also show clear difference between

emulsions before and after pH increase; most of the inner droplets have disappeared leaving a small number of tiny water droplets in the oil phase, regardless of the size of multiple emulsion droplets. In fact, we estimate that more than 90 vol% of the encapsulated water phase has been released, indeed confirming that mild agitation can drastically accelerate the triggered release from Janus particle-stabilized multiple emulsions.

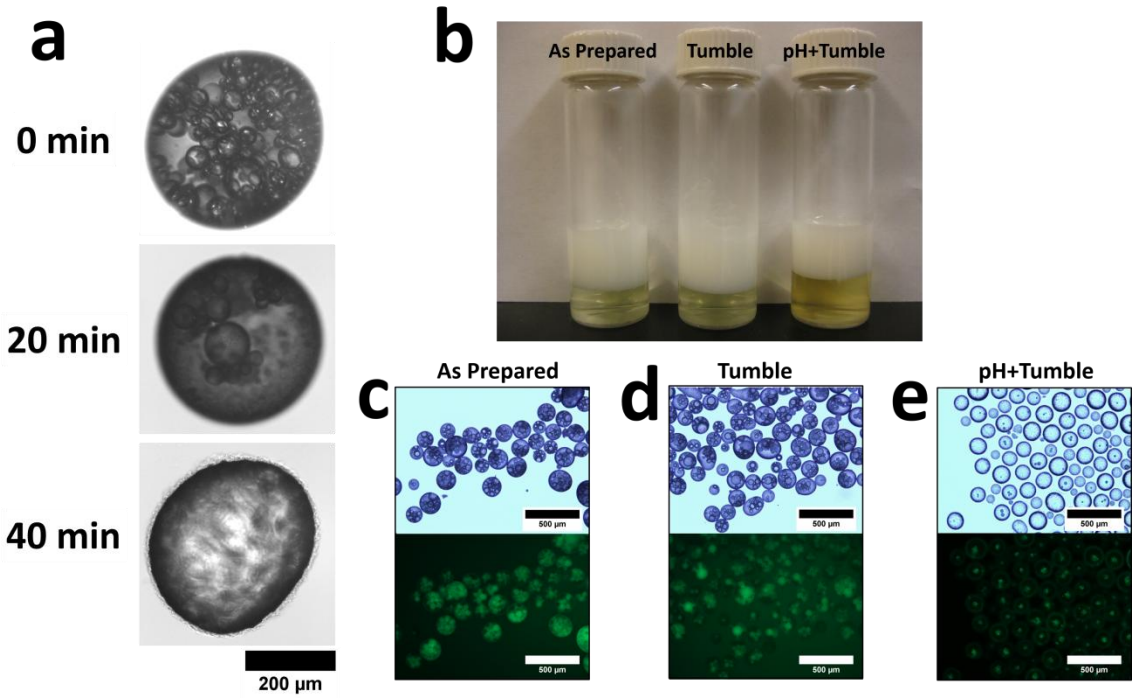

Figure 4.11 (a) Microscopy images of evolution of a multiple emulsion drop upon pH increase. Multiple emulsions are made from 0.5 wt% (Sty50/AA50) Janus particle dispersed in pH2.2 water and toluene with ϕ_o = 0.2. (b) Photo and microscopy images of (c) as-prepared multiple emulsion, (d) multiple emulsion with tumble only and (e) multiple emulsion tumbled with increasing pH. Multiple emulsions are made from 1 wt% (Sty50/AA50) Janus particle dispersed in deionized water and toluene with ϕ_o = 0.4.

1.5×10-4 wt% calcein added in the water phase. The scale bar is 200 μm for (a) and 500 μm for (c), (d) and (e).

4.4 Conclusions

In conclusion, we have demonstrated that highly stable W/O/W multiple emulsions can be generated with Janus particles via one-step emulsification, enabling the one-step encapsulation of hydrophilic species in multiple emulsions. More importantly, increasing the solution pH triggers the destabilization of aqueous compartments and subsequent release of encapsulants from these multiple emulsions. Our study is a powerful demonstration of the versatility of Janus particles as solid surfactants. It shows that indeed Janus particles can exhibit functionalities that are not easily realized using conventional molecular surfactants. Since these pH-responsive Janus particles can be generated in large quantities, we believe these Janus particles have significant potential in impacting a number of areas that require stable double emulsion products that can release actives upon changes in the local environment. We believe microscale studies that would uncover how these Janus particles stabilize inner water/oil and outer oil/water fluid interfaces and subsequently induce triggered release upon pH change would lead to deeper understanding on the mechanism of one-step formation of multiple emulsions and triggered release of encapsulants.

Chapter 5. Synthesis of Janus Particles with Pure Compartments and Anisotropic Particles

5.1 Introduction

During the past two decades, we have witnessed a great effort of using Janus particles in both fundamental studies and practical applications.[18] Unlike homogeneous particles, Janus particles have anisotropic interactions with the environment and themselves, thus they can assemble into novel structures such as chain structure and tube structure, which are seldome observed with homogeneous particles.[166] One example is that colloidal fibers made of Janus ellipsoids have shape-memory properties that can be actuated on application of an external alternating-current electric field.[167] Janus particles are also used as nano-/micro motor which are able to self-propell in solution or at interfaces. A major goal is to mimic biological functions and develop vehicles for cargo transport and delivery application.[168] The asymmetric catalytic properties on the two sides of Janus particles induce non-equilibrium distribution of matter such as gaseous bubbles propelling the particles forward.[169] Another interesting application of Janus particles with different catalytic properties is to use them as interfacial catalyst with phase selectivity. A recent study showed that Janus particles with catalyst only on the hydrophobic face had better phase selectivity than the particles with catalyst on both sides. Such phase-selectivity is especially important for bio-fuel refining processes involving numerous

reactions where phase-selectivity is crucial to achieve high yield and to avoid competing reactions from hampering product formation. They have also described the advantages of using Janus particles as "interfacial catalyst emulsifiers", such as high conversion because of high interfacial area and easy separation of the catalyst and reaction product.[20]

All the interesting properties and applications of Janus particles reported relies on the distinct properties on the two sides of the particles, thus methods for producing such particles is imperative. In *Chapter 3,* we introduced a bulk synthesis method for making uniform amphiphilic Janus particles with a styrene-rich and an acrylic acid-rich domes as the hydrophobic and the hydrophilic side, respectively. These Janus particles are promising for making particles with anisotropic optic, magnetic and catalytic properties because studies have shown that microgels with acrylic acid can be used as nano-reactor for synthesizing various nanoparticles including metal, metal oxide and semi-conductor.[170,171] However, the Janus particles synthesized using our method do not have pure compartments. That is, there is some amount of acrylic acid and styrene existing in the hydrophobic and hydrophilic side, respectively. Thus it is likely that the distribution of nanoparticles in the Janus particles will not be asymmetric. To overcome this problem, synthesis methods that can produce Janus particles with pure compartments are highly desirable.

In this chapter, a modified method is developed to generate Janus particles with pure hydrophobic and hydrophilic compartments by investigating the effect of several parameters of the synthesis scheme of *Chapter 3* on the final morphologies of Janus

particles. Surfactants and the type of monomer used during the synthesis are found to be of critical importance. The newly developed synthesis method also allows us to generate highly uniform anisotropic particles in a large quantity.

5.2 Experimental Section

5.2.1 Synthesis of Particles

Particles are synthesized by seeded emulsion polymerization followed by acid hydrolysis. The monodisperse seed particles composed of linear polystyrene (LPS) are synthesized by dispersion polymerization. First, 0.03 gram polyvinylpyrrolidone (PVP, Mw ~ 55,000) is dissolved in 75 ml isopropyl alcohol (IPA, 99.9%) in a 100 ml flask. Then 9 ml deionized (DI) water containing 0.02 gram ammonium persulfate (APS, 98%) as initiator is added to the flask followed by adding 6.6 ml styrene (≥99%). After the flask is sealed with a rubber stopper and Teflon® tape, the mixture is well mixed by shaking the flask for 60 seconds. Subsequently the mixture is purged with nitrogen for 5 minutes. The flask is mounted onto a tumbler (IKA® RW16 basic) and immersed in oil bath at 70 ℃. The flask is tumbled at 100 revolutions per minute (rpm) for 24 hours for polymerization. After polymerization, the particles are washed four times with DI water using centrifugation. 20 wt% LPS dispersion is prepared by dispersing LPS particles in either 1 wt% poly vinyl alcohol (PVA, Mw 13,000-23,000, 87-89% hydrolyzed) aqueous solution or 0.4 wt% sodium dodecyl sulfate (SDS) aqueous solution. A monomer emulsion is

prepared by vortexing a mixture consisting of either styrene or toluene, either *tert*-butyl acrylate (*t*BA, 98%) or *tert*-butyl methacrylate (*t*BMA), with or without 1 vol% divinyl benzene (DVB, 55%) and 0.5 wt% initiator 2,2'-Azobis(2.4-dimethyl valeronitrile) (V-65B) (Wako) with either 1 wt% PVA aqueous solution or 0.4 wt% SDS aqueous solution. LPS particles are swollen with the monomer mixture by mixing the LPS dispersion and the monomer emulsion. The particle-monomer mixture is mounted on a rotator (Glas-Col®) and rotated for 8 hours at 60 rpm. Seeded emulsion polymerization is performed by tumbling the particle-monomer mixture in an oil bath at 70 ℃ at 100 rpm for 10 hours. If the particles are prepared with toluene in the monomer mixture, these particles are placed in a water bath of 50 ℃ overnight to evaporate the toluene after seed emulsion polymerization. If there is no toluene in the monomer mixture, no evaporation is needed. Then particles are washed with DI water for least 6 times by centrifugation to remove surfactants and unreacted monomer. The particles from seeded emulsion polymerization are then stirred in an acid mixture consisting of 80 vol% trifluoroacetic acid (TFA, 99%) and 20 vol% formic acid (FA, ≥95%) at 1200 rpm for 24 hours for hydrolysis of *t*BA. The volume ratio of particles and acid mixture is 1:40. The hydrolyzed particles are washed with DI water for at leaset 6 times by centrifugation.

5.3 Results and Discussions

The main reason for the presence of some amount of styrene and acrylic acid in acrylic acid-rich side and styrene-rich side of Janus particles, respectively, discussed in the previous two chapters is that the monomer mixture consists of both styrene and *tert*-butyl acrylate (*t*BA). The polymer chain produced during seeded emulsion polymerization is a copolymer network of both styrene and *t*BA which could have considerable miscibility with the linear polystyrene (LPS) seed particles. In order to synthesize a pure polymer network of poly *tert*-butyl acrylate (P*t*BA) during seeded emulsion polymerization, we replace styrene with toluene because toluene is non-polymerizable and can be removed by evaporation after polymerization of *t*BA. There is a significant change in the morphology of Janus particle when we switch from styrene to toluene as shown in Figure 5.1. With monomer mixture containing toluene, the polymer network is pure polyacrylic acid (PAA) after hydrolysis. Thus it shrinks significantly after removal of water losing its structure integrity and hides in the center of a PS hemispherical particle as shown in Figure 5.1 (a). Janus particles synthesized with monomer mixture containing styrene remains almost spherical after removal of water as shown in Figure 5.1 (b). This is probably because the polymer network synthesized from the monomer mixture contains considerable amount of styrene in it whose polymer has a much higher glass transition temperature, which helps the Janus particles to maintain their structure. However, using toluene instead of styrene does not seem to promote complete phase separation as

indicated by the dimples on the PS hemisphere as shown in Figure 5.1 (a) which might be micro-phase separated domains of PAA.

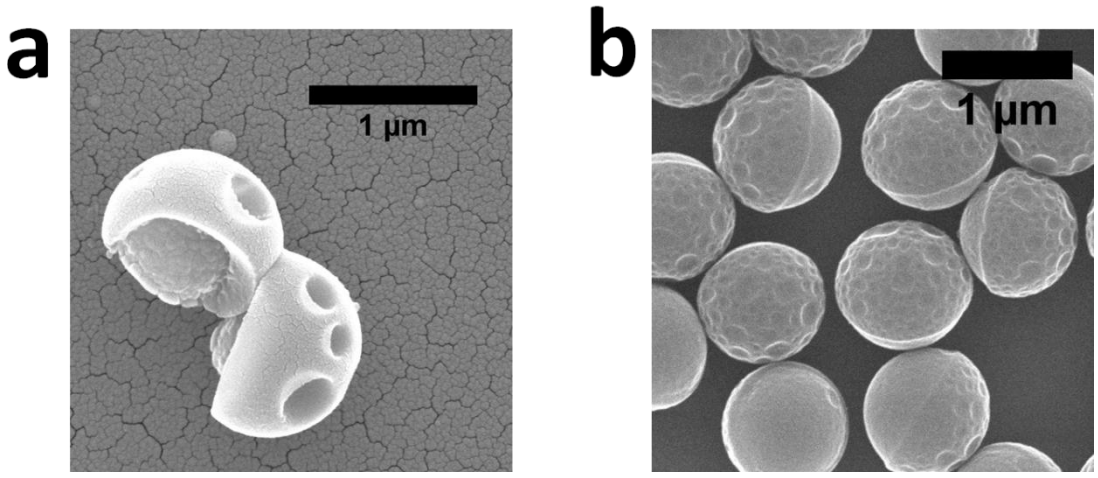

Figure 5.1 Scanning electron microscopy images of Janus particles synthesized with monomer mixture containing (a) toluene and (b) styrene. The monomer mixture consists of 50 vol% of either toluene or styrene and 1 vol% divinyl benzene as cross-linker. The rest monomer is *t*BA. LPS dispersion and monomer emulsion are prepared with 1 wt% PVA aqueous solution. The volume ratio between monomer mixture and LPS is 4:1. The scale is 1 μm.

Another reason for this incomplete phase separation could be the presence of 1 vol% cross-linker, divinyl benzene (DVB) because cross-linked polymer network will greatly reduce the mobility of polymer chain thus retarding the phase separation. Therefore, we remove DVB from the monomer mixture and still use toluene instead of styrene in the monomer mixture. After hydrolysis, however, the only remaining part is the PS dome as shown in Figure 5.2. This is interesting but not surprising because, without the cross-linker, what is synthesized during the seeded emulsion polymerization is linear P*t*BA

which is converted to linear PAA after hydrolysis. Linear PAA is highly soluble in water thus they are washed away during the washing step after hydrolysis as shown by the schematic in Figure 5.3. The remaining PS dome, however, still has several dimples on it indicating incomplete phase separation even if there is no cross-linker added during the synthesis. Therefore, the amount of cross-linker used in our synthesis might not be the main factor for the incomplete phase separation.

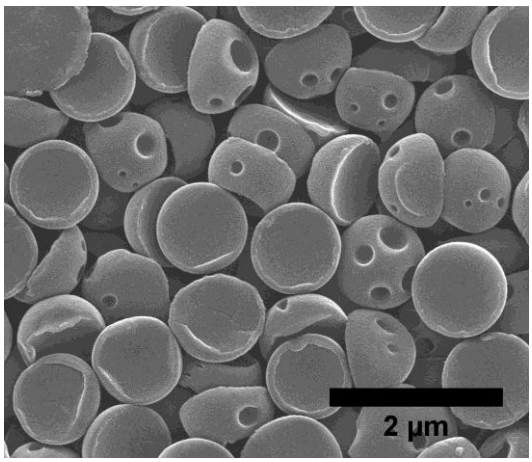

Figure 5.2 The scanning electron microscopy image of particles synthesized with a monomer mixture containing toluene and *t*BA without cross-linker DVB. LPS dispersion and monomer emulsion are prepared with 1 wt% PVA aqueous solution. The volume ratio between monomer mixture and LPS is 4:1. The scale is 2 µm.

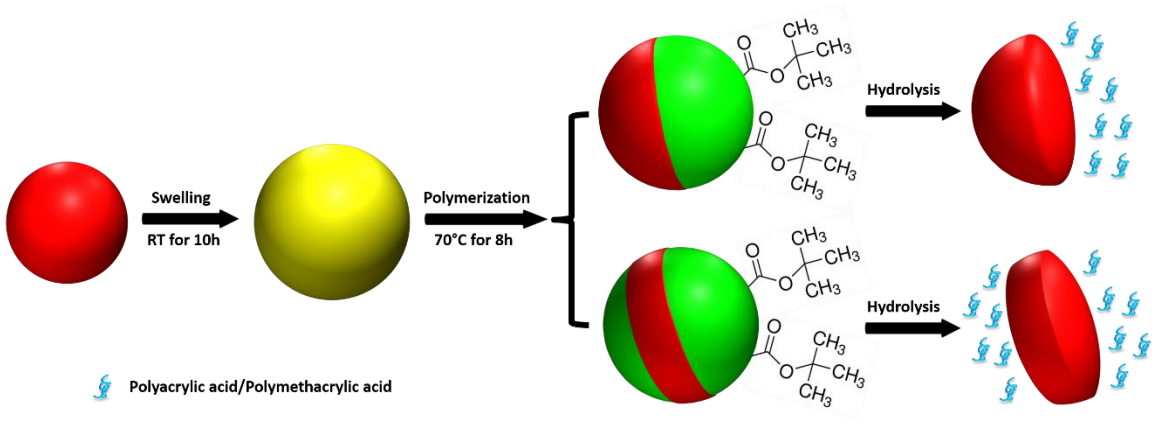

Figure 5.3 Schematic of the procedure for synthesizing geometrically anisotropic particles

Studies have shown that the type of surfactant is an important factor in controlling the phase separation of two immiscible polymers inside a composite particle because such phase separation is dominated by interfacial energy. Thus the minimization of interfacial energy determines the equilibrium morphology of composite particles, which is given as

$$\Delta G = \sum \gamma_i A_i - \gamma_0 A_0 \quad (5\text{-}1)$$

where γ_i stands for the interfacial tension between the two polymers or between aqueous phase and the two polymers, while and A_i represents the area of corresponding interface.[172] Sodium dodecyl sulfate (SDS) has been shown to be critical for moon-like morphology particles formed by evaporating the organic solvent of a droplet containing PS and polymethyl methacrylate (PMMA), because SDS is able to significantly reduce the interfacial tensions between PS in toluene and aqueous phase ($\gamma_{PS\text{-}T/W}$) and also between PMMA in toluene and aqueous phase ($\gamma_{PMMA\text{-}T/W}$) to a similar value (3~6

mN/m).[173] Thus we use SDS instead of PVA for preparing LPS dispersion and monomer emulsion. Particles are synthesized with monomer mixture containing toluene with and without cross-linker. Without cross-linker in the monomer mixture, the particles we get after hydrolysis have smooth surface as shown in Figure 5.4 (a) which is an indication of complete phase separation between PS and P*t*BA. No dimples are observed on the surface of particles like particles synthesized with PVA aqueous solution as shown in Figure 5.2. This is strong evidence that the type of surfactant has a significant effect on the phase separation of two incompatible polymers confined in a droplet of a common solvent. With cross-linker in the monomer mixture, we notice that PAA polymer network converted from poly P*t*BA after acid hydrolysis collapses. Dimples on the hard PS domes are still observed, however the depth of the dimples as shown in Figure 5.4 (b) are not as significant as particles shown in Figure 5.1 (a), which we believe comes from the fact that SDS is better than PVA at promoting complete phase separation.

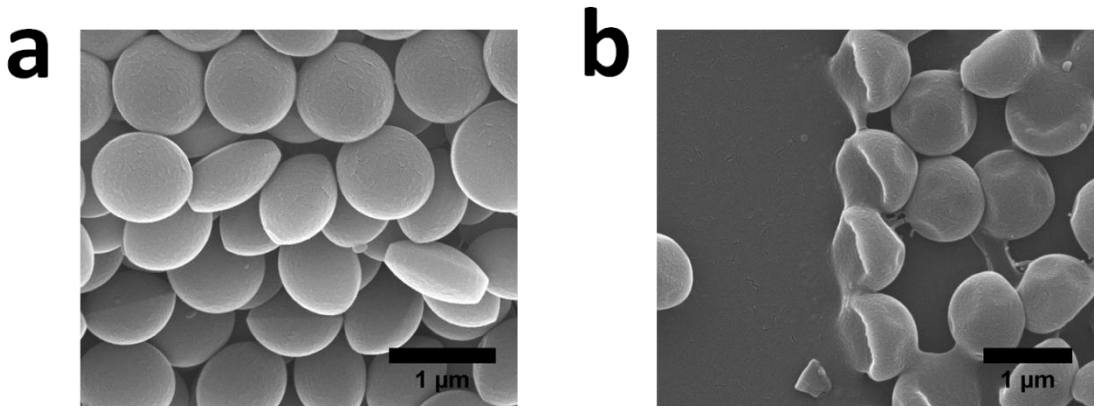

Figure 5.4 Scanning electron microscopy images of particles synthesized with a monomer mixture containing toluene and *t*BA (a) without and (b) with 1 vol % cross-

linker DVB. LPS dispersion and monomer emulsion are prepared with 0.4 wt% SDS aqueous solution. The volume ratio between monomer mixture and LPS is 4:1. The scale is 1 μm.

In addition to the type of surfactant, the glass transition temperature of the two polymers also affects the extent of phase separation. It has been reported that composite particles made of two polymers with higher glass transition temperature have more distinctive phase separation.[174] Therefore, we use *tert*-butyl methacrylate (*t*BMA) instead of *t*BA in the monomer mixture for seeded emulsion polymerization because the addition of an extra methyl group gives poly *tert*-butyl methacrylate (P*t*BMA) a higher glass transition temperature than P*t*BA. Under the same condition for hydrolyzing P*t*BA, P*t*BMA can be converted to poly methacrylic acid (PMAA) which is also one type of hydrogel materials. As shown in Figure 5.5 (a), the use of *t*BMA does promote better phase separation as indicated by the smooth surface of the hemisphere. Because of the evaporation of water, PMAA hydrogel network shrinks and hide in the center of the hemisphere. When these particles are dispersed in deionized water, we observe that these particles all have a dark part and the other part is almost transparent under optic microscope as shown in Figure 5.5 (b). We believe the dark part is PS. The part that is almost transparent is PMAA hydrogel network. Because the pKa of methacrylic acid (MAA) (~4.66) is lower than the pH of deionized water (5~6), the PMAA hydrogel takes a fully swollen state with a lot of water molecules inside which makes it almost transparent.

To demonstrate that better phase separation is achieved with toluene and *t*BMA as monomer mixture and SDS aqueous solution, we dyed (Sty50/AA50) Janus particles in

Chapter 3 and particles as shown in Figure 5.5 (a) with a hydrophobic fluorescent dye Nile Red. This is done by placing a droplet of toluene containing 0.01 wt% Nile Red in the particle dispersion with a volume ratio of 1:100 and heat the particle dispersion in a closed glass vial at a water bath of 60 °C for 24 hours. The particle concentration for both particle dispersions is 1wt%. During heat, toluene carrying Nile Red will diffuse into the particles and accumulate at PS domain. Then the cap of the glass vial is removed to evaporate excess toluene. These dyed particles are imaged under a fluorescent microscope. As shown in Figure 5.6, both particles show a strong red fluorescence on one side. For (Sty50/AA50) Janus particles, the side that shows strong red fluorescence is the styrene-rich side. For particles in shown Figure 5.5 (a), we believe the smooth PS side is showing red fluorescence. There is also a big difference between these two types of particles. For (Sty50/AA50) particles shown in Figure 5.6 (a), we are also able to see weak red fluorescence on the opposite side of styrene-rich side. As we discussed before, there is likely some amount of styrene existing in the acrylic acid-rich side thus Nile Red could also accumulate at the PS domains within the acrylic-acid-rich side. The fluorescent images in Figure 5.6 (a) clearly support our idea. However, particles in Figure 5.5 (a) only show fluorescence on one side and no fluorescence is observed as shown in Figure 5.6 (b) on the other side. We even observe two particles whose fluorescent sides separate from the side that does not show fluorescence as shown Figure 5.6 (b). These observations all indicate complete phase separation is achieved in particles shown in Figure 5.5. With the use of toluene and *t*BMA in the monomer mixture and SDS for

preparing LPS dispersion and monomer emulsion, Janus particles with pure compartments are synthesized.

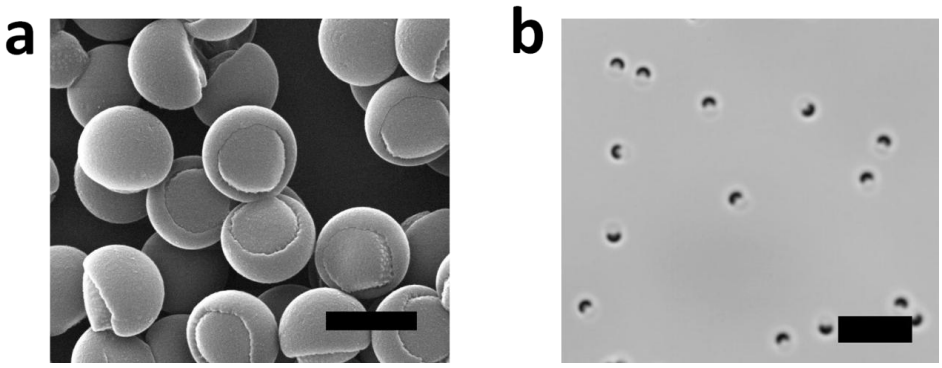

Figure 5.5 (a) The scanning electron microscopy and (b) optic microscopy images of Janus particles synthesized with a monomer mixture containing toluene (50 vol%), *t*BMA and DVB (1 vol%) as cross-linker. LPS dispersion and monomer emulsion are prepared with 0.4 wt% SDS aqueous solution. The volume ratio between monomer mixture and LPS is 4:1. The scale in (a) and (b) are is 1 μm and 5 μm, respectively.

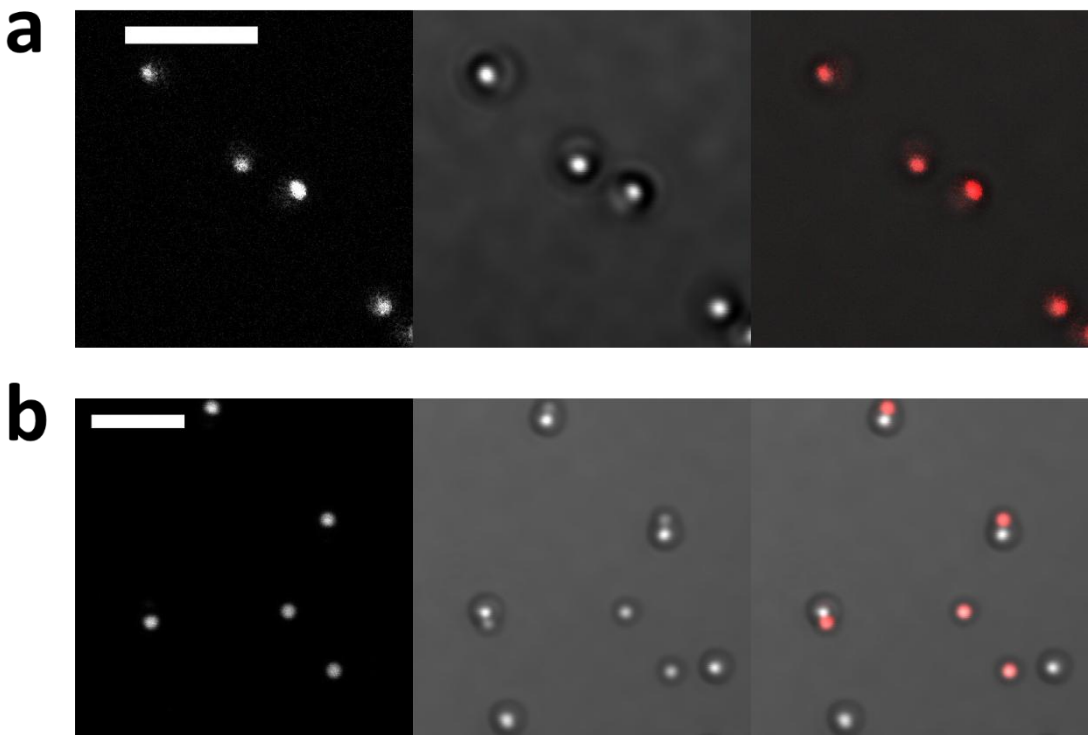

Figure 5.6 Microscopy images and fluorescent images of (a) (Sty50/AA50) Janus particles from *Chapter 3* and (b) Janus particles shown in Figure 5.5. Particles are dyed with a hydrophobic dye Nile Red. The scale bars are (a) 3 μm and (b) 10 μm, respectively.

Another interesting finding is that, this synthesis scheme for making Janus particles can be adapted to generate geometrically anisotropic particles in a large quantity. This can be done by using monomer mixture without cross-linker so that polymer synthesized during seeded emulsion polymerization is linear polymer. After hydrolysis, either PAA or PMAA will be water soluble thus can be removed by washing with deionized water. The remained PS dome will be the actual geometrically anisotropic particles. As shown in Figure 5.4 (a), there are two types of anisotropic particles. One has an oblate like shape. The other one has a disk-like shape. Previous studies have shown that the thermodynamic

morphology of a composite particle consisting of two incompatible polymers should adopt either core-shell or moon-like morphology.[175] That means the oblate-like particles are from composite particles with equilibrium morphology while the disk-like particles are from composite particles with kinetic stable or meta-stable morphology.[175] The main reason for the appearance of kinetic stable morphology is high viscosity inside the particle that prevents it from reaching equilibrium morphology.[176] In order to generate uniform anisotropic particles, we increase the volume of toluene used for preparing the monomer mixture which will reduce the viscosity of the composite particle. The volume ratio of LPS, *t*BA and toluene originally used is 1:2:2 therefore toluene consists of 40 vol%. We first use the volume ratio of LPS, *t*BA and toluene that is 1:2:27 so that toluene content is 90 vol%. As shown in Figure 5.7 (a), the disk-like particles disappear and all the particles are oblate-like indicating the reduced viscosity does help the composite particles reach their equilibrium morphology. Then we also try another volume ratio of LPS, *t*BA and toluene that is 1:1:18 so that the volume fraction of toluene is still 90 vol%. Due to the dcrease amount of *t*BA, the remaining anisotropic particles are almost hemispherical as shown in Figure 5.7 (b) and they are all adopting only one shape which resulted from equilibrium morphology. This also demonstrates the tunability of our synthesis scheme for making uniform anisotropic particles in a large quantity.

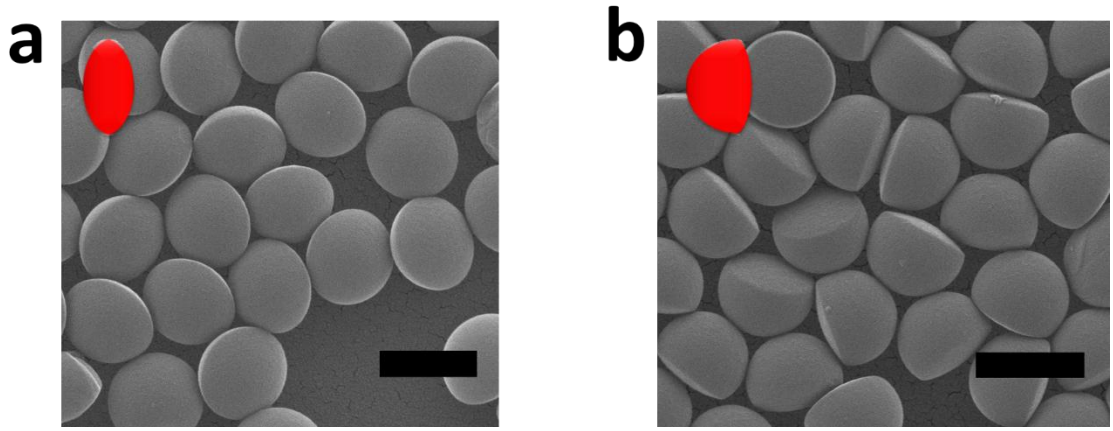

Figure 5.7 Scanning electron microscopy images of anisotropic particles synthesized using (a) 1:2:27 and (b) 1:1:18 for the volume ratio of LPS, tBA and toluene. No DVB is used in the monomer mixture. LPS dispersion and monomer emulsion are prepared with 0.4 wt% SDS aqueous solution. The scale is 1 μm.

5.4 Conclusions

By investigating the effect of cross-linker, monomer and surfactants on the morphology of Janus particles using the method from *Chapter 3*, a synthesis scheme for making Janus particles with pure hydrophilic and hydrophobic compartments are developed. Surfactants and the type of monomer used during the synthesis are found to be of critical importance. Based on the synthesis scheme developed here, a simple way of making geometrically anisotropic particles in a large quantity is also found. The tunability of the shape of these anisotropic particles is also demonstrated.

Chapter 6. Conclusions and Outlook

6.1 Conclusions

In *Chapter 1* of this dissertation, different types of emulsions and emulsifiers are introduced. In addition, the stabilizing mechanism of different emulsifiers including surfactants and colloidal particles are discussed. Janus particles are promising candidates for emulsion stabilization. The following chapters are the theoretical and experimental works done for demonstrating this idea.

Chapter 2 shows that the use of Janus dumbbells as emulsion stabilizers leads to the formation of thermodynamically stable emulsions which is advantageous over kinetically stable emulsion stabilized by surfactant molecules or homogeneous particles. For a given volume fraction of Janus dumbbells in the mixture system of a given composition, there exists thermodynamically preferred interfacial area, which can be achieved when all of the Janus dumbbells in the system are adsorbed to the droplet interface and form close-packed monolayers. Furthermore, we examine the effect of asymmetry of dumbbells and show that increasing the asymmetry of dumbbells increase the average droplet radius when the volume fraction of Janus dumbbells is fixed, whereas the average droplet radius decreases when the number of Janus dumbbells is kept constant. These theoretical results will provide critical insights into the design and application of Janus dumbbells as colloid surfactants to generate thermodynamically stable Pickering emulsion.

Chapter 3 presents a bulk synthesis scheme for generating highly uniform pH-responsive Janus particles. These Janus particles not only drastically change their shape but also completely reverse their amphiphilicity in response to changes in the solution pH. It is demonstrated that the type of emulsions generated using these amphiphilicity-reversing and shape-tunable Janus particles depends strongly on the acidity/basicity of the aqueous phase and that emulsions can be inverted to the opposite types by either lowering or raising the pH of the aqueous phases. The phase inversion is attributed to the ability of these Janus particles to change their shape and amphiphilicity in response to pH stimuli. The pH-dependent aggregation/dispersion behavior of our Janus particles are utilized to generated both attractive and repulsive emulsions at low and high pH conditions, respectively. Furthermore, attractive and repulsive interactions between emulsion droplets can be controlled on demand by changing the pH of continuous phase.

Chapter 4 demonstrates that highly stable W/O/W multiple emulsions can be generated with Janus particles via one-step emulsification, enabling the one-step encapsulation of hydrophilic species in multiple emulsions. Increasing the solution pH triggers the destabilization of aqueous compartments and subsequent release of encapsulants from these multiple emulsions, which is a powerful demonstration of the versatility of Janus particles as solid surfactants.

Chapter 5 presents the development of a synthesis scheme for making Janus particles with pure hydrophilic and hydrophobic compartments by investigating the effect of cross-linker, monomer and surfactants on the morphology of Janus particles using the method

from *Chapter 3*. Surfactants and the type of monomer used during the synthesis are found to be of critical importance. Based on the synthesis scheme developed, a simple way of making geometrically anisotropic particles in a large quantity is also found, which also offers good tunability.

6.2 Outlook for Future Research

6.2.1 Janus Particles with Positively Charged Hemisphere

The Janus particles synthesized using method developed in this *Chapter 3* only generate Janus particles with negatively charged hemisphere. This approach relies on the fact that *tert*-butyl acrylate (*t*BA) is not miscible with water but is highly hydrophilic after hydrolysis. After hydrolysis, *t*BA is converted to acrylic acid with a carboxylic acid functional group which makes the hydrophilic part negatively charged. In order to widen the toolbox of Janus particles for application, Janus particles with positively charged hemisphere are also needed especially Janus particles with hemispheres that are decorated with primary amine functional groups because primary amine is very easy for other bio-conjugation reactions, which could widen the biomedical application of Janus particles.

6.2.2 Janus Particles with Different Stimuli-responsive Properties

Janus particles developed in this dissertation are pH-responsive. The pH-responsive property comes from the presence of polymer network of weak acid: acrylic acid. Emulsions stabilized by these Janus particles are also pH-responsive. There are many applications in which other type of stimuli-responsive properties are desired. For example, thermo-responsive emulsions that are stable at one temperature and unstable at another temperature require Janus particles with thermo-responsive properties. Novel photo-responsive Janus particles will also find application in stabilizing smart emulsions.

6.2.3 Self-assembly of Janus particles

There have been various studies reported for using Janus particles as building blocks for making new structure that are not observed with homogeneous particles due to the anisotropic interactions between Janus particles. One of the most interesting self-assembly structure of surfactant molecules is micelles that have fix number of surfactant molecules. The structure of micelle is mainly determined by the geometry or packing parameter of surfactant molecules. Can Janus particles, as colloidal analogue of surfactant molecules, also form micelles that only contain a fixed number of particles? This will be a very interesting question to investigate, which could help us gain insight on micelle formation and similarities and differences between Janus particles and surfactant molecules.

6.2.4 Janus Particles with Functional Nanoparticles

Polyelectrolyte network is a very good template for synthesizing functional nanoparticles. It has been reported that microgels containing carboxylic acid groups are versatile nanoreactor for growing metal, metal oxide and semi-conducting nanoparticles.[170] Janus particles developed in this dissertation has a polyacrylic acid network as the hydrophilic side thus making these Janus particles suitable for nanoreactor for functional nanoparticles. For example, Janus particles functionalized with magnetic iron oxide can be used as building blocks to study the assembly structures under magnetic field. In addition, emulsions stabilized by such Janus particles are magnetic responsive which will allow us to manipulate the emulsions and recycle the Janus particles using magnetic field.[177] The Janus particles developed in this dissertation could also be used as micro-motor if functionalized with nanoparticles having catalytic properties such as platinum. Another promising application of Janus particles functionalized with catalyst is to use them as "interfacial catalyst emulsifiers". How this works is that the Janus particles not only stabilize emulsion but also function as catalyst to catalyze reaction at the oil-water interface. Because catalyst embedded in only one side of the Janus particles, they only catalyze reactions in one phase reducing by-product due to unnecessary catalytic reactions in the other phase, which could substantially increase the phase-selectivity of the system.[20]

APPENDIX

Controlling the Stability and Size of Double Emulsion-Templated Poly(lactic-co-glycolic)acid Microcapsules

A.1 Introduction

Hollow microcapsules encapsulating active ingredients such as drugs,[178-187] genes,[188-194] proteins[195-200] and living cells[201-211] inside a polymer shell are essential for targeted delivery and sustained release applications.[212-216] Hollow microcapsules made of PLGA are ideal systems for numerous biomedical applications because of their excellent biocompatibility and tunable biodegradability.[217-219] Conventionally, PLGA microcapsules are fabricated by a technique that involves double emulsification followed by solvent evaporation/extraction.[220,221] In this method, an aqueous solution containing active ingredients is emulsified in a PLGA-containing organic solution to form water-in-oil (W/O) emulsions. Subsequently, these W/O emulsion are emulsified in another aqueous solution such as PVA or PVP solution to form water-in-oil-in-water (W/O/W) double emulsions. To remove the organic solvent and form PLGA-shelled microcapsules, the W/O/W emulsion is either kept in a reduced pressure or a large water reservoir to accelerate the removal of the organic solvent.

Although great progress in biomedical applications of PLGA microcapsules has been achieved, the conventional method presents a number of challenges that limit the utilization of these microcapsules. For example, the conventional double emulsification method has a low encapsulation efficiency, which leads to a significant loss of actives.[222,223] In addition, these PLGA microcapsules are very polydisperse in size; therefore, their properties can vary from batch to batch, making it difficult for subsequent characterization and utilization. Furthermore, the shell of these PLGA microcapsules tends to be highly porous, which is thought to be the main reason for the undesirable burst release of encapsulated materials.[224]

Recent studies have shown that microfluidic techniques provide a versatile means to generate microparticles and hollow microcapsules with high uniformity and encapsulation efficiency.[225-232] A microfluidic technique that is particularly useful for the generation of hollow microcapsules relies on generating monodisperse water-in-oil-in-water (W/O/W) double emulsions, which are subsequently used to template microcapsule formation. The ability to produce monodisperse droplets also enables precise characterization and investigation of double emulsions and resulting microcapsules.[233] This double emulsion template method is versatile because it allows the use of different types of materials besides polymers to construct hollow microcapsules.[226,227,230,234,235] Another important advantage of the microfluidic approach is that double emulsion generation becomes a continuous process. This is a significant advantage over other techniques that may be able to provide monodisperse microcapsules.

Controlling the size of double emulsions while maintaining high stability and encapsulation efficiency is essential for a variety of applications. Recent studies, however, have shown that it is challenging to control the size of double emulsions and that of resulting microcapsules over a wide range without changing the channel dimensions of the microfluidic device or the properties of the fluids, such as viscosity, drastically.[236] It was found that a rather small window of flow rates exists, within which monodisperse double emulsions can be consistently generated. Outside this window, single emulsions or double emulsions with multiple inner drops are generated, making it difficult to control the size of double emulsions while maintaining high encapsulation efficiency. Even if the system is in the stable regime to generate monodisperse double emulsions, the possibility of changing the dimension of double emulsions (e.g., radius of the inner droplets) by tuning the flow rates was found to be rather limited.[236] For example, it is extremely difficult to generate double emulsions that would template microcapsules with inner diameters of 10 and 100 μm using a single microfluidic device, even if the flow rates are changed drastically. A new microfluidic device with appropriate dimensions would have to be fabricated to generate a double emulsion of specific dimensions.[233] Therefore, a facile method to control the size of monodisperse double emulsions without the need to fabricate a new microfluidic device with different channel dimensions would be highly desirable.

The objectives of this study are two folds. We study the stability of PLGA-containing double emulsions and find that the stability of PLGA double emulsions depends on the

pH of the inner aqueous phase. We also demonstrate that the size of double emulsions can be controlled within a wide range without utilizing multiple microfluidic devices. We develop a method to control the size of double emulsions and the resulting microcapsules using osmotic pressure difference between the inner and outer phases of the double emulsions. Although osmotic pressure has been previously used to vary the size and properties of double emulsions, its use has been limited to highly polydisperse emulsions[237-241], complicating the quantitative analysis of the process. The use of highly monodisperse double emulsions from microfluidics enables quantitative analysis and prediction of the size of double emulsions and resulting microcapsules. More importantly, this osmotic annealing technique overcomes a major drawback of microfluidic techniques, which do not allow for variation in the size of double emulsions and microcapsules over a wide range using a single microfluidic device. This technique can also be used to concentrate the encapsulated species, which could potentially be useful for encapsulating highly concentrated biomolecular solutions and colloidal suspensions.

A.2 Experimental Section

A.2.1 Materials

Deionized water is generated from Barnstead NANOpure (Thermo Scientific). Ester-terminated PLGA with composition 50:50 (Intrinsic Viscosity (η_i) = 0.41 dL g^{-1} in

hexafluoroisopropanol (HFIP)), 65:35 (Intrinsic Viscosity (η_i) = 0.55-0.75 dL g^{-1} in HFIP), 85:15 (Intrinsic Viscosity (η_i) = 0.66 dL g^{-1} in $CHCl_3$) are purchased from Durect Corp. Silica nanoparticles suspension (KE-E30) is obtained from Nippon Shokubai, Japan. Polyvinyl alcohol (PVA, 87-89% hydrolyzed, average M_w = 13,000-23,000), phosphate buffered saline (PBS) and calcein are purchased from Sigma-Aldrich. Chloroform ($CHCl_3$), tetrahydrofuran (THF), sodium chloride (NaCl), sodium sulfate (Na_2SO_4), sodium sulfite (Na_2SO_3), sodium nitrate ($NaNO_3$), sodium bicarbonate ($NaHCO_3$), sodium carbonate (Na_2CO_3), sodium hydroxide (NaOH), sodium phosphate monobasic (NaH_2PO_4), sodium phosphate dibasic (Na_2HPO_4), potassium chloride (KCl) and potassium phosphate dibasic (K_2HPO_4) are purchased from Fisher Scientific. Sodium phosphate tribasic (Na_3PO_4) is purchased from Acros Organics. Alizarin Yellow R is purchased from GFS Chemicals.

A.2.2 Double emulsion generation

Water-in-oil-in-water (W/O/W) double emulsions are generated using a glass capillary microfluidic device, as described previously.[242] To generate double emulsions, three different fluid phases are injected into a microfluidic device by three syringe pumps (PHD, Harvard Apparatus) with controlled flow rates. The outer phase is 2 wt% PVA aqueous solution. The middle phase is 0.9 wt% PLGA in $CHCl_3$. Different salt solutions are used as the inner phase. To generate double emulsions containing a pH indicator dye,

Alizarin Yellow R is dissolved in 0.01M and 1M NaOH solution with a concentration of 100 mg/L. These solutions are used as the inner phase. The middle phase is 0.9 wt% PLGA (50:50) (mol % of lactide : mol % of glycolide) in $CHCl_3$ and the outer phase is a 2 wt% PVA solution. The double emulsions generated using 0.01M NaOH and 1M NaOH solutions as inner phases are collected in 1M NaCl and 0.01M NaCl solutions, respectively, to prevent dilution of the inner phase due to the difference in osmotic pressure between the inner phase and the solution used to collect the double emulsions. These double emulsions are collected in small vials to compare the change in the color of the inner droplets.

A.2.3 Stability of PLGA double emulsions

PLGA-containing double emulsions encapsulating aqueous solutions of different pH are generated and collected in a petri dish with deionized water. PLGA with composition (50:50), (65:35) and (85:15) are used. Solution pH is tuned by adding NaOH in deionized water. The double emulsions are observed under an upright optical microscope as soon as they are generated. A full set of images for one sample is taken in between 5 and 10 minutes after emulsion collection. All of the stable double emulsions become PLGA microcapsules in around 2 hours during which the organic solvent in the middle phase is completely evaporated or removed. The fraction of stable double emulsions is determined by dividing the number of stable double emulsions by the total number of double

emulsions collected. Stable double emulsions refer to double emulsions whose inner aqueous droplets remain inside the middle phase until they become PLGA microcapsules. Unstable double emulsions refer to double emulsions whose inner aqueous droplets coalesce with the outer aqueous phase and become single oil-in-water droplets. Unstable double emulsions that become single oil-in-water droplets do not undergo coalescence with each other because they are stabilized by PVA (see Figure S1 in Supporting Information). The total number of generated double emulsions is determined by counting the number of stable double emulsions and that of single emulsions (unstable double emulsions) in optical microscopy images. We analyze over 3200 double emulsions for each data point to obtain the average and standard deviation.

A.2.4 Interfacial tension measurement

Interfacial tension between the oil phase (i.e., 0.9 wt% PLGA with three compositions in $CHCl_3$) and the aqueous phase (i.e., aqueous solution with different pH) is determined by pendant drop tensiometry (Attension, Theta). The pH of the aqueous solution is tuned by adding NaOH to the aqueous solution.

A.2.5 PLGA molecular weight determination

0.9 wt% PLGA in $CHCl_3$ is mixed with 1M NaOH and PBS solution with volume ratios of 3:0.6 and 3:1, respectively. The mixture is vigorously agitated using a vortex mixer (Fisher Scientific). After vigorous mixing, 2ml of the oil phase is transferred to another vial. The $CHCl_3$ is removed by evaporation under vacuum. 11ml THF is added to the vial to dissolve the solid residue. The vial is placed in a sonicator to help dissolve the PLGA. PLGA in THF is used to determine the molecular weight of PLGA by gel permeation chromatography (Waters) equipped with a refractive index detector.

A.2.6 Controlling the size of double emulsions and PLGA microcapsules using osmotic annealing

Double emulsions are generated with 2 wt% PVA solution and 0.9 wt% PLGA (85:15) as the outer phase and the middle phase, respectively. 0.1M NaCl solution with 5mM Na_2CO_3 is used as the inner phase to shrink the inner droplet of double emulsions, whereas 0.8M NaCl is used as the inner phase to swell the inner drops. Generated double emulsions are collected in cuvettes filled with 0.1, 0.2, 0.4 and 0.8M NaCl solutions. Upon collection of double emulsions, the cuvettes are capped with stoppers to suppress the evaporation of $CHCl_3$. After the inner droplets reach their equilibrium size, stoppers are removed to allow fast evaporation of $CHCl_3$. PLGA microcapsules are formed after complete evaporation of $CHCl_3$.

A.2.7 Concentrating encapsulated species using osmotic annealing

NaH_2PO_4 and Na_2HPO_4 are added to deionized water with a mole ratio of 22.6 : 77.4 to make 0.5mM phosphate buffered saline (PBS). Then a fluorescent dye, calcein, is added to this 0.5mM PBS solution to make its concentration to be 0.1mg/L. This calcein-containing solution is used as the inner phase to generate double emulsions. Generated double emulsions are collected in either 0.5mM PBS solution or 0.2M NaCl solution. Both bright field and fluorescent images are taken after PLGA microcapsules are formed.

To encapsulate silica particles, the original silica nanoparticle suspension (concentration: 20 wt%) is centrifuged at 8000 RPM for 5 minutes. After the removal of supernatant, deionized water is added and the sample is placed in a sonicator for 15 minute to re-disperse silica nanoparticles. The process is repeated five times. Subsequently, silica nanoparticles are dried under vacuum. These dried silica nanoparticles are added to 5mM Na_2CO_3 aqueous solution to prepare 0.5 wt% silica nanoparticles. After nanoparticles are re-dispersed by sonication, the nanoparticle suspension is used as the inner phase to generate double emulsions with 0.9 wt% PLGA (50:50) in $CHCl_3$ and 2 wt% PVA solution as middle phase and outer phase, respectively. Generated double emulsions are collected in 1.0M NaCl solution and observed under an upright optical microscope.

A.3 Results and Discussions

A.3.1 Stability of PLGA-containing double emulsions

Our previous study has shown that PLGA can stabilize the inner water-oil interface of water-in-oil-in-water (W/O/W) double emulsions without extra surfactants present in the oil phase.[243] However, we find that when double emulsions are generated with deionized water (pH 5.5 – 6.0) as the inner phase, such double emulsions are unstable as shown in Figure A.1 (a). Interestingly, when a PBS solution is used as the inner phase, the inner droplets remain stable inside the oil phase, and hollow PLGA microcapsules can be generated by removing the solvent.[243] These results indicate that either the ionic strength and/or the pH of the inner phase play important roles in controlling the stability of PLGA-containing double emulsions. To gain insights into stabilization of double emulsion by PLGA, we explore parameters such as ionic strength and pH of the inner phase as well as the composition of PLGA.

We investigate the effect of ionic species in the inner phase. Two types of salts are tested: one that dissociates in water but does not significantly affect the pH of the solution such as NaCl, Na_2SO_4, $NaNO_3$ and KCl, and one that dissociates and forms basic solutions such as Na_3PO_4, K_2HPO_4, Na_2SO_3 and Na_2CO_3. Table A.1 summarizes the effect of each salt on the pH of the aqueous phase. We find that salts that do not make the inner phase basic fail to stabilize double emulsions, whereas those that increase the pH of the inner phase are able to stabilize the double emulsions as shown in Figure A.1. These results lead us to relate the stability of PLGA-containing double emulsions to the pH of the inner phase rather than the ionic strength.

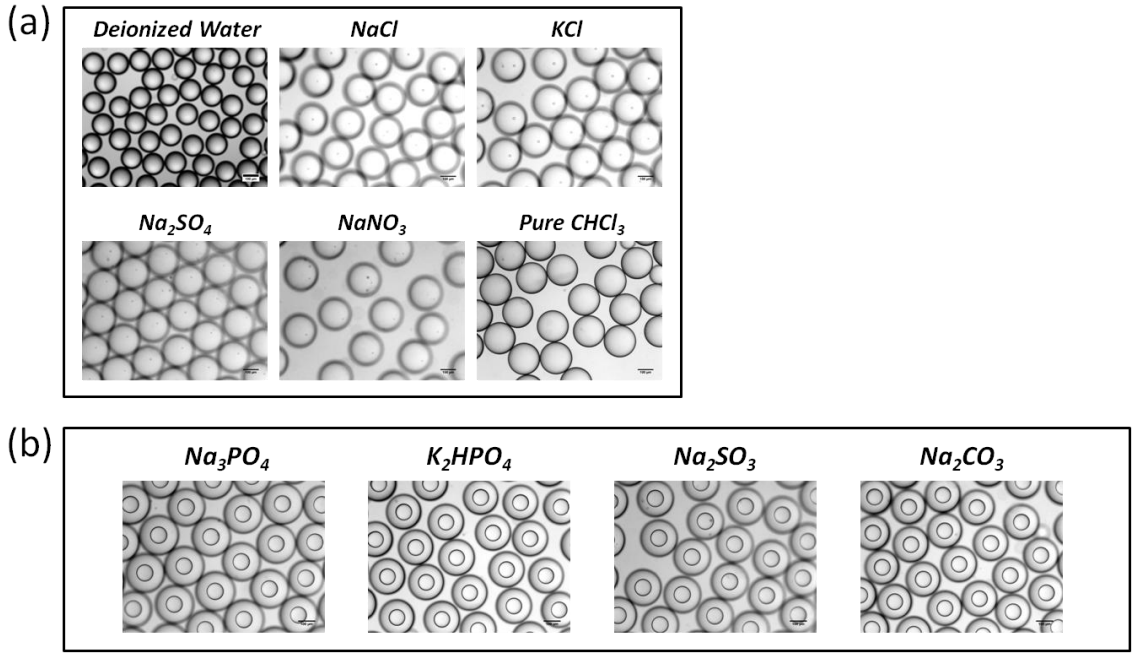

Figure A.1 Stability of double emulsions with inner drops containing different salts. The middle and outer phases are 0.9 wt% PLGA (85:15) in $CHCl_3$ and 2 wt% PVA solution, respectively. (a) and (b) are optical microscopy images of double emulsions that are unstable and stable, respectively. All the scale bars are 100 μm.

We test our hypothesis by generating PLGA-containing double emulsions with inner phase of varying pH without extra added salt. For all three types of PLGA used in this study, the stable fraction abruptly increases as the pH of the inner phase reaches 12.[244] Double emulsions generated with inner phase of pH 11 or smaller are unstable as shown in Figure A.2 and A.3. This result again clearly indicates that basic condition (i.e., presence of hydroxide anions) leads to stable double emulsions. It is also important to note that PLGA in the middle phase is necessary to maintain the stability of double emulsions. Double emulsions generated without PLGA in the middle phase, regardless of

the inner phase condition, are unstable as shown in Figure A.1 (a). Therefore, both basic inner phase and PLGA are necessary to stabilize the double emulsions.

Table A.1 Salts used to test the stability of PLGA-containing double emulsions.

Middle Phase	Inner Phase	pH	Stability
0.9 wt% PLGA (85:15) in $CHCl_3$	0.05M K_2HPO_4	9.00	**Stable**
	0.05M Na_2SO_3	9.70	
	0.005M Na_3PO_4	11.34	
	0.05M Na_2CO_3	11.29	
0.9 wt% PLGA (85:15) in $CHCl_3$	Deionized Water	5.91	**Unstable**
	0.05M NaCl	5.81	
	0.05M KCl	5.75	
	0.05M Na_2SO_4	6.14	
	0.05M $NaNO_3$	5.94	
Pure $CHCl_3$	0.05M Na_2CO_3	11.29	

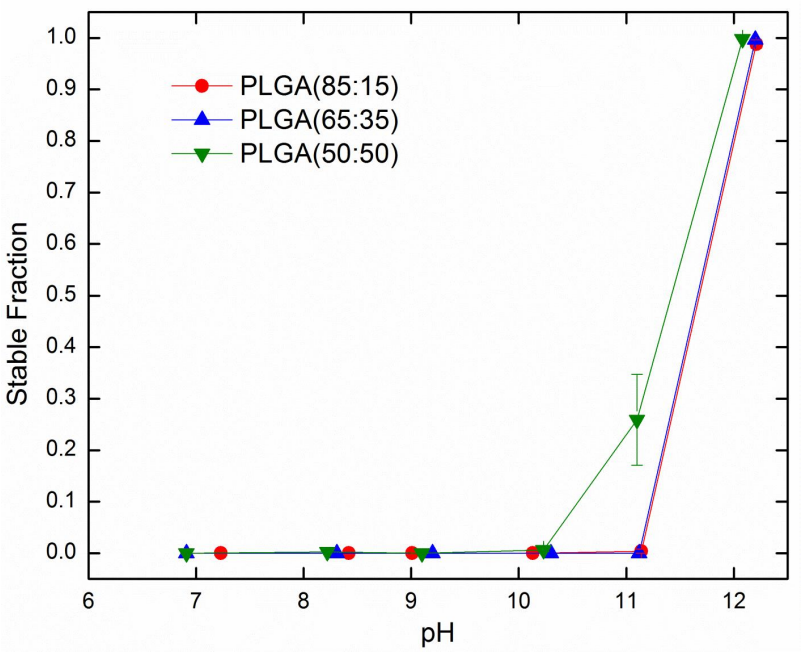

Figure A.2 Stability of double emulsions containing PLGA of different composition as a function of solution pH. Red circle, blue triangle and green inverted triangle represent the double emulsions containing 85:15, 65:15 and 50:50 PLGA, respectively.

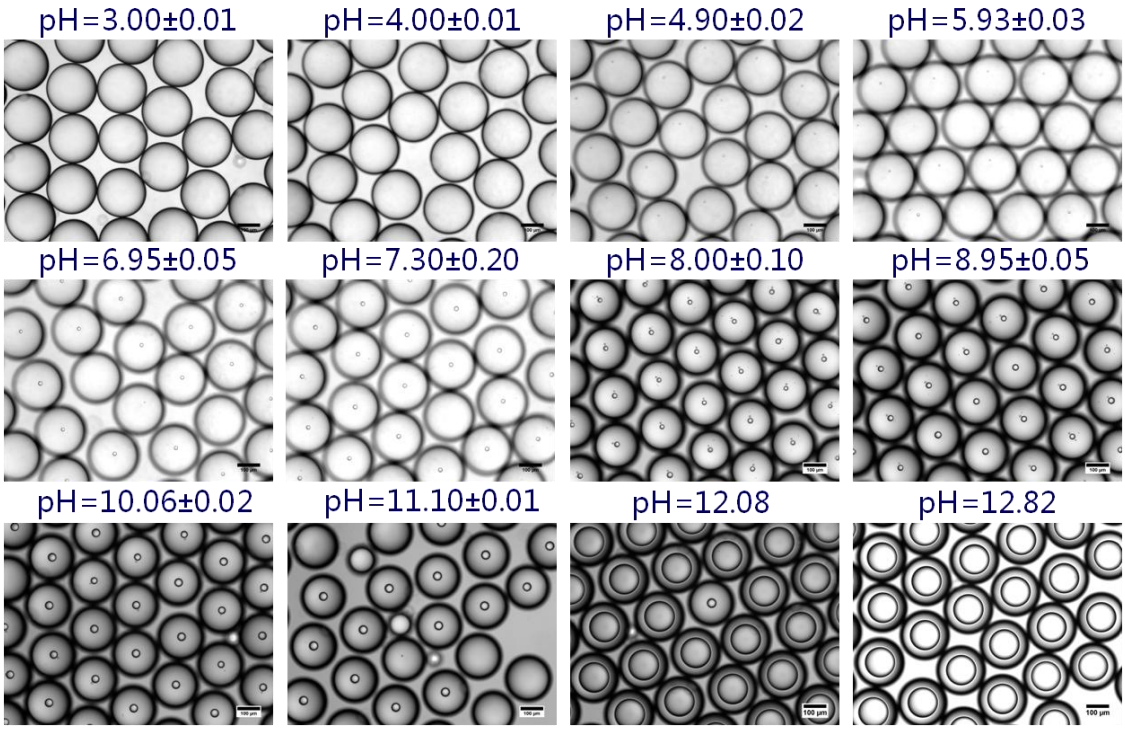

Figure A.3 Stability of PLGA (85:15)-containing double emulsions as a function of the pH of the inner phase. All scale bars are 100 μm.

We study the effect of inner phase pH on the interfacial tension between the aqueous phase and PLGA-containing oil phase using pendant drop tensiometry. We measure the interfacial tension between chloroform, with and without PLGA, and an aqueous solution as a function of solution pH. Consistent with the ability of PLGA to stabilize double emulsions, PLGA is found to decrease the interfacial tension between the aqueous and oil phases, as shown in Figure A.4. Interestingly, the surface activity depends on the composition of PLGA. We believe the hydrophile-lipophile balance (HLB) of PLGA increases as the fraction of more hydrophilic glycolide is increased in the backbone of PLGA. More importantly, the interfacial tension between the aqueous phase and PLGA-

containing chloroform decreases significantly as the pH of the aqueous phase is increased, whereas the change in the interfacial tension between aqueous phase and pure chloroform as a function of pH is negligible. These results indicate that high pH condition enhances the surface activity of PLGA.

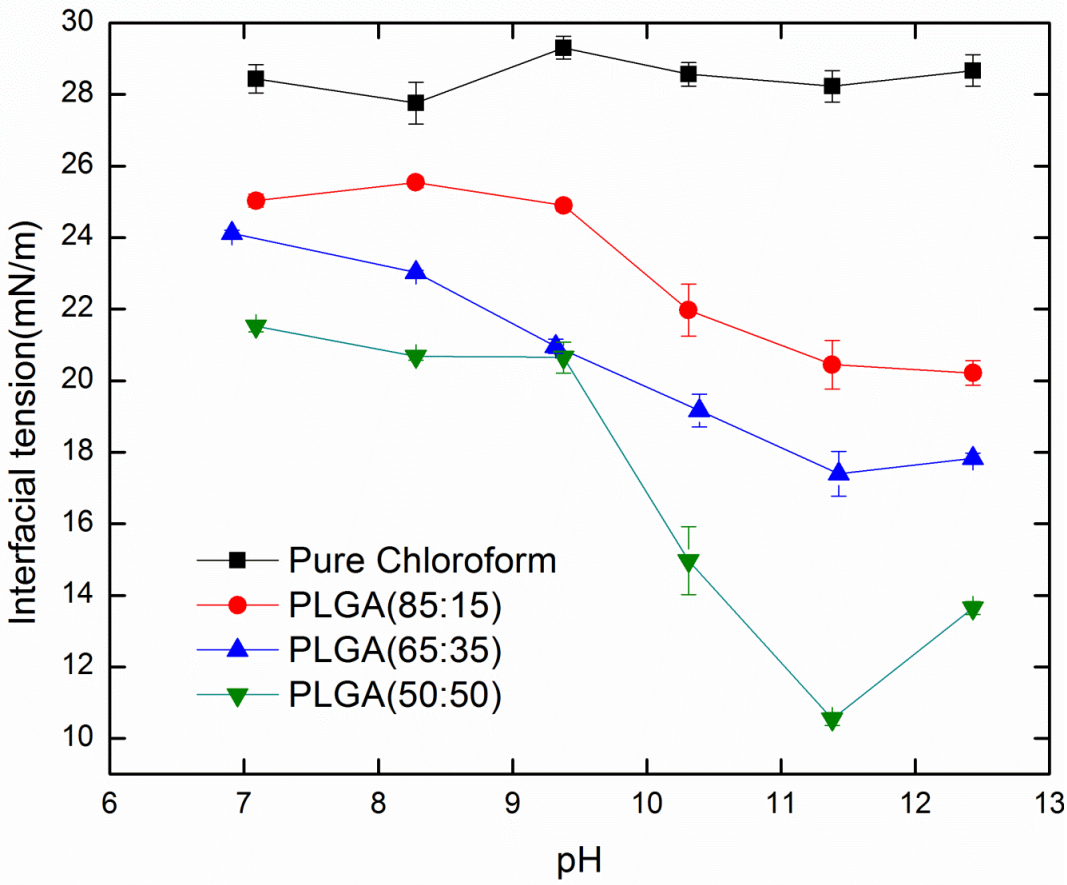

Figure A.4 Interfacial tension between a PLGA solution in chloroform and an aqueous solution as a function of solution pH. Black square represents pure chloroform. Red circle, blue triangle and green inverted triangle represent chloroform solutions with 85:15, 65:35 and 50:50 PLGA, respectively.

Table A.2 Weight averaged molecular weight (g/mol) of PLGA after contacting 1M NaOH solution and of with PBS solution.

Aqueous phase	1M NaOH			PBS
Type of PLGA	PLGA (50:50)	PLGA (65:35)	PLGA (85:15)	PLGA (50:50)
0 min	*63.1 ± 2.9 K*	*50.8 ± 1.7 K*	*68.0 ± 1.7 K*	*62.0 ± 1.8 K*
30 min	*48.6 ± 8.5 K*	*38.7 ± 0.2 K*	*64.5 ± 1.8 K*	*53.5 ± 5.3 K*
50 min	*43.7 ± 2.4 K*	*31.6 ± 0.9 K*	*50.9 ± 1.8 K*	*53.9 ± 5.2 K*[a]

[a]Molecular weight is measured after PLGA solution was in contact with the PBS solution for 1 hr instead of 50 min.

We further explore the importance of the interaction between basic solutions and PLGA by monitoring the change in the molecular weight of PLGA upon contact with high pH solutions. To monitor the change in the molecular weight of the polymer, PLGA in $CHCl_3$ is mixed with 1M NaOH solution or PBS solution and agitated for different periods of time. Although the oil phase and aqueous phase are immiscible, a significant reduction in the average molecular weight of PLGA is observed with time (Table A.2). These results indicate that PLGA undergoes hydrolysis upon contact with basic solutions. Basic solutions have previously been used to render PLGA scaffolds hydrophilic, which have been attributed to the base-catalyzed hydrolysis of ester bonds in PLGA and the formation of carboxylic acid end groups as shown in Figure A.5.[245-254] In particular, it has been shown that the rate of hydrolysis increases by five orders of magnitude when the solution pH increases from 7 to 12.[247]

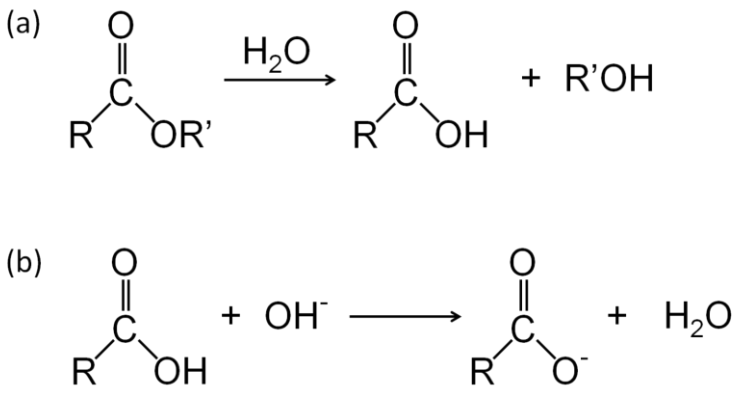

Figure A.5 (a) Hydrolysis of ester bond and (b) ionization of carboxylic acid group by acid-base reaction.

We further investigate the importance of basic condition by monitoring the consumption of hydroxide anions in the inner phase of PLGA-containing double emulsions. To enable this study, we add a pH indicator dye, Alizarin Yellow R, as a probe. Alizarin Yellow R is soluble in water but insoluble in chloroform, thus dose not diffuse out of the double emulsions. This dye changes its color from dark red to light yellow when the solution pH changes from 12.1 to 10.0 or below. When the dye is dissolved in 0.01M and 1M NaOH solutions, there is no observable difference in the color of the two NaOH solutions containing Alizarin Yellow R as shown in Figure A.6. The color of PLGA double emulsions with 0.01M NaOH inner phase changes its color from dark red to light yellow upon collection, whereas PLGA double emulsions with 1.0M NaOH inner phase remains red.[255] These results indicate that a large amount of hydroxide anions in the inner phase are consumed likely due to the ionization of carboxylic acid end groups of PLGA, leading to the change in the color of PLGA double emulsions and the subsequent pH

reduction. It is also likely that monomers of PLGA are released upon hydrolysis.[256] Because both monomers, lactic acid and glycolic acid, are highly soluble in water, they could partition into the aqueous phase and contribute to the shift in the pH of the inner droplets.

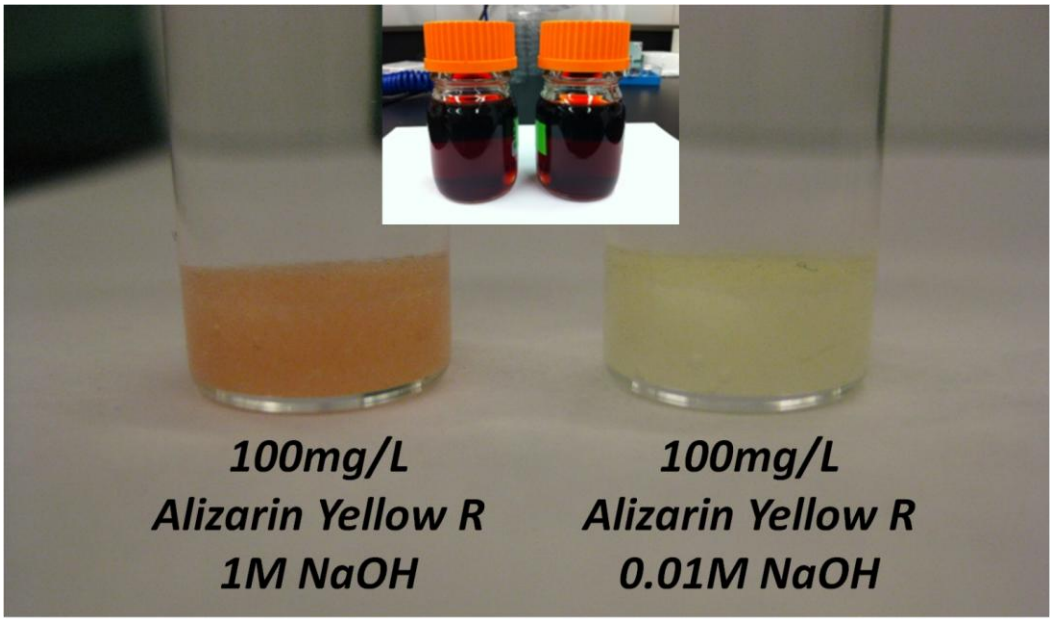

Figure A.6 Change in the color of PLGA double emulsions containing Alizarin Yellow R in the inner phase. Double emulsion on the left are generated using 100mg/L Alizarin Yellow R in 1.0M NaOH as the inner phase, and one on the right are generated using 100mg/L Alizarin Yellow R in 0.01M NaOH as the inner phase. The inset shows Alizarin Yellow R in 1.0M NaOH and 0.01M NaOH.

Based on these results, we conclude that the ionization of carboxylic acid end groups that form due to the hydrolysis of PLGA chains as shown in Figure A.5 is responsible for the stabilization of PLGA-containing double emulsions. As evidenced by the molecular weight reduction, base-catalyzed hydrolysis of PLGA provides carboxylic acid end

groups. Acid-base reaction between the carboxylic acid end groups of PLGA and hydroxide anions in the inner aqueous phase generates ionized carboxylate groups, which are highly hydrophilic. These ionized end groups facilitate the anchoring of PLGA at the oil-water interface, which, in turn, enhances the surface activity of PLGA and its stabilization of the inner droplets of double emulsions. Such a mechanism is consistent with the enhanced double emulsion stability and PLGA surface activity (Figure A.4) at a high pH (> 12.0). A similar mechanism likely is responsible for the stabilization of W/O/W double emulsions when a PBS solution (pH 7.4) is used as the inner phase. The PBS solution is able to maintain the pH of inner phase and ionize the carboxylic acid end groups of PLGA, although the hydrolysis of PLGA is not as significant as high pH aqueous solution (Table A.2). We believe that a small amount of carboxylic acid groups that were originally present in PLGA could also play an important role in the surface activity of PLGA and the subsequent stabilization of W/O/W double emulsions.[257]

A.3.2 Controlling the size of double emulsions and PLGA microcapsules

As described in Introduction, it is difficult to control the size of double emulsions over a wide range using a single microfluidic device. We overcome this limitation by making use of osmotic pressure. To tune the size of double emulsion-templated microcapsules by what we call osmotic annealing, we separate the formation of microcapsules from double emulsions into two steps, as illustrated in Figure A.7. We generate double emulsions with

a salt solution of a given concentration as the inner aqueous phase. Subsequently, we collect double emulsions into a glass cuvette. The glass cuvette is filled with a solution of a different salt concentration. The cuvette is sealed to suppress the removal of the organic solvent in the middle phase. The difference in electrolyte concentrations between the inner droplet and the collection solution induces water to diffuse into and out of the inner droplet leading to their swelling and shrinkage, respectively. After the inner droplet reaches its equilibrium size, we expose the emulsion suspension to open air to allow the removal of the organic solvent, chloroform. PLGA microcapsules are formed after complete removal of the organic solvent as shown in Figure A.7.

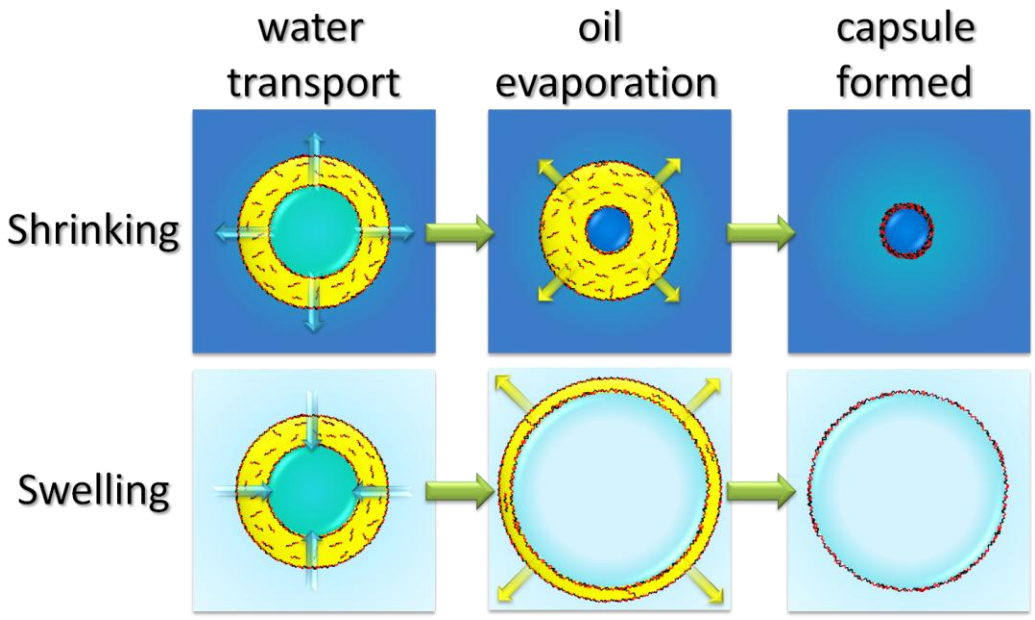

Figure A.7 Schematic illustration of tuning the size of double emulsions and microcapsules by osmotic annealing.

To test the feasibility of this osmotic annealing, we generate eight samples of double emulsions with the same initial dimensions as shown in Figure A.8. Based on the results from the first part of this study, 5mM Na_2CO_3 is added to the inner phase to enhance the stability of PLGA-containing double emulsions while NaCl in the inner phase is used to provide osmotic pressure difference for osmotic annealing. When the concentration of NaCl in the inner droplets is higher than that in the collection solution, the inner droplets swell. In contrast, the inner droplets shrink if the situation is the opposite. These swelling and shrinking behaviors can be understood by considering the difference in osmolarity (i.e., chemical potential of water) of the inner droplet and the collection solution. When the inner phase is more concentrated, water in the collection solution has a higher chemical potential than that of the inner phase; therefore, water diffuses into the inner droplets from the collection solution through the middle phase. This transport of water makes the inner droplets swell. The inner droplets reach their equilibrium diameter within two hours of osmotic annealing, which can be inferred from the plateau of the diameter evolution curves in Figure A.8 (b). PLGA microcapsules ranging from 80 μm to ~ 300 μm in diameter are formed from one double emulsion (initial inner and outer diameters were ~ 150 and 250 μm, respectively) using osmotic annealing as shown in Figure A.8 (a).

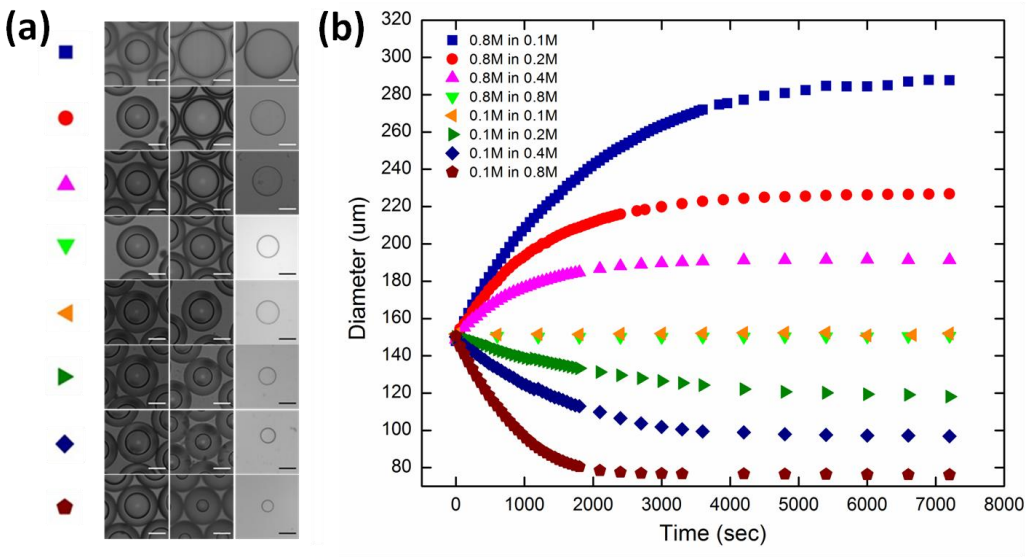

Figure A.8 (a) PLGA microcapsules formed using osmotic annealing and (b) the diameter evolution of the inner droplets of double emulsions under osmotic annealing. The first, second and third columns in (a) represent the initial double emulsions, double emulsions at equilibrium and PLGA microcapsules formed, respectively, under different conditions. All the scales bar in (a) are 100 μm. The legend in (b) represents different conditions under which PLGA microcapsules are formed. For example, blue squares with "0.8M in 0.1M" represent double emulsions generated using 0.8M NaCl solution (also containing 5 mM Na_2CO_3) as the inner phase and collected in 0.1M NaCl solution.

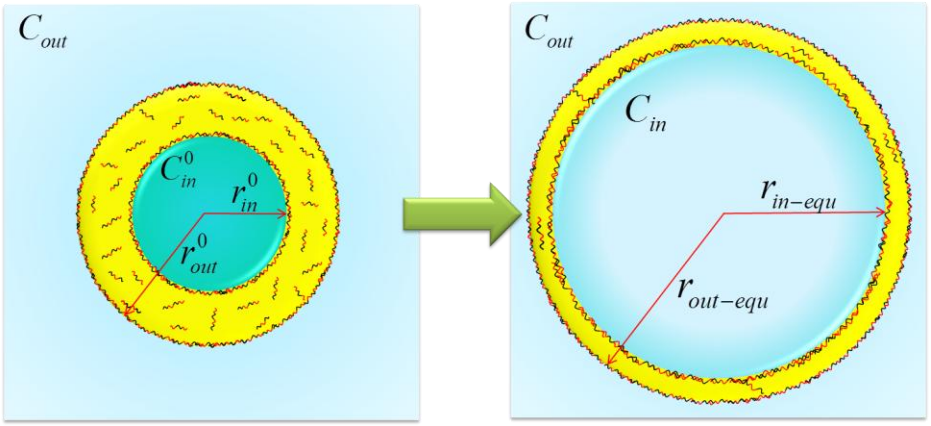

Figure A.9 Schematic representation of parameters used in the calculation of the equilibrium diameter of the inner droplets of double emulsions after osmotic annealing.

The equilibrium diameter of the inner droplets of double emulsions is determined by the balance of osmotic pressure due to the concentration difference between the inner droplet and the collection solution, and the Laplace pressure due to interfacial tension at the two oil-water interfaces. To derive the relationship between the salt concentration ratio and the equilibrium diameter of the inner droplet, we assume that there is negligible transport of the ionic species across the middle phase, which is reasonable since the solubility of the ions in chloroform is extremely low. Laplace pressure associated with the two oil-water interfaces is

$$P = \frac{2\gamma_{im}}{r_{in}} + \frac{2\gamma_{om}}{r_{out}}, \qquad \text{(A-1)}$$

where γ_{im} is the interfacial tension between the inner and middle phases, and γ_{om} represents the interfacial tension between the outer and middle phases. r_{in} and r_{out} represent the radii of the inner and outer droplets, respectively. Osmotic pressure difference between the inner and outer phases can be represented by van't Hoff's Law[258]:

$$\Pi = 2(C_{in} - C_{out})RT. \qquad \text{(A-2)}$$

C_{in} and C_{out} are the concentrations of NaCl in the inner droplets and the collection solution at equilibrium as shown in Figure A.9. R is the gas constant, and T is the absolute temperature. The equilibrium diameter of the inner droplets is determined by equating Equation (A-1) and Equation (A-2) as shown in Equation (A-3):

$$2(C_{in} - C_{out})RT = \frac{2\gamma_{im}}{r_{in-equ}} + \frac{2\gamma_{om}}{r_{out-equ}}, \quad \text{(A-3)}$$

where $r_{in\text{-}equ}$ and $r_{out\text{-}equ}$ are the radii of the inner and outer droplets at equilibrium, respectively. Neglecting the transport of the ionic species, the concentration of NaCl in the inner droplet at equilibrium is related with its original value by Equation (A-4), which implies the conservation of ionic species in the inner droplets:

$$C_{in} = C_{in}^0 \left(\frac{r_{in}^0}{r_{in-equ}} \right)^3. \quad \text{(A-4)}$$

Substituting Equation (A-4) into Equation (A-3) we obtain

$$C_{in}^0 \left(\frac{r_{in}^0}{r_{in-equ}} \right)^3 - C_{out} = \frac{1}{RT} \left(\frac{\gamma_{im}}{r_{in-equ}} + \frac{\gamma_{om}}{r_{out-equ}} \right). \quad \text{(A-5)}$$

Solving Equation (A-5), the ratio of $r_{in\text{-}equ}$ and $r_{in}{}^0$ can be expressed as

$$\frac{r_{in-equ}}{r_{in}^0} = \left(\frac{C_{in}^0}{C_{out} + \frac{1}{RT} \left(\frac{\gamma_{im}}{r_{in-equ}} + \frac{\gamma_{om}}{r_{out-equ}} \right)} \right)^{1/3}. \quad \text{(A-6)}$$

Using R=8.314 $J/mol{\cdot}K$, T=293.15 K, γ_{im}=21 mN/m (interfacial tension between the inner and middle phases of double emulsions that have (85:15) PLGA), γ_{om}=5 mN/m (interfacial tension between 2 wt% PVA solution and PLGA containing middle phase[243]),

$r_{in\text{-}equ}$=10 μm and $r_{out\text{-}equ}$=10 μm, the numerical value of the term in Equation (A-6) $1/RT(\gamma_{im}/\gamma_{in\text{-}equ}+\gamma_{om}/\gamma_{out\text{-}equ})=1.07\times10^{-3}$ M . This value is approximately one percent of 0.1M NaCl solution and much less than one percent of 0.8M NaCl solution. Thus, we can simplify Equation (A-6) by neglecting the effect of interfacial tension on the equilibrium diameter of the inner droplet. Thus, we obtain a very simple relationship between the initial and the equilibrium radii of the inner droplet as shown in Equation (A-7):

$$\frac{r_{in-equ}}{r_{in}^{0}}=\left(\frac{C_{in}^{0}}{C_{out}}\right)^{1/3} . \qquad \text{(A-7)}$$

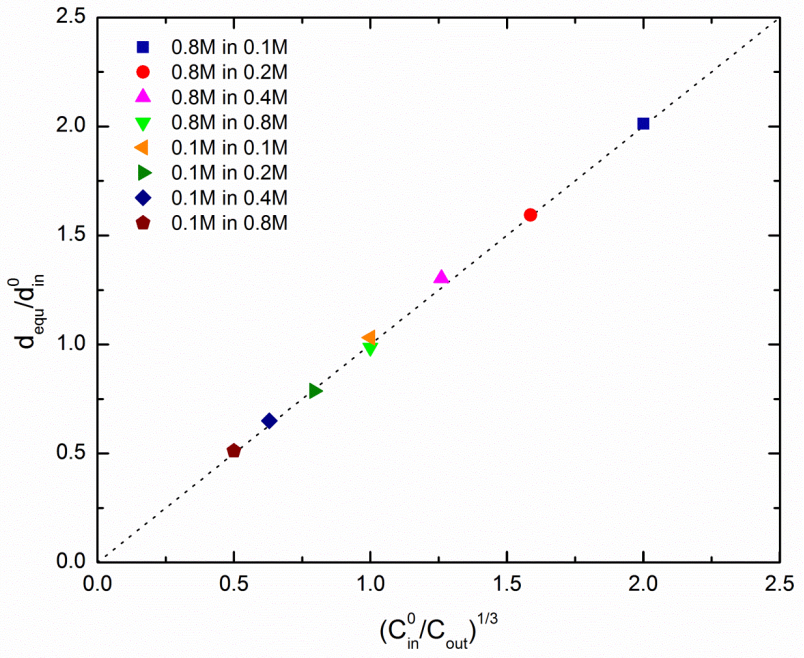

Figure A.10 The ratio of initial and equilibrium diameter of inner droplets as a function of the NaCl concentration ratio of the inner and collection solutions. The dotted line in (b) represents the prediction based on Equation (A-7). The legend has the same interpretation as that in Figure A-8.

The diameter of the inner droplets after osmotic annealing can be accurately predicted by the theoretical model as represented by Equation (A-7). The relationship between the one third power of the concentration ratio ($(C_{in}^{0}/C_{out})^{1/3}$) and the radii ratio ($r_{in\text{-}equ}/r_{in}^{0}$) for eight different concentration ratios is shown in Figure A.10. Note that the diameter of the inner droplet measured from optical microscopy is different from its actual diameter due to the difference in the refractive indices of water and organic solvent. All data for the diameter of the inner droplets are corrected using a method provided elsewhere.[236] It can be clearly seen that the experimental data from Figure A.8 all lie on the line determined by Equation (A-7), indicating that the experimental results agree well with our hypothesis and prediction. Most importantly, these results strongly support that we can readily tune the size of microcapsules and that of the inner droplets of double emulsions from a single device under one set of double emulsion formation conditions by simply changing the ratio of the solute concentrations of the inner and collection solutions. The thickness of microcapsule shell is an important factor that determines the release of encapsulated species. The average shell thickness can be determined based on the concentration of PLGA in the middle phase, the volume of middle phase, the density of PLGA and the equilibrium inner diameter of PLGA microcapsules. The average shell thickness of PLGA microcapsules can be derived based on conservation of mass:

$$\frac{4}{3}\pi\left(r_{in-equ}+h\right)^{3}-\frac{4}{3}\pi\left(r_{in-equ}\right)^{3}=\frac{VW}{\rho} \qquad \text{(A-8)}$$

where $r_{in\text{-}equ}$ is the equilibrium inner radius of PLGA microcapsules obtained from Equation (A-7) and h is the average shell thickness. V is the volume of middle phase per double emulsion, W is the concentration (g/ml) of PLGA in middle phase and ρ is the density of PLGA used. The average thickness h can be obtained by numerically solving Equation (A-8). If the thickness of the shell is much smaller than the equilibrium inner radius ($h << r_{in\text{-}equ}$), h can be expressed explicitly as

$$h = \frac{1}{4\pi r_{in-equ}^2}\frac{VW}{\rho} . \qquad \text{(A-9)}$$

We can further make use of osmotic annealing to concentrate encapsulated species in double emulsions and microcapsules. We use 0.5mM phosphate buffer solution (PBS) with 0.1 mg/L calcein in the inner phase as a probe dye to generate double emulsions. When these double emulsions are collected in 0.5 mM PBS and converted into PLGA microcapsules, very little fluorescence intensity is detected due to the low concentration of calcein (Figure A-11 (a)). In contrast, when these double emulsions are collected in 0.2M NaCl solution, water inside the inner droplets diffuse out through the oil phase due to the difference in osmolarity between the inner and outer phases, while calcein remains encapsulated in the inner droplets. Consequently, the concentration of calcein and, in turn, the fluorescence intensity of the inner phase increases substantially. The increase in fluorescence intensity is quite drastic as seen in Figure A-11 (b) and (c), which shows a line scan of fluorescence in microcapsules generated with and without osmotic annealing. It is worth noting that in our swelling experiment the volume of the inner droplets is

increased by a factor of 8 (Figure A-8 (b)), whereas in the shrinking experiment, the volume of inner droplets is decreased by a factor of ~270 (Figure A-11 (a) and (b)); thus, our results indicate that the volume of the inner droplets and, in turn, the concentration of the encapsulated solute, can be tuned by at least three orders of magnitude using the osmotic annealing method.

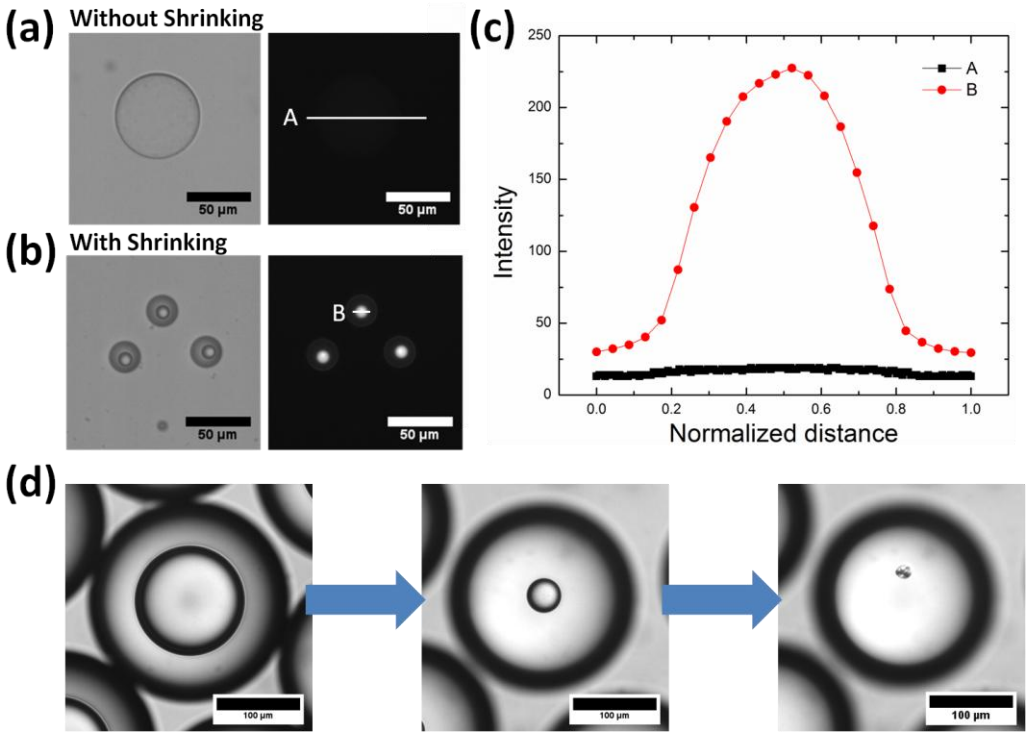

Figure A.11 Concentrating encapsulated species using osmotic annealing. (a) and (b) show bright field and fluorescent images of the PLGA microcapsules without and with osmotic annealing. (c) Fluorescence intensity of encapsulated species along the white lines in (a) and (b). (d) Optical microscopy images showing the shrinkage of encapsulated silica suspension to an agglomerate of silica particles under osmotic annealing. Double emulsions are generated with 0.5 wt% silica particle suspensions in 5mM Na_2CO_3 as the inner phase and collected in 1.0M NaCl solution.

This concentration method using osmotic annealing is especially useful in encapsulating highly concentrated solid suspensions such as colloidal particles. Typically, microfluidic channels clog rapidly when highly concentrated solutions of suspensions are used.[259,260] We can readily encapsulate highly concentrated particle suspension by annealing double emulsions containing a low initial concentration of particles in a high salt solution. We demonstrate this by essentially squeezing out all of water from encapsulated particle suspension, which leaves an agglomerate of particles in the core of oil droplets as shown in Figure A-11 (d).

A.4 Conclusions

We have demonstrated that the stability and size of PLGA-containing double emulsions and resulting PLGA microcapsules can be controlled by varying the composition of each phase of the double emulsions. In particular, it is important to adjust the pH of the inner phase to enable stabilization of inner droplets of PLGA-containing double emulsions. Hydrolysis of PLGA and, more importantly, the ionization of carboxylic acid end groups enhance the surface activity of PLGA at the oil-water interface and, in turn, the stabilization of PLGA-containing double emulsions. We have also shown that the size of double emulsions can be precisely tuned by changing the concentration ratio of a solute in the inner and outer phases of double emulsions. It is possible to change the volume of internal compartment of PLGA microcapsules by more than three orders of magnitude,

illustrating the effectiveness and reliability of this new method in changing the size of microcapsules and, in turn, the concentration of the encapsulated species. This approach overcomes the difficulty in generating monodisperse double emulsions and microcapsules over a wide range of dimensions using a single microfluidic device. We believe that the osmotic annealing method will be useful for generating drug delivery systems, encapsulating high concentration of biomacromolecules such as proteins,[261] and also for generating capsules encapsulating high concentration solid suspensions while avoiding clogging of microfluidic devices.

BIBLIOGRAPHY

(1) Adams, F.; Walstra, P.; Brooks, B.; Richmond, H.; Binks, B. P. *Modern aspects of emulsion science*; Royal Society of Chemistry, 1998.

(2) Tadros, T. F. *Emulsion science and technology. Wiley-VCH, Weinheim* **2009**, 1.

(3) Matsumoto, S.; Kita, Y.; Yonezawa, D. *Journal of Colloid and Interface Science* **1976**, *57*, 353.

(4) Rosen, M. J.; Kunjappu, J. T. *Surfactants and interfacial phenomena*; John Wiley & Sons, 2012.

(5) Israelachvili, J. N. *Intermolecular and surface forces: revised third edition*; Academic press, 2011.

(6) McClements, D. J. *Soft Matter* **2012**, *8*, 1719.

(7) Ramsden, W. *Proceedings of the Royal Society of London* **1903**, 156.

(8) Pickering, S. U. *Journal of the Chemical Society, Transactions* **1907**, *91*, 2001.

(9) Binks, B. P. *Current Opinion in Colloid & Interface Science* **2002**, *7*, 21.

(10) Aveyard, R.; Binks, B. P.; Clint, J. H. *Advances in Colloid and Interface Science* **2003**, *100*, 503.

(11) Finkle, P.; Draper, H. D.; Hildebrand, J. H. *Journal of the American Chemical Society* **1923**, *45*, 2780.

(12) Schulman, J. H.; Leja, J. *Transactions of the Faraday Society* **1954**, *50*, 598.

(13) Binks, B. P.; Lumsdon, S. O. *Langmuir* **2000**, *16*, 8622.

(14) Aveyard, R. *Soft Matter* **2012**, *8*, 5233.

(15) Tadros, T. F.; Vincent, B. *Encyclopedia of emulsion technology* **1983**, *1*, 129.

(16) Casagrande, C.; Fabre, P.; Raphael, E.; Veyssie, M. *Europhysics Letters* **1989**, *9*, 251.

(17) de Gennes, P. G. *Reviews of Modern Physics* **1992**, *64*, 645.

(18) Jiang, S.; Granick, S.; Schneider, H.-J. *Janus particle synthesis, self-assembly and applications*; Royal Society of Chemistry, 2012.

(19) Walther, A.; Müller, A. H. E. *Chemical Reviews* **2013**, *113*, 5194.

(20) Faria, J.; Ruiz, M. P.; Resasco, D. E. *Advanced Synthesis & Catalysis* **2010**, *352*, 2359.

(21) Glaser, N.; Adams, D. J.; Böker, A.; Krausch, G. *Langmuir* **2006**, *22*, 5227.

(22) Jiang, S.; Chen, Q.; Tripathy, M.; Luijten, E.; Schweizer, K. S.; Granick, S. *Advanced Materials* **2010**, *22*, 1060.

(23) Kim, J.-W.; Lee, D.; Shum, H. C.; Weitz, D. A. *Advanced Materials* **2008**, *20*, 3239.

(24) Kim, J.-W.; Larsen, R. J.; Weitz, D. A. *Journal of the American Chemical Society* **2006**, *128*, 14374.

(25) Mejia, A. F.; Diaz, A.; Pullela, S.; Chang, Y.-W.; Simonetty, M.; Carpenter, C.; Batteas, J. D.; Mannan, M. S.; Clearfield, A.; Cheng, Z. *Soft Matter* **2012**, *8*, 10245.

(26) Walther, A.; Matussek, K.; Müller, A. H. E. *ACS Nano* **2008**, *2*, 1167.

(27) Bahrami, R.; Löbling, T. I.; Gröschel, A. H.; Schmalz, H.; Müller, A. H. E.; Altstädt, V. *ACS Nano* **2014**, *8*, 10048.

(28) Walther, A.; Hoffmann, M.; Müller, A. H. E. *Angewandte Chemie International Edition* **2008**, *47*, 711.

(29) Fan, H.; Striolo, A. *Soft Matter* **2012**, *8*, 9533.

(30) Binks, B.; Fletcher, P. *Langmuir* **2001**, *17*, 4708.

(31) Hong, L.; Jiang, S.; Granick, S. *Langmuir* **2006**, *22*, 9495.

(32) Jiang, S.; Granick, S. *Langmuir* **2008**, *24*, 2438.

(33) McClements, D. J. *Food emulsions: principles, practices, and techniques*; CRC, 2004.

(34) Aveyard, R.; Clint, J. H.; Horozov, T. S. *Physical Chemistry Chemical Physics* **2003**, *5*, 2398.

(35) Binks, B.; Lumsdon, S. *Langmuir* **2000**, *16*, 8622.

(36) Juárez, J. A.; Whitby, C. P. *Journal of Colloid and Interface Science* **2012**, *368*, 319.

(37) Fujii, S.; Yokoyama, Y.; Miyanari, Y.; Shiono, T.; Ito, M.; Yusa, S.-i.; Nakamura, Y. *Langmuir* **2013**, *29*, 5457.

(38) Levine, S.; Bowen, B. D. *Colloids and Surfaces* **1991**, *59*, 377.

(39) Perro, A.; Reculusa, S.; Ravaine, S.; Bourgeat-Lami, E.; Duguet, E. *Journal of Materials Chemistry* **2005**, *15*, 3745.

(40) Wurm, F.; Kilbinger, A. F. M. *Angewandte Chemie International Edition* **2009**, *48*, 8412.

(41) Hu, J.; Zhou, S.; Sun, Y.; Fang, X.; Wu, L. *Chemical Society Reviews* **2012**, *41*, 4356.

(42) Takei, H.; Shimizu, N. *Langmuir* **1997**, *13*, 1865.

(43) Fujimoto, K.; Nakahama, K.; Shidara, M.; Kawaguchi, H. *Langmuir* **1999**, *15*, 4630.

(44) Paunov, V. N.; Cayre, O. J. *Advanced Materials* **2004**, *16*, 788.

(45) Roh, K.-H.; Martin, D. C.; Lahann, J. *Nature Materials* **2005**, *4*, 759.

(46) Nie, Z.; Li, W.; Seo, M.; Xu, S.; Kumacheva, E. *Journal of the American Chemical Society* **2006**, *128*, 9408.

(47) Nisisako, T.; Torii, T.; Takahashi, T.; Takizawa, Y. *Advanced Materials* **2006**, *18*, 1152.

(48) Shepherd, R. F.; Conrad, J. C.; Rhodes, S. K.; Link, D. R.; Marquez, M.; Weitz, D. A.; Lewis, J. A. *Langmuir* **2006**, *22*, 8618.

(49) Nisisako, T.; Torii, T. *Advanced Materials* **2007**, *19*, 1489.

(50) Takahara, Y. K.; Ikeda, S.; Ishino, S.; Tachi, K.; Ikeue, K.; Sakata, T.; Hasegawa, T.; Mori, H.; Matsumura, M.; Ohtani, B. *Journal of the American Chemical Society* **2005**, *127*, 6271.

(51) Suzuki, D.; Tsuji, S.; Kawaguchi, H. *Journal of the American Chemical Society* **2007**, *129*, 8088.

(52) Liu, B.; Wei, W.; Qu, X.; Yang, Z. *Angewandte Chemie International Edition* **2008**, *47*, 3973.

(53) Perro, A.; Meunier, F.; Schmitt, V.; Ravaine, S. *Colloids and Surfaces A: Physicochemical and Engineering Aspects* **2009**, *332*, 57.

(54) Sheu, H. R.; El-Aasser, M. S.; Vanderhoff, J. W. *Journal of Polymer Science Part A: Polymer Chemistry* **1990**, *28*, 629.

(55) Mock, E. B.; De Bruyn, H.; Hawkett, B. S.; Gilbert, R. G.; Zukoski, C. F. *Langmuir* **2006**, *22*, 4037.

(56) Park, J. G.; Forster, J. D.; Dufresne, E. R. *Journal of the American Chemical Society* **2010**, *132*, 5960.

(57) Yoon, K.; Lee, D.; Kim, J. W.; Kim, J.; Weitz, D. A. *Chemical Communications* **2012**, *48*, 9056.

(58) Kuhn, H.; Försterling, H.-D.; Waldeck, D. H. *Principles of physical chemistry*; Wiley-Interscience, 2009.

(59) Park, B. J.; Lee, D. *ACS Nano* **2011**, *6*, 782.

(60) Park, B. J.; Lee, D. *Soft Matter* **2012**, *8*, 7690.

(61) Brugarolas, T.; Park, B. J.; Lee, M. H.; Lee, D. *Advanced Functional Materials* **2011**, *21*, 3924.

(62) Park, B. J.; Brugarolas, T.; Lee, D. *Soft Matter* **2011**, *7*, 6413.

(63) Kumar, A.; Park, B. J.; Tu, F.; Lee, D. *Soft Matter* **2013**, *9*, 6604.

(64) Kralchevsky, P. A.; Denkov, N. D.; Danov, K. D. *Langmuir* **2001**, *17*, 7694.

(65) Stamou, D.; Duschl, C.; Johannsmann, D. *Physical Review E* **2000**, *62*, 5263.

(66) Even if the particles are close-packed, there will be 12 particles that have five nearest neighbours. However, when the radius of a droplet is large compared to the radius of an adsorbed particle, the fraction of particles with five nearest neighbours is very small; thus negligible.

(67) Hirose, Y.; Komura, S.; Nonomura, Y. *The Journal of Chemical Physics* **2007**, *127*, 054707.

(68) Berg, J. C. *Introduction to Interfaces and Colloids*; World Scientific Publishing Company Incorporated, 2009.

(69) Levine, S.; Bowen, B. D.; Partridge, S. J. *Colloids and Surfaces* **1989**, *38*, 325.

(70) Levine, S.; Bowen, B. D.; Partridge, S. J. *Colloids and Surfaces* **1989**, *38*, 345.

(71) Israelachvili, J. N.; Pashley, R. M. *Nature* **1983**, *306*, 249.

(72) Molina-Bol ívar, J. A.; Ortega-Vinuesa, J. L. *Langmuir* **1999**, *15*, 2644.

(73) The radii of droplets after the adsorption of Janus dumbbells are slightly larger than 10 μm

(74) R. H. Hardin, N. J. A. Sloane and W. D. Smith, Published

online at http://www2.research.att.com/~njas/icosahedral.codes//.

(75) Arditty, S.; Whitby, C. P.; Binks, B. P.; Schmitt, V.; Leal-Calderon, F. *The European Physical Journal E: Soft Matter and Biological Physics* **2003,** *11*, 273.

(76) Abismaïl, B.; Canselier, J. P.; Wilhelm, A. M.; Delmas, H.; Gourdon, C. *Ultrasonics Sonochemistry* **1999,** *6*, 75.

(77) Vladisavljević, G. T.; Schubert, H. *Journal of Membrane Science* **2003,** *225*, 15.

(78) Thompson, K. L.; Armes, S. P.; York, D. W. *Langmuir* **2011,** *27*, 2357.

(79) Sauter, J. D*ie Größenbestimmung der im Gemischnebel von Verbrennungskraftmaschinen vorhandenen Brennstoffteilchen;* VDI-Verl, 1926.

(80) In the non-dimensionalized form, if all other parameters are kept constant, the absolute values of volume of oil and aqueous phases do not change the non-dimensionalized average droplet radius as long as the the ratio between these two is kept constant.

(81) With the fixed number of Janus dumbbells, we are not able to derive an expression for non-dimensional average droplet radius; therefore, the change in the average droplet radius in the absolute unit is presented.

(82) Jiang, S.; Granick, S.; Schneider, H. J. *Janus particle synthesis, self-assembly and applications;* Royal Society of Chemistry, 2012.

(83) Walther, A.; Hoffmann, M.; Müller, A. H. E. *Angewandte Chemie* **2008,** *120*, 723.

(84) Liu, B.; Liu, J.; Liang, F.; Wang, Q.; Zhang, C.; Qu, X.; Li, J.; Qiu, D.; Yang, Z. *Macromolecules* **2012,** *45,* 5176.

(85) Yoon, J.; Kota, A.; Bhaskar, S.; Tuteja, A.; Lahann, J. *ACS Applied Materials & Interfaces* **2013,** *5,* 11281.

(86) Tu, F.; Park, B. J.; Lee, D. *Langmuir* **2013,** *29,* 12679.

(87) Sacanna, S.; Kegel, W. K.; Philipse, A. P. *Physical Review Letters* **2007,** *98,* 158301.

(88) Aveyard, R.; Binks, B. P.; Clint, J. H. *Advances in Colloid and Interface Science* **2003,** *100–102,* 503.

(89) Glaser, N.; Adams, D. J.; Böker, A.; Krausch, G. *Langmuir* **2006,** *22,* 5227.

(90) Walther, A.; André, X.; Drechsler, M.; Abetz, V.; Müller, A. H. E. *Journal of the American Chemical Society* **2007,** *129,* 6187.

(91) Ruhland, T. M.; Gröschel, A. H.; Walther, A.; Müller, A. H. E. *Langmuir* **2011,** *27,* 9807.

(92) Fernandez-Rodriguez, M. A.; Song, Y.; Rodríguez-Valverde, M. Á.; Chen, S.; Cabrerizo-Vilchez, M. A.; Hidalgo-Alvarez, R. *Langmuir* **2014,** *30,* 1799.

(93) Faria, J.; Ruiz, M. P.; Resasco, D. E. *Advanced Synthesis & Catalysis* **2010,** *352,* 2359.

(94) Zhou, W.-J.; Fang, L.; Fan, Z.; Albela, B.; Bonneviot, L.; De Campo, F.; Pera-Titus, M.; Clacens, J.-M. *Journal of the American Chemical Society* **2014,** *136,* 4869.

(95) Park, B. J.; Choi, C.-H.; Kang, S.-M.; Tettey, K. E.; Lee, C.-S.; Lee, D. *Soft Matter* **2013,** *9,* 3383.

(96) Park, B. J.; Choi, C.-H.; Kang, S.-M.; Tettey, K. E.; Lee, C.-S.; Lee, D. *Langmuir* **2013,** *29,* 1841.

(97) Ruhland, T. M.; Gröschel, A. H.; Ballard, N.; Skelhon, T. S.; Walther, A.; Müller, A. H. E.; Bon, S. A. F. *Langmuir* **2013,** *29,* 1388.

(98) Mathur, A. M.; Drescher, B.; Scranton, A. B.; Klier, J. *Nature* **1998,** *392,* 367.

(99) Khoukh, S.; Perrin, P.; Bes de Berc, F.; Tribet, C. *ChemPhysChem* **2005,** *6,* 2009.

(100) Zhang, L.; Yu, K.; Eisenberg, A. *Science* **1996,** *272,* 1777.

(101) Zhang, L.; Eisenberg, A. *Macromolecules* **1996,** *29,* 8805.

(102) Christian, D. A.; Tian, A.; Ellenbroek, W. G.; Levental, I.; Rajagopal, K.; Janmey, P. A.; Liu, A. J.; Baumgart, T.; Discher, D. E. *Nature Materials* **2009,** *8,* 843.

(103) Perrin, P.; Porcar, I.; Tribet, C. *Polymer International* **2003,** *52,* 465.

(104) Besnard, L.; Marchal, F.; Paredes, J. F.; Daillant, J.; Pantoustier, N.; Perrin, P.; Guenoun, P. *Advanced Materials* **2013,** *25,* 2844.

(105) Tanaka, T.; Okayama, M.; Minami, H.; Okubo, M. *Langmuir* **2010,** *26,* 11732.

(106) Yang, H.; Liang, F.; Wang, X.; Chen, Y.; Zhang, C.; Wang, Q.; Qu, X.; Li, J.; Wu, D.; Yang, Z. *Macromolecules* **2013,** *46,* 2754.

(107) Lu, C.; Urban, M. W. *ACS Macro Letters* **2014,** *3,* 346.

(108) Tang, C.; Zhang, C.; Liu, J.; Qu, X.; Li, J.; Yang, Z. *Macromolecules* **2010,** *43,* 5114.

(109) Park, J.-G.; Forster, J. D.; Dufresne, E. R. *Journal of the American Chemical Society* **2010,** *132,* 5960.

(110) Du, J.; O'Reilly, R. K. *Chemical Society Reviews* **2011,** *40,* 2402.

(111) Loget, G.; Kuhn, A. *Journal of Materials Chemistry* **2012,** *22,* 15457.

(112) van Ravensteijn, B. G. P.; Kamp, M.; van Blaaderen, A.; Kegel, W. K. *Chemistry of Materials* **2013,** *25,* 4348.

(113) Hautekeer, J. P.; Varshney, S. K.; Fayt, R.; Jacobs, C.; Jerome, R.; Teyssie, P. *Macromolecules* **1990,** *23,* 3893.

(114) Davis, K. A.; Matyjaszewski, K. *Macromolecules* **2000,** *33,* 4039.

(115) Becer, C. R.; Paulus, R. M.; Hoogenboom, R.; Schubert, U. S. *Journal of Polymer Science Part A: Polymer Chemistry* **2006,** *44,* 6202.

(116) Durécault, A.; Taton, D.; Destarac, M.; Leising, F.; Gnanou, Y. *Macromolecules* **2004,** *37,* 5513.

(117) Yeo, S. J.; Kang, H.; Kim, Y. H.; Han, S.; Yoo, P. J. *ACS Applied Materials & Interfaces* **2012,** *4,* 2107.

(118) Xu, C.; Fu, X.; Fryd, M.; Xu, S.; Wayland, B. B.; Winey, K. I.; Composto, R. J. *Nano Letters* **2006,** *6,* 282.

(119) McConnell, M. D.; Lee, M. H.; Composto, R. J.; Yang, S. *Polymer Preprints* **2007,** *48,* 1000.

(120) Odian, G. *Principles of polymerization;* John Wiley & Sons, 2004.

(121) Ratzsch, M.; Stephan, L. *Plaste Kautsch.* **1968,** *15,* 884.

(122) Escale, P.; Save, M.; Lapp, A.; Rubatat, L.; Billon, L. *Soft Matter* **2010,** *6,* 3202.

(123) Cho, I.; Lee, K.-W. *Journal of Applied Polymer Science* **1985,** *30,* 1903.

(124) Wang, H.; Singh, V.; Behrens, S. H. *The Journal of Physical Chemistry Letters* **2012,** *3,* 2986.

(125) We denote the composition of the monomer mixture that is used to generate these Janus particles. (Sty50/AA50), for example, indicate that the ratio of styrene and tBA in the monomer mixture is 50:50.

(126) Hong, L.; Cacciuto, A.; Luijten, E.; Granick, S. *Nano Letters* **2006,** *6,* 2510.

(127) Lattuada, M.; Hatton, T. A. *Journal of the American Chemical Society* **2007,** *129,* 12878.

(128) Isojima, T.; Lattuada, M.; Vander Sande, J. B.; Hatton, T. A. *ACS Nano* **2008,** *2,* 1799.

(129) Chen, Q.; Whitmer, J. K.; Jiang, S.; Bae, S. C.; Luijten, E.; Granick, S. *Science* **2011,** *331,* 199.

(130) Binks, B. P.; Lumsdon, S. O. *Langmuir* **2000,** *16,* 2539.

(131) Kralchevsky, P. A.; Ivanov, I. B.; Ananthapadmanabhan, K. P.; Lips, A. *Langmuir* **2004,** *21,* 50.

(132) Gautier, F.; Destribats, M.; Perrier-Cornet, R.; Dechezelles, J.-F.; Giermanska, J.; Heroguez, V.; Ravaine, S.; Leal-Calderon, F.; Schmitt, V. *Physical Chemistry Chemical Physics* **2007,** *9,* 6455.

(133) Golemanov, K.; Tcholakova, S.; Kralchevsky, P. A.; Ananthapadmanabhan, K. P.; Lips, A. *Langmuir* **2006,** *22,* 4968.

(134) Destribats, M.; Lapeyre, V.; Sellier, E.; Leal-Calderon, F.; Schmitt, V.; Ravaine, V. *Langmuir* **2011,** *27,* 14096.

(135) Binks, B. P. *Modern aspects of emulsion science;* Royal Society of Chemistry, 1998.

(136) Binks, B. P.; Rodrigues, J. A. *Angewandte Chemie* **2005,** *117,* 445.

(137) Binks, B. P.; Murakami, R.; Armes, S. P.; Fujii, S. *Angewandte Chemie* **2005,** *117,* 4873.

(138) Sun, G.; Li, Z.; Ngai, T. *Angewandte Chemie* **2010,** *122,* 2209.

(139) Datta, S. S.; Gerrard, D. D.; Rhodes, T. S.; Mason, T. G.; Weitz, D. A. *Physical Review E* **2011,** *84,* 041404.

(140) Hermes, M.; Clegg, P. S. *Soft Matter* **2013,** *9,* 7568.

(141) Leal-Calderon, F.; Schmitt, V.; Bibette, J. *Emulsion science: basic principles;* Springer, 2007.

(142) Garti, N. *Colloids and Surfaces A: Physicochemical and Engineering Aspects* **1997,** *123–124,* 233.

(143) Lindenstruth, K.; Müller, B. W. *European Journal of Pharmaceutics and Biopharmaceutics* **2004,** *58,* 621.

(144) Miyazawa, K.; Yajima, I.; Kaneda, I.; Yanaki, T. *Journal of Cosmetic Science* **2000,** *51,* 239.

(145) Garti, N.; Aserin, A. *Advances in Colloid and Interface Science* **1996,** *65,* 37.

(146) McClements, D. J. *Food emulsions: principles, practice, and techniques;* CRC press, 1998.

(147) Binks, B.; Dyab, A.; Fletcher, P.; Barthel, H. G*erman Patent assigned to Wacker-Chemie GmbH, DE10211313, filed 14y3y2002* **2003.**

(148) Ficheux, M. F.; Bonakdar, L.; Leal-Calderon, F.; Bibette, J. *Langmuir* **1998,** *14,* 2702.

(149) Jiménez-Colmenero, F. *Food Research International* **2013,** *52,* 64.

(150) Besnard, L.; Protat, M.; Malloggi, F.; Daillant, J.; Cousin, F.; Pantoustier, N.; Guenoun, P.; Perrin, P. *Soft Matter* **2014,** *10,* 7073**.**

(151) He, Y.; Wu, F.; Sun, X.; Li, R.; Guo, Y.; Li, C.; Zhang, L.; Xing, F.; Wang, W.; Gao, J. *ACS Applied Materials & Interfaces* **2013,** *5,* 4843.

(152) Binks, B. P.; Fletcher, P. D. I.; Thompson, M. A.; Elliott, R. P. *Langmuir* **2013,** *29,* 5723.

(153) Hong, L.; Sun, G.; Cai, J.; Ngai, T. *Langmuir* **2012,** *28,* 2332.

(154) White, K. A.; Schofield, A. B.; Wormald, P.; Tavacoli, J. W.; Binks, B. P.; Clegg, P. S. *Journal of Colloid and Interface Science* 2**011,** *359,* 126.

(155) Nonomura, Y.; Kobayashi, N.; Nakagawa, N. *Langmuir* **2011,** *27,* 4557.

(156) Hanson, J. A.; Chang, C. B.; Graves, S. M.; Li, Z.; Mason, T. G.; Deming, T. J. *Nature* **2008,** *455,* 85.

(157) Binks, B. P.; Rodrigues, J. A. *Langmuir* **2003,** *19,* 4905.

(158) Zhang, Y.; Gou, J.; Sun, F.; Geng, S.; Hu, X.; Zhang, K.; Lin, X.; Xiao, W.; Tang, X. *Colloids and Surfaces B: Biointerfaces* **2014,** *122,* 368.

(159) Yamagami, T.; Kitayama, Y.; Okubo, M. *Langmuir* **2014,** *30,* 7823.

(160) Lu, C.; Urban, M. W. *ACS Macro Letters* **2014,** *3,* 346.

(161) Ji, X.; Zhang, Q.; Liang, F.; Chen, Q.; Qu, X.; Zhang, C.; Wang, Q.; Li, J.; Song, X.; Yang, Z. *Chemical Communications* **2014,** *50,* 5706.

(162) Tu, F.; Lee, D. *Journal of the American Chemical Society* **2014,** *136***,** 9999**.**

(163) Binks, B. P.; Murakami, R. *Nature Materials* **2006,** *5,* 865.

(164) Zambrano, N.; Tyrode, E.; Mira, I.; Márquez, L.; Rodríguez, M.-P.; Salager, J.-L. *Industrial & Engineering Chemistry Research* **2002,** *42,* 50.

(165) Groeneweg, F.; Agterof, W. G. M.; Jaeger, P.; Janssen, J. J. M.; Wieringa, J. A.; Klahn, J. K. *Chemical Engineering Research and Design* **1998,** *76,* 55.

(166) Yan, J.; Bloom, M.; Bae, S. C.; Luijten, E.; Granick, S. *Nature* **2012,** *491,* 578.

(167) Shah, A. A.; Schultz, B.; Zhang, W.; Glotzer, S. C.; Solomon, M. J. *Nature Materials* **2015,** *14,* 117.

(168) Jurado-Sánchez, B.; Sattayasamitsathit, S.; Gao, W.; Santos, L.; Fedorak, Y.; Singh, V. V.; Orozco, J.; Galarnyk, M.; Wang, J. *Small* **2015,** *11,* 499.

(169) Wang, S.; Wu, N. *Langmuir* **2014,** *30,* 3477.

(170) Zhang, J.; Xu, S.; Kumacheva, E. *Journal of the American Chemical Society* **2004,** *126,* 7908.

(171) Zhang, J.; Xu, S.; Kumacheva, E. *Advanced Materials* **2005,** 1*7,* 2336.

(172) Chen, Y.-C.; Dimonie, V.; El-Aasser, M. S. *Journal of Applied Polymer Science* **1991,** *42,* 1049.

(173) Saito, N.; Kagari, Y.; Okubo, M. *Langmuir* **2006,** 2*2,* 9397.

(174) Ivarsson, L. E.; Karlsson, O. J.; Sundberg, D. C. *Macromolecular Symposia* **2000,** *151,* 407.

(175) Chen, Y. C.; Dimonie, V.; El-Aasser, M. S. *Macromolecules* **1991,** *24,* 3779.

(176) Chen, Y.-C.; Dimonie, V. L.; Shaffer, O. L.; El-Aasser, M. S. *Polymer International* **1993,** *30,* 185.

(177) Akimoto, M.; Morimoto, Y. *Biomaterials* **1983,** *4,* 49.

(178) Waeckerle-Men, Y.; Groettrup, M. *Advanced Drug Delivery Reviews* **2005,** *57,* 475.

(179) Zhao, Q.; Han, B.; Wang, Z.; Gao, C.; Peng, C.; Shen, J. *Nanomedicine: Nanotechnology, Biology and Medicine* **2007,** *3,* 63.

(180) Liu, X.; Gao, C.; Shen, J.; Möhwald, H. *Macromolecular Bioscience* **2005,** *5,* 1209.

(181) An, Z.; Lu, G.; Möhwald, H.; Li, J. *Chemistry – A European Journal* **2004,** *10,* 5848.

(182) Fundueanu, G.; Constantin, M.; Esposito, E.; Cortesi, R.; Nastruzzi, C.; Menegatti, E. *Biomaterials* **2005,** *26,* 4337.

(183) Lu, L.; Huang, K. *Journal of Polymer Science Part A: Polymer Chemistry* **2005,** *43,* 2468.

(184) Wang, S.-B.; Xu, F.-H.; He, H.-S.; Weng, L.-J. *Macromolecular Bioscience* **2005,** *5,* 408.

(185) Huang, S.-L.; MacDonald, R. C. *Biochimica et Biophysica Acta (BBA) - Biomembranes* **2004,** *1665,* 134.

(186) Wang, C.; Ye, W.; Zheng, Y.; Liu, X.; Tong, Z. *International Journal of Pharmaceutics* **2007,** *338,* 165.

(187) Song, W.; He, Q.; Mohwald, H.; Yang, Y.; Li, J. *Journal of Controlled Release* **2009,** *139,* 160.

(188) Ando, S.; Putnam, D.; Pack, D. W.; Langer, R. *Journal of Pharmaceutical Sciences* **1999,** *88,* 126.

(189) Wang, D.; Robinson, D. R.; Kwon, G. S.; Samuel, J. *Journal of Controlled Release* **1999,** *57,* 9.

(190) Capan, Y.; Woo, B. H.; Gebrekidan, S.; Ahmed, S.; DeLuca, P. P. *Pharmaceutical Research* **1999,** *16,* 509.

(191) Luo, D.; Woodrow-Mumford, K.; Belcheva, N.; Saltzman, W. M. *Pharmaceutical Research* **1999,** *16,* 1300.

(192) Wang, C.; Ge, Q.; Ting, D.; Nguyen, D.; Shen, H.-R.; Chen, J.; Eisen, H. N.; Heller, J.; Langer, R.; Putnam, D. *Nature Materials* **2004,** *3,* 190.

(193) Walter, E.; Moelling, K.; Pavlovic, J.; Merkle, H. P. *Journal of Controlled Release* **1999,** *61,* 361.

(194) Walter, E.; Dreher, D.; Kok, M.; Thiele, L.; Kiama, S. G.; Gehr, P.; Merkle, H. P. *Journal of Controlled Release* **2001,** *76,* 149.

(195) Yang, Y.-Y.; Chia, H.-H.; Chung, T.-S. *Journal of Controlled Release* **2000,** *69,* 81.

(196) Christian, D. A.; Cai, S.; Bowen, D. M.; Kim, Y.; Pajerowski, J. D.; Discher, D. E. *European Journal of Pharmaceutics and Biopharmaceutics* **2009,** *71,* 463.

(197) Maulding, H. V. *Journal of Controlled Release* **1987,** *6,* 167.

(198) Elvassore, N.; Bertucco, A.; Caliceti, P. *Industrial & Engineering Chemistry Research* **2001,** *40,* 795.

(199) Balabushevitch, N. G.; Sukhorukov, G. B.; Moroz, N. A.; Volodkin, D. V.; Larionova, N. I.; Donath, E.; Mohwald, H. *Biotechnology and Bioengineering* **2001,** *76,* 207.

(200) Caruso, F.; Trau, D.; Mohwald, H.; Renneberg, R. *Langmuir* **2000,** *16,* 1485.

(201) Tan, W. H.; Takeuchi, S. *Advanced Materials* **2007,** *19,* 2696.

(202) Chia, S. M.; Wan, A. C. A.; Quek, C. H.; Mao, H. Q.; Xu, X.; Shen, L.; Ng, M. L.; Leong, K. W.; Yu, H. *Biomaterials* **2002,** *23,* 849.

(203) Peirone, M.; Ross, C. J. D.; Hortelano, G.; Brash, J. L.; Chang, P. L. *Journal of Biomedical Materials Research* **1998,** *42,* 587.

(204) Blasi, P.; Giovagnoli, S.; Schoubben, A.; Ricci, M.; Rossi, C.; Luca, G.; Basta, G.; Calafiore, R. *International Journal of Pharmaceutics* **2006,** *324,* 27.

(205) Matthew, H. W.; Salley, S. O.; Peterson, W. D.; Klein, M. D. *Biotechnology Progress* **1993,** *9,* 510.

(206) Chandy, T.; Mooradian, Daniel L.; Rao, Gundu H. R. *Artificial Organs* **1999,** *23,* 894.

(207) Keen, P. H. R.; Slater, N. K. H.; Routh, A. F. *Langmuir* **2012,** *28,* 1169.

(208) Trongsatitkul, T.; Budhlall, B. M. *Langmuir* **2012,** *27,* 13468.

(209) Hamad, S. A.; Dyab, A. F. K.; Stoyanov, S. D.; Paunov, V. N. *Journal of Materials Chemistry* **2012,** *21,* 18018.

(210) Mazumder, M. A. J.; Burke, N. A. D.; Shen, F.; Potter, M. A.; Stover, H. D. H. *Biomacromolecules* **2009,** *10,* 1365.

(211) Rossow, T.; Heyman, J. A.; Ehrlicher, A. J.; Langhoff, A.; Weitz, D. A.; Haag, R.; Seiffert, S. *Journal of the American Chemical Society* **2012,** *134,* 4983.

(212) Langer, R. *Nature* **1998,** *392,* 5.

(213) Sukhorukov, G. B.; Rogach, A. L.; Garstka, M.; Springer, S.; Parak, W. J.; Muñoz-Javier, A.; Kreft, O.; Skirtach, A. G.; Susha, A. S.; Ramaye, Y.; Palankar, R.; Winterhalter, M. *Small* **2007,** *3,* 944.

(214) Orive, G.; Hernandez, R. M.; Gascon, A. R.; Calafiore, R.; Chang, T. M. S.; Vos, P. D.; Hortelano, G.; Hunkeler, D.; Lacik, I.; Shapiro, A. M. J.; Pedraz, J. L. *Nature Medicine* **2003,** *9,* 104.

(215) Putnam, D. *Nature Materials* **2006,** *5,* 439.

(216) Luo, D.; Saltzman, W. M. *Nature Biotechnology* **2000,** *18,* 33.

(217) Anderson, J. M.; Shive, M. S. *Advanced Drug Delivery Reviews* **1997,** *28,* 5.

(218) Bala, I.; Hariharan, S.; Kumar, M. N. *Critical reviews in therapeutic drug carrier systems* **2004,** *21,* 387.

(219) Athanasiou, K. A.; Niederauer, G. G.; Agrawal, C. M. *Biomaterials* **1996,** *17,* 93.

(220) Freitas, S.; Merkle, H. P.; Gander, B. *Journal of Controlled Release* **2005,** *102,* 313.

(221) Rajeev A, J. *Biomaterials* **2000,** *21,* 2475.

(222) Nihant, N.; Schugens, C.; Grandfils, C.; Jerome, R.; Teyssie, P. *Journal of Colloid and Interface Science* **1995,** *173,* 55.

(223) Yeo, Y.; Park, K. *Archives of Pharmacal Research* **2004,** *27,* 1.

(224) Wang, H. T.; Schmitt, E.; Flanagan, D. R.; Linhardt, R. J. *Journal of Controlled Release* **1991,** *17,* 23.

(225) Xu, S.; Nie, Z.; Seo, M.; Lewis, P.; Kumacheva, E.; Stone, H. A.; Garstecki, P.; Weibel, D. B.; Gitlin, I.; Whitesides, G. M. *Angewandte Chemie* **2005,** *117,* 734.

(226) Shum, H. C.; Kim, J.-W.; Weitz, D. A. *Journal of the American Chemical Society* **2008,** *130,* 9543.

(227) Shum, H. C.; Lee, D.; Yoon, I.; Kodger, T.; Weitz, D. A. *Langmuir* **2008,** *24,* 7651.

(228) Choi, S.-W.; Zhang, Y.; Xia, Y. *Advanced Functional Materials* **2009,** *19,* 2943.

(229) Stachowiak, J. C.; Richmond, D. L.; Li, T. H.; Liu, A. P.; Parekh, S. H.; Fletcher, D. A. *Proceedings of the National Academy of Sciences* **2008,** *105,* 4697.

(230) Kim, J.-W.; Utada, A. S.; Fernández-Nieves, A.; Hu, Z.; Weitz, D. A. *Angewandte Chemie* **2007,** *119,* 1851.

(231) Lee, M. H.; Lee, D. *Soft Matter* **2010,** *6,* 4326.

(232) Lee, M. H.; Prasad, V.; Lee, D. *Langmuir* **2009,** *26,* 2227.

(233) Utada, A. S.; Lorenceau, E.; Link, D. R.; Kaplan, P. D.; Stone, H. A.; Weitz, D. A. *Science* **2005,** *308,* 537.

(234) Kamat, N. P.; Lee, M. H.; Lee, D.; Hammer, D. A. *Soft Matter* **2012,** *7,* 9863.

(235) Lee, D.; Weitz, D. A. *Advanced Materials* **2008,** *20,* 3498.

(236) Erb, R. M.; Obrist, D.; Chen, P. W.; Studer, J.; Studart, A. R. *Soft Matter* **2011,** *7,* 8757.

(237) Mezzenga, R.; Folmer, B. M.; Hughes, E. *Langmuir* **2004,** *20,* 3574.

(238) Herrmann, J.; Bodmeier, R. *Journal of Controlled Release* **1995,** *36,* 63.

(239) K. F. Pistel, T. K. *Journal of Microencapsulation* **2000,** *17,* 467.

(240) Han, K.; Lee, K.-D.; Gao, Z.-G.; Park, J.-S. *Journal of Controlled Release* **2001,** *75,* 259.

(241) Jiang, G.; Thanoo, B. C.; DeLuca, P. P. *Pharmaceutical Development and Technology* **2002,** *7,* 391.

(242) Shah, R. K.; Shum, H. C.; Rowat, A. C.; Lee, D.; Agresti, J. J.; Utada, A. S.; Chu, L.-Y.; Kim, J.-W.; Fernandez-Nieves, A.; Martinez, C. J.; Weitz, D. A. *Materials Today* **2008,** *11,* 18.

(243) Lee, M. H.; Hribar, K. C.; Brugarolas, T.; Kamat, N. P.; Burdick, J. A.; Lee, D. *Advanced Functional Materials* **2012,** *22,* 131.

(244) Although the effect of PLGA composition is not overwhelming, 50:50 PLGA seems to stabilize double emulsions most effectively. At pH 11.0, the fraction of stable double emulsions containing 50:50 PLGA is greater than those containing 65:35 and 85:15.

(245) Miller, D. C.; Thapa, A.; Haberstroh, K. M.; Webster, T. J. *Biomaterials* **2004,** *25,* 53.

(246) Gao, J.; Niklason, L.; Langer, R. *Journal of Biomedical Materials Research* **1998,** *42,* 417.

(247) Croll, T. I.; O'Connor, A. J.; Stevens, G. W.; Cooper-White, J. J. *Biomacromolecules* **2004,** *5,* 463.

(248) Park, G. E.; Pattison, M. A.; Park, K.; Webster, T. J. *Biomaterials* **2005,** *26,* 3075.

(249) Smith, L. L.; Niziolek, P. J.; Haberstroh, K. M.; Nauman, E. A.; Webster, T. J. *International Journal of Nanomedicine* **2007,** *2,* 383.

(250) Nam, Y. S.; Yoon, J. J.; Lee, J. G.; Park, T. G. *Journal of Biomaterials Science, Polymer Edition* **1999,** *10,* 1145.

(251) Khang, G.; Choee, J.-H.; Rhee, J. M.; Lee, H. B. *Journal of Applied Polymer Science* **2002,** *85,* 1253.

(252) Pattison, M. A.; Wurster, S.; Webster, T. J.; Haberstroh, K. M. *Biomaterials* **2005,** *26,* 2491.

(253) Thapa, A.; Miller, D. C.; Webster, T. J.; Haberstroh, K. M. *Biomaterials* **2003,** *24,* 2915.

(254) Thapa, A.; Webster, T. J.; Haberstroh, K. M. *Journal of Biomedical Materials Research Part A* **2003,** *67A,* 1374.

(255) 1M NaOH solution is not suitable for the encapsulation of active ingredients. This basic solution, however, is used to study of the effect of the inner solution basicity on the hydrolysis of PLGA in the oil phase and ionization of carboxylic acid groups.

(256) Giunchedi, P.; Conti, B.; Scalia, S.; Conte, U. *Journal of Controlled Release* **1998,** *56,* 53.

(257) Although ester-terminated PLGA is used, PLGA may undergo slow hydrolysis during storage at a low temperature (= -17 ℃). PLGA has been shown to undergo hydrolysis at 0 ℃.

(258) Atkins, P.; de Paula, J. P*hysical Chemistry;* 7th ed.; W. H. Freeman and Company: New York, 2001.

(259) Wyss, H. M.; Blair, D. L.; Morris, J. F.; Stone, H. A.; Weitz, D. A. *Physical Review E* **2006,** *74,* 061402.

(260) Kanai, T.; Lee, D.; Shum, H. C.; Weitz, D. A. S*mall* 2**010,** *6,* 807.

(261) Shire, S. J.; Shahrokh, Z.; Liu, J. *Journal of Pharmaceutical Sciences* **2004,** *93,* 1390.